Molecular and Environmental Studies of Bacterial Arsenate Respiration

Thesis by

Davin Malasarn

In Partial Fulfillment of the Requirements

for the Degree of

Doctor of Philosophy

CALIFORNIA INSTITUTE OF TECHNOLOGY

Pasadena, California

2007

(Defended February 8, 2007)

Acknowledgements

I moved into my home on Wilson Avenue on December 24, 2000, just days before I started my rotation in Dianne Newman's lab. Now, in February of 2007, I'm attempting to thank everyone who has helped me throughout my studies at Caltech. It's impossible, of course, and I'm sure over the years, names and faces of additional people who I don't mention here will creep up in happy memories.

Dianne, I'm so grateful to you for taking me into your lab. It has been an honor to work under someone as intellectually elegant and as scientifically daring as you. I really appreciate your support and your nurturing attitude. Being systematic and organized is not my strongest suit, but you helped me get better at that, and you always encouraged my creative side. Graduate school is the hardest and most rewarding thing I have ever done so far, and I feel very fortunate to have you as my guide in science and in life.

To my committee, past and present, I'm grateful to be able to rely on a group of professors that inspire me. Paul Sternberg, you were the reason I came to Caltech, and I always appreciate your openness and your passion. Harry Gray, I deeply admire the fact that you make all of your hard work and brilliance look so easy. Pamela Bjorkman, you helped me clarify my image of what it takes to be a successful scientist. You helped me find ways to feel more secure in my work. And, Jim Howard, thank you for your infinite patience as I took my first steps into biochemistry.

Now for the people in the trenches. Kate Campbell, what would I have done without you? You motivated me in the lab, you taught me how to be a better scientist,

and you filled my hours of time courses with fascinating conversation about writing. I've really come to appreciate your finesse in the lab, from color coding to describing the quality of the reagents we used. Your huge contributions are a part of nearly every chapter of this thesis, and it has been a joy to have you in my life.

Chad Saltikov, thanks for giving birth to ANA-3 genetics. You taught me everything I needed to know about cloning and (trying) to surf on a short board.

Tracy Teal, you've been my closest officemate and lab bench bay buddy in the lab. Thanks for singing your campfire songs. More importantly, thanks for saving me over and over again on both a technical level and an emotional level. You helped me stay positive whenever the program was beating me down.

Yongqin Jiao, what words are there to describe you? I really appreciate you being willing to make yourself look silly to keep all of us amused. That personality only works because you have the hard work and intellect behind it. You've been a wonderful friend.

Thanks to:

Anthea Lee for teaching me how to deal with acid spills.

Laura Croal for giving me older-sister advice.

Lars E. P. Dietrich for shaking my hand on my birthday.

Doug Lies for caring so much for his cat.

Nicky Caiazza for not being able to whistle but trying anyway.

Alexa Price-Whelan for being so precocious.

Mariu Hernandez for being the first student to graduate from Dianne's Lab.

Tanja for making tiramisu.

Everyone else in the Newman Lab for making it so much fun.

To Curt Riesberg and Lea Cox, thanks for constantly reminding me that there is a world outside the lab. You helped me connect my left-brain with my right-brain, and my brain to my heart, because you are so connected yourselves. And, you both have given me the same haunting advice to make sure I get arrested at some point in my life…I can't wait.

To my family: Mom, you are responsible for every good thing I do in my life. I love you, and I thank you. Dad, you have always encouraged me to make something of my life. Thank you so much for lifting me up. Auntie, you helped me so much in school and in life. Thank you, thank you! Keng, I'm so grateful to have a brother so different from me. I know I'll always admire you. I know I will always be able to come to you for advice. During my time at Caltech, I've experienced new beginnings and sad endings. My brother got married in 2000, just months before I came back down to live in Southern California. His wife, Maria, has been a great addition to my life. My goofball nephew, Dylan, was born in April of 2003. Dylan, kiddo, you've helped to remind me how easy it is to access the best part of the world. And, just a few months ago, my loving dogs, Dragon and Knight, passed away after being a part of the family for fifteen years. I miss you both, and I hope you had a good time while you were with us. Thank you.

To the scientific world, thank you for creating a place where truth can be found. I am so grateful that I have the opportunity to learn something new everyday.

Abstract

Arsenate [As(V)]-respiring bacteria that reduce As(V) to arsenite, As(III), for energy production have been implicated as possible catalysts for arsenic mobilization into drinking water supplies. To understand how this metabolism contributes to arsenic geochemistry, this thesis explores the dynamics of As(V)-respiratory gene expression, the impact of As(V) respiration on microbial ferric [Fe(III)] reduction, and biochemical properties of the arsenate respiratory reductase, ARR.

Using sequences for *arrA*, a gene encoding the terminal reductase involved in As(V) respiration, degenerate PCR primers were designed to amplify a diagnostic region of the gene in multiple As(V)-respiring isolates. These primers were used to track *arrA* transcription in microcosm studies involving synthetic sediments. *arrA* was required for As(V) reduction in this context, and the gene was expressed in contaminated sediments at Haiwee Reservoir in Olancha, CA.

To understand the impact of As(V) respiration on Fe(III) reduction, native microbial consortia from Haiwee Reservoir and pure cultures of the genetically tractable *Shewanella* sp. strain ANA-3 were incubated with As-sorbed hydrous ferric oxide (HFO), and rates of As(V) and Fe(III) reduction were determined. As(V) reduction occurred simultaneously with or prior to Fe(III) reduction, consistent with the idea that electron acceptor utilization is determined by thermodynamic favorability. Furthermore, the presence of sorbed As(III) increased rates of Fe(III) reduction, potentially by increasing HFO surface area.

Lastly, the expression, assembly, and kinetic properties of ARR from ANA-3 were characterized. ARR is a soluble periplasmic heterodimer that is expressed during early exponential growth and persists into late stationary phase. The enzyme contains molybdenum, Fe, and sulfur cofactors. It has a K_m of 5 μM, a V_{max} of 11,111 μmol As(V) reduced · min^{-1} · mg $protein^{-1}$, and reduces only As(V). Mutational analysis of the residues corresponding to the diagnostic region of *arrA* mentioned above resulted in loss of enzyme activity.

This work brings us closer to being able to quantify and predict the contribution of As(V) respiration to the solubilization of arsenic from sediments. Structural studies, the development of probes to detect ARR, and comparisons of ARR from different bacterial species are now possible.

Table of Contents

List of Figures

List of Tables

Chapter 1

Introduction

1.1. Motivation

In the early 1970s, world aid agencies sponsored the installation of millions of tube wells throughout Bangladesh in the hopes of accessing cleaner water supplies. For over a decade the solution seemed promising, but beginning in 1983, doctors in West Bengal started receiving patients seeking a cure for black, gangrenous lesions on the palms of their hands and the bottom of their feet (Saha 1996; Chowdhury 2004). What was the cause of this mysterious new illness? The doctors determined that the symptoms resulted from chronic arsenic poisoning, and the source of the contamination was traced back to the tube wells. Today, tens of millions of people still rely on these wells for water, and the public health crisis has been called "the largest mass poisoning of a population in history" (Smith et al. 2000).

Early studies revealed that the arsenic in groundwater supplies originated from underlying sediments that are typically iron-rich. A series of microcosm studies using sediment from contaminated sites showed that the addition of antibiotics or formaldehyde could inhibit the mobilization of arsenic from the solid phase to the aqueous phase, suggesting that the action was due to microbial activity. Multiple metabolic reactions

could be responsible for this arsenic mobilization: reduction of the oxidized form of arsenic, arsenate [As(V)], to arsenite [As(III)] as a result of detoxification or respiratory systems could change the sorptive properties of arsenic. Reductive iron dissolution could reduce the amount of sediment material onto which the arsenic could sorb. Other reactions, such as sulfide oxidation, might release arsenic from arsenic-bearing minerals.

With these potentially important mechanisms in mind, the challenge was to understand the contribution of each microbial reaction in contaminated environments. To begin to parse out this complex problem, I have focused on the role of As(V) respiration and biochemical studies of the key enzyme involved in this metabolism, the arsenate respiratory reductase (ARR). I proposed to answer the following questions:

1. Is there a molecular marker for respiratory As(V) reduction? If so, can we use this marker to determine if As(V) respiration is active and significant in contaminated environments?

2. How does respiratory As(V) reduction impact bacterial dissimilatory iron reduction, another microbial metabolism that may influence arsenic mobilization?

3. What are the dynamics of post-transcriptional expression of ARR, and what mechanisms are involved in the assembly of active enzyme?

1.2. Overview

In this thesis I present our progress in addressing these questions. Chapter 2 reviews background topics relevant to the study of arsenic contamination. This begins with discussions of health problems caused by chronic arsenic ingestion, sources of arsenic in the environment, and a review of the microbes that transform arsenic between As(V) and As(III). The mechanisms involved for arsenic detoxification, As(III) oxidation, and respiratory As(V) reduction proceeds. This is followed by a discussion of bacterial contributions to arsenic mobilization in the environment based on microcosm studies. I then present the significance of these reactions in relation to two specific environmental sites: first, I describe the mineralogy and potentially important microbial reactions in Bangladesh. Second, I characterize Haiwee Reservoir, a contaminated field site studied in later chapters. The chapter concludes with a brief discussion of how molecular biology can help to answer environmental questions regarding arsenic mobilization. Sections of this chapter were published in *Annual Review of Genetics 38: 175-202 (2004)*.

Chapter 3 presents the development and application of a genetic marker for As(V) respiration in the environment. We sequenced homologs of *arrA*, a key gene required for As(V) respiration, from a subset of known As(V)-respirers, and designed a set of degenerate PCR primers to amplify a diagnostic region of the gene from a broad range of isolates. Then, using a pure culture of an As(V)-respiring bacterium and a mutant form of the strain that lacked *arrA*, we evaluated the importance of this gene in an environmental context. We characterized the transcription of *arrA* in relation to As(V)

reduction in this setting. Finally, we applied the degenerate primers at Haiwee Reservoir to determine if the gene was expressed. This work was performed in collaboration with Dr. Kate Campbell and Professor Janet Hering in the Division of Engineering and Applied Science at Caltech and Dr. Joanne Santini in the Department of Microbiology at La Trobe University. Sections of this chapter were published in *Science 306: 455 (2004).*

In Chapter 4, we characterize the impact of microbial As(V) respiration on iron reduction. Using a sediment analog and microcosm experiments, we tracked the reduction of As(V) and iron by native microbial consortia from Haiwee Reservoir. The results were used to design additional experiments with pure cultures of *Shewanella* sp. strain ANA-3 and additional sediment analogs sorbed with As(V), As(III), or analogs without any sorbed species. In these experiments, we observed that the presence of sorbed As(III), either at the onset of the experiment or as a result of As(V) respiration, increased the rates of bacterial iron reduction. This work was performed in collaboration with Dr. Kate Campbell and Professor Janet Hering in the Division of Engineering and Applied Science at Caltech. Sections of this chapter were published in *Environmental Science & Technology 40(19): 5950-5955 (2006)*.

In Chapter 5 we present the biochemical characterization of the arsenate respiratory reductase, ARR. Because *arrA* gene expression was observed in contaminated sediments, and because As(V) respiration is significant in environmental contexts, our objective was to characterize the post-transcriptional expression of ARR. We measured the dynamics of native ARR activity during the growth of ANA-3 cultures and determined the intracellular localization of ARR. After the characterization of the

enzyme in the native strain, we heterologously expressed ARR in *E. coli* strain C43. We identified the conditions required for the assembly of active enzyme. Also, we purified the protein and characterized it in terms of molecular mass, metal cofactors, and enzyme kinetics for the purified ARR complex and the individual subunits ArrA and ArrB.

Chapter 6 contains a brief summary of the key findings presented in this thesis, concluding remarks about the future of this work, and enticing questions that remain unanswered.

Finally, three appendices are included. Appendix A provides supplemental instructions for the use of degenerate primers to amplify *arrA* in the environment (Sections of this appendix were published in *The Manual of Environmental Microbiology, 3rd edition (2006)*). Appendix B contains homology modeling and preliminary mutational analysis of ARR. Appendix C contains work that attempts to explain the mechanisms involved in the increased rate of iron reduction upon sorption of As(III). We characterized this phenomenon using microscopy, chemical techniques, and fluorescent derivatives of *Shewanella* to observe differences in cell adhesions.

1.3. References

Chowdhury, A. M. (2004). "Arsenic crisis in Bangladesh." Scientific American **291**(2): 86-91.

Saha, D. P. (1996). "Arsenic poisoning in West Bengal." Science **274**(5291): 1287.

Smith, A. H., E. O. Lingas, et al. (2000). "Contamination of drinking-water by arsenic in Bangladesh: a public health emergency." Bulletin from the World Health Organization **78**(9): 1093-1103.

Chapter 2

Background

This chapter includes sections from:

Croal, L. R., J. Gralnick, D. Malasarn, D. K. Newman. 2004. "The Genetics of Geochemistry." Annual Review of Genetics 38: 175-202.

2.1. Arsenic Contamination: A Global Concern

Evidence of people suffering from chronic arsenic exposure has been recorded throughout history, even in Greek mythology where the depiction of Hephaestus with deformed legs is believed to have been inspired by metalsmiths who suffered from polyneuropathy caused by working with As (Aterman 1999). In more recent times, arsenic is problematic because it contaminates drinking water supplies, where chronic exposure causes neurological damage, black-foot disease, skin cancer, other cancers of the internal organs, and respiratory problems (Mazumder et al. 1998). Though it is only the 20th most abundant element in the earth's crust, present at about 1.8 parts per million (Klein 2002), its toxicity is problematic in many parts of the world. The World Health Organization recommends As guideline values of 10 μg/L (World Health Organization), but As concentrations in Argentina, Chile, Canada, Bangladesh, Cambodia, Vietnam, West Bengal, and the United States often exceed this limit. In Bangladesh alone, where

As concentrations reach as high as 1000 μg/L (Nickson et al. 1998), as many as 50-60 million people are exposed to As-contaminated drinking water, and thousands of cases of arsenicosis are diagnosed each year.

Used in metallurgy, wood preservation, painting, medicine, pest control, and as an additive to chicken feed where it increases growth (Nriagu 2002; Silver et al. 2002), anthropogenic sources contribute to some incidents of As contamination (Spliethoff and Hemond 1996). However, volcanic action, low temperature volatilization (World Health Organization) and natural weathering (Wilkie and Hering 1998; Armienta et al. 2001) of As-containing minerals are the greatest sources of As in the environment. Arsenic can exist in the form of arsine gas, arsenosugars, or other organoarsenicals, such as arsenobetaine, but the major species present in natural waters are arsenate ($HAsO_4^{2-}$; As(V)) and arsenite (H_3AsO_3; As(III)) (Francesconi and Kuehnelt 2002). These two oxyanions readily interconvert, and their different chemical properties determine whether they are sequestered in solid form or mobilized into the aqueous phase (Newman and Kolter 2000). In sedimentary environments that are not dominated by Fe, As(III) is generally more mobile than As(V), thus, understanding what stimulates As(III) oxidation and/or limits As(V) reduction is relevant for management of contaminated sites (Harvey et al. 2002).

2.2. Arsenic-transforming Microbes

Microorganisms that transform As between As(V) and As(III) are diverse in their phylogeny and overall physiology (Table 2.1). By far the most genetic work on As(V) reduction comes from studies of the As detoxification systems in *Staphylococcus aureus* and *E. coli* (Hedges and Baumberg 1973; Silver et al. 1981; Mobley et al. 1983; Broer et al. 1993; Wu and Rosen 1993; Dey and Rosen 1995; Xu et al. 1996). These systems do not generate energy. Microorganisms that utilize As for energy fall into two classes: the chemolithoautotrophic As(III) oxidizers and the heterotrophic As(V) reducers. Chemolithoautotrophs gain energy from coupling the oxidation of As(III) to the reduction of oxygen (Ilyaletdinov and Abdrashitova 1981; Santini et al. 2000) or nitrate (Oremland et al. 2002; Senn and Hemond 2002). They include members of the *Alcaligenes* (Philips and Taylor 1976), *Agrobacterium/Rhizobium* (Santini et al. 2000), *Ectothiorhodospora* (Oremland et al. 2002), *Pseudomonas* (Macur et al. 2004) and *Thermus* (Gihring and Banfield 2001) genera among others. Not all As(III)-oxidizing bacteria conserve energy from As(III) oxidation, however; several As(III)-oxidizing heterotrophs do not appear to utilize As(III) as an electron donor for respiration, suggesting that As(III) oxidation may be incidental or a form of detoxification in these strains (Anderson et al. 1992; Ellis et al., 2001; Salmassi et al. 2002). A diverse group of heterotrophic bacteria can utilize As(V) as a terminal electron acceptor for respiration. These organisms comprise members of the gamma-, delta-, and epsilon- *Proteobacteria*, gram-positive bacteria, thermophilic eubacteria, and *Crenarchaetoa* (Oremland and Stolz 2003). Most As(V)-respiring strains couple the oxidation of lactate to acetate to support As(V) reduction to As(III) (Table

2.1), although some isolates can mineralize acetate to CO_2 (Macy et al. 1996) and/or use H_2 as an electron donor (Huber et al. 2000). While most known As(V) respirers are obligate anaerobes, a few are facultative aerobes, and one, *Shewanella* species strain ANA-3, has been particularly useful in genetic studies.

Metabolism	Reaction	Genes
Lactate-mediated arsenate reduction	$CH_3CHOHCOO^- + 2HAsO_4^{2-} + 3H^+ \rightarrow CH_3COO^- + 2HAsO_2 + 2H_2O + HCO_3^-$	*arrA, arrB*
Acetate-mediated arsenate reduction	$CH_3COO^- + 4HAsO_4^{2-} + 7H^+ \rightarrow 2HCO_3^- + 4HAsO_2 + 4H_2O$	*arrA, arrB*
Nitrate-dependent arsenite oxidation	$HAsO_2 + NO_3^- + H_2O \rightarrow HAsO_4^{2-} + NO_2^- + 2H^+$	None known
Oxygen-dependent arsenite oxidation	$2HAsO_2 + 2H_2O + O_2 \rightarrow 2HAsO_4^{2-} + 4H^+$	*aroA, aroB*

Table 2.1. Reactions catalyzed by As-metabolizing microorganisms.

2.3. Mechanisms of Bacterial As(V) Reduction and As(III) Oxidation

2.3.1. Detoxification: the *ars* system

As(V) enters Gram-negative cells through nonselective porins in the outer membrane. Because arsenate is an analog of phosphate, it is thought to enter into the cytoplasm mainly through the Pit phosphate transport system, a low affinity-high velocity system (Silver et al. 1981). *E. coli* that rely on the Pit system cannot grow in the presence of 10 mM arsenate, whereas *pit* mutants that rely on the Pst phosphate transport system—which has a higher affinity for phosphate than the Pit system—can grow (Willsky and Malamy 1980). Once As(V) enters the cells, it uncouples oxidative phosphorylation and inhibits ATP synthesis. In contrast, As(III) appears to enter the cell through aquaglyceroporins (Rosen 2002), one of which, GlpF, was identified in a screen for genes responsible for antimonite [Sb(III)] sensitivity (Sanders et al. 1997). As(III) is much more toxic than As(V) due to its strong affinity for sulfhydryl groups in proteins (Oremland and Stolz 2003). Paradoxically, although As(III) is more toxic than As(V), As(V) reduction to As(III) may provide cells with an advantage in exporting As (Silver et al. 2002).

The most well-studied As detoxification system involves the *ars* operon from *E. coli* plasmid R773 (Hedges and Baumberg 1973). This operon encodes five genes, *arsRDABC*, that are cotranscribed from one promoter region. *arsR* and *arsD* encode two regulatory elements. *arsR* encodes a helix-turn-helix repressor that binds the operator

region of the *ars* operon as a dimer until As(III) or Sb(III) binds to it and induces its release (Wu and Rosen 1991; Xu et al. 1996). *arsD* is believed to be a trans-acting inducer-independent secondary regulator (Wu and Rosen 1993). It is expressed in the presence of As(III), and has no effect on the expression of the operon when ArsR is repressing the system (Wu and Rosen 1993). *arsA* encodes a membrane-associated ATPase subunit that interacts with the *arsB* gene product (Tisa and Rosen 1990; Kaur and Rosen 1992). ArsB is the efflux pump responsible for the extrusion of As(III) and Sb(III). Interestingly, in association with ArsA, it uses the energy from ATP hydrolysis for this function, however, when ArsA is not present, ArsB is still functional (Dey and Rosen 1995). *arsC* encodes a small cytoplasmic arsenate reductase.

Not every *ars* operon contains these five genes, however. Most of the operons identified in bacteria contain only three genes, *arsRBC*. In addition, although almost all of the operons contain the small As(V) reductase encoded by *arsC*, two distinct families of these reductases exist. The *E. coli* ArsC receives reducing equivalents from glutathione and glutaredoxin (Shi et al. 1999) whereas the *S. aureus* ArsC receives them from thioredoxin (Ji and Silver 1992). Structural studies of ArsC from *Bacillus subtilis*, which shares 65% identity with the *S. aureus* ArsC, revealed its similarity to low molecular weight tyrosine phosphatases, both of which rely on three conserved cysteines to carry out their redox chemistry (Bennett et al. 2001). Additional genes, such as *arsH* from *Yersinia* (Neyt et al. 1997) and ORF2 from *Bacillus subtilis* (Sato and Kobayashi 1998) have been identified in *ars* operons, and sometimes *arsB* and *arsH* are transcribed in the opposite direction, suggesting complex regulation (Butcher et al. 2000). A wide

variety of bacteria have been found to contain *ars* operons on their chromosomes (Sofia et al. 1994; Sato and Kobayashi 1998; Butcher et al. 2000).

2.3.2. As(III) Oxidation and As(V) Respiration

2.3.2.1. The DMSO Reductase Family

The key enzymes involved in arsenite oxidation and respiratory arsenate respiration belong to the DMSO reductase family. Enzymes in this family (Kisker et al. 1997; Romao et al. 1997) rely on a molybdenum (Mo) atom or a tungsten (W) atom to carry out two-electron redox reactions. These enzymes are found in a variety of bacteria, often serving as an oxidase or a terminal reductase in the electron transport chain. The Mo or W atom is coordinated to two molybdopterin guanine dinucleotide (MGD) cofactors arbitrarily named the P-pterin and the Q-pterin. These cofactors lie antiparallel to one another in the center of the roughly spherical enzyme. This configuration positions the transition metal atom at the bottom of a funnel-shaped active site (41 x 33 x 25 Å in the DMSO reductase) where electron transfer with the substrate takes place. Typically, the Mo or W atom is coordinated to three dithiolene sulfurs of the pterin groups and one amino acid, either serine, cysteine, or selenocysteine, in the polypeptide. The MGD-containing subunit is organized into four domains. Together, domains I-III create the active site, and domains II and III are structurally symmetrical and form the two sides of the funnel. Domain IV is between domains II and III on the opposite side of the funnel. These enzymes may or may not have an iron sulfur cluster associated with

them. And, in DMSO reductase, a disordered region containing one Trp residue is predicted to form a lid that can shield the active site (Schindelin et al. 1996).

2.3.2.2. As(III) Oxidation: the *aox* and *aro* system

The arsenite oxidase was first purified from *Alcaligenes faecalis* (Anderson et al. 1992). This enzyme was identified as an 85 kDa monomer containing Mo, Fe, and inorganic sulfide. Native azurin and a *c*-type cytochrome, both periplasmic proteins, served as electron acceptors for the enzyme, and a K_m of 8 µM As(III) was measured in kinetic studies. The crystal structure of the *A. faecalis* arsenite oxidase heterodimer was determined to 1.64 Å resolution (Ellis et al. 2001). Studies of the presumed active site revealed that, unlike other members of the DMSO reductase family, the arsenite oxidase does not have a polypeptide ligand to the Mo. However, other structural features of the DMSO family are conserved.

Transposon mutagenesis in strain ULPAs1 (Weeger et al. 1999), a chemoorganotrophic member of the ß-*Proteobacteria*, identified two genes, *aoxA* and *aoxB*, required for As(III) oxidation (Muller et al. 2003). Protein purification and N-terminal sequencing allowed the identification of another pair of As(III) oxidoreductase genes (*aroA* and *aroB*) from strain NT-26, a chemolithoautotrophic As(III)-oxidizing bacterium. Deletion of *aroA* resulted in the loss of As(III) oxidation and the ability to grow chemoautotrophically with arsenite (Santini and vanden Hoven 2004). *aroA* is 48% identical at the amino acid level to *aoxB*, and *aroB* is 52% identical to *aoxA*. Translated sequences of these genes share high identity with proteins from *A. faecalis* and putative

proteins from the archaea *Aeropyrum pernix* and *Sulfolobus tokodaii* and the phototroph, *Chloroflexus aurantiacus*.

Subunit stoichiometry among the arsenite oxidases may vary. The purified oxidase from NT-26 has a native molecular mass of 219 kDa, suggesting an $\alpha_2ß_2$ configuration. Additionally, in *Hydrogenophaga* sp. str. NT-14, the membrane-associated arsenite oxidase consists of two subunits of molecular mass 86 and 16 kDa while having a native molecular mass of 306 kDa, suggesting an $\alpha_3ß_3$ configuration (vanden Hoven and Santini 2004).

The regulation of *aoxAB* was studied in *A. tumefaciens*. RT-PCR experiments determined that, in addition to being upregulated by As(III) and AoxR, in the absence of As(III), *aoxAB* was upregulated in late stationary phase or in the presence of supernatants from late stationary phase cultures, implying that regulation is partially controlled by quorum sensing (Kashyap et al. 2006).

2.3.2.3. Respiratory As(V) Reduction: the *arr* system

Recently, our laboratory established a genetic system in *Shewanella* species strain ANA-3 (Saltikov et al. 2003) that led to the discovery that this organism has two independent systems for reducing As(V) (Figure 2.1.). The first system belongs to the *ars* detoxification family, and is not required for anaerobic respiration, although it provides an advantage at high arsenic concentrations (Saltikov et al. 2003). The second system comprises two genes, *arrA* and *arrB*, required for respiratory arsenate reduction. The operon encoding these genes is proximal to the *ars* operon on the chromosome, but

is divergently transcribed (Saltikov and Newman 2003). These genes appear to be under the control of a promotor that senses anaerobiosis, arsenate, and arsenite (Saltikov et al. 2005). Additionally, the sequence region at the start of the *arrA* gene contains a putative twin arginine signal sequence (TAT) known to be involved in Sec-independent transport of folded proteins with metal cofactors, suggesting that the *arr* genes are translocated to the periplasm. The *arrA* gene has a cysteine rich motif that typically binds iron sulfur clusters and a canonical molybdopterin binding domain. *arrB* is downstream of *arrA* and its translated product is predicted to be similar to proteins that contain iron sulfur clusters. c-type cytochromes have recently been shown to be involved in the electron transport pathway to As(V) in strain ANA-3. Our current model of the respiratory complex is that it interacts with a CymA homolog in ANA-3, and genetic studies reveal that *cymA* is required for As(V) respiration (Murphy and Saltikov 2007) (Figure 2.2.).

Figure 2.1. As(V) reduction genes from *Shewanella* sp. strain ANA-3.

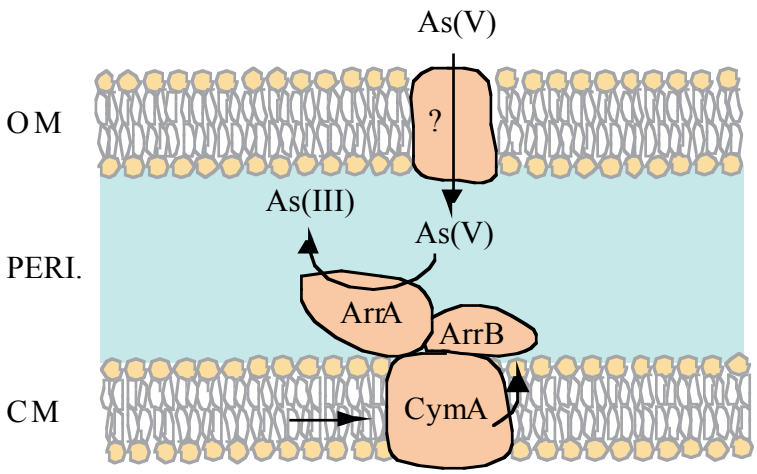

Figure 2.2. Cartoon drawings of a model pathway showing the major components involved in electron transfer for As(V) reduction by *Shewanella* sp. strain ANA-3. The arrows between the components point in the direction of electron flow from reductant to oxidant. The question mark indicates an unidentified porin.

ARR has been purified natively from two distantly related bacteria, *Chrysiogenes arsenatis* (Krafft and Macy 1998) and *Bacillus selenitireducens* (Afkar et al. 2003). In both cases, the enzyme was isolated as a heterodimer consisting of a larger A subunit and a smaller B subunit. In *C. arsenatis*, ARR is localized the periplasmic space. It has a K_m of 0.3 mM and a V_{max} of 7,013 µmol As(V) reduced · min^{-1} · mg $protein^{-1}$. Molybdenum, iron, acid-labile sulfur, and zinc were all found to be associated with the enzyme. The arsenate reductase from *B. selenitireducens* was only solubilized in the presence of detergent, suggesting that it is associated with the cell membrane. It has a K_m of 34 µM and a V_{max} of 2.5 µmol As(V) reduced · min^{-1} · mg $protein^{-1}$. Optimal activity of this enzyme was found at pH 9.5 and 150 g per L of NaCl. And, unlike the enzyme from *C.*

arsenatis, the enzyme from *B. selenitireducens* was also able to reduce arsenite, selenate, and selenite. Molybdenum and iron were present at low levels, possibly due to loss of metal during purification. Further biochemical and structural studies have not been performed.

2.4. Bacterial Contributions to Arsenic Mobilization

Arsenic-transforming microbes are known to contribute in large part to arsenic speciation in some environments (Cullen and Reimer 1989; Newman et al. 1998; Oremland and Stolz 2003). In particular, As(V) respiration has been a central focus because of its ability to convert the sequestered form of arsenic to the more dangerous As(III).

Evidence of bacterial dissimilatory arsenate reduction in the environment was discovered over a decade ago (Dowdle et al. 1996). Anoxic sediment from a San Francisco Bay salt marsh in Palo Alto, California revealed arsenate reduction capacity in the absence of oxygen. Addition of nitrate, another potential electron acceptor that provides more energy than arsenate, was shown to inhibit arsenate reduction. The addition of electron donors such as lactate and glucose increased the rates, whereas addition of antibiotics or respiratory inhibitors/uncouplers including rotenone, dinitrophenol, and cyanide inhibited reduction.

The environmental occurance of arsenate respiration can contribute significantly to carbon cycling. In Mono Lake, California, arsenate respiration may account for as much as 14.2% of total carbon mineralization in the stratified region of the lake during

meromixis (Oremland et al. 2000). Radioassays determined that rates of arsenate reduction in this alkaline, hypersaline environment reached 5.9 μmol/L per day. The contribution of arsenate reduction to carbon cycling was second only to sulfate reduction, which accounted for approximately 23.8-41.2% carbon mineralization.

The role of arsenate respiration for mobilization of arsenic in the environment has been investigated in several studies. Incubation of anoxic sediments from the Halls Brook Storage Area (affiliated with the Aberjona Watershed near Boston, MA) with ferric arsenate ($FeAsO_4 \cdot 2H_2O$) or ferrous arsenate ($Fe_3(AsO_4)_2$) revealed arsenate reduction capacity, resulting in an increase in aqueous As(III) that could be inhibited by formaldehyde (Ahmann et al. 1997). Incubation of ferrous arsenate with a pure arsenate respiring culture MIT-13 (Ahmann et al. 1994) also showed reduction and dissolution of arsenate in the form of arsenite, and when MIT-13 was mixed with sterilized contaminated sediment, the same observation was shown. Microcosm experiments with Bengal delta sediments incubated in simulated groundwater amended with acetate also showed an increase is aqueous arsenite.

The fate of arsenic is not solely dependent on its redox state, however. The sediment mineralogy on which the arsenic is sorbed also determines its partitioning. Because of its vast abundance and because both As(V) and As(III) adsorb onto $Fe(OH)_3$, the fate of As is often linked to that of Fe (Figure 2.3.). Microbes that reduce Fe(III) to Fe(II) have been studied on an environmental, physiological, and molecular level. The largest contributors to iron geochemistry are thought to be dissimilatory iron reducers (Lovley 1993). This group couples iron reduction to the oxidation of organic carbon sources such as acetate and lactate, requiring enzymes such as c-type cytochromes

localized to the outer membrane. Studies with *Shewanella alga* strain BrY, a model organism for dissimilatory iron reduction, showed that it is able to mobilize arsenate from scorodite ($FeAsO_4 \cdot 2H_2O$) and As(V) sorbed to sediments (Cummings 1999).

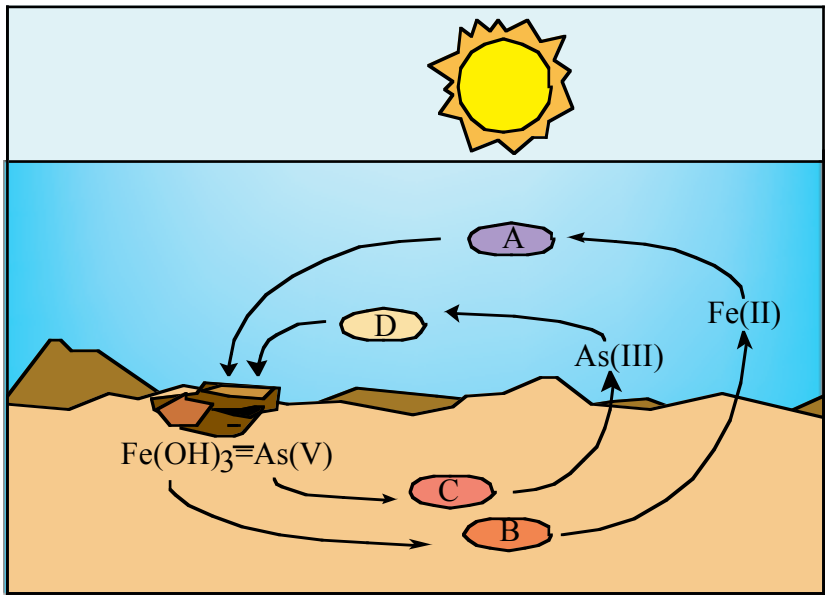

Figure 2.3. Simplified cartoon of the Fe-As biogeochemical cycle, showing the effect of representative microbial processes that either oxidize or reduce metal(loids). The speciation of Fe and As are neglected (with the exception of $Fe(OH)_3$), and only the dominant oxidation states are represented. The organism labeled "A" catalyzes Fe(II) oxidation through a light-dependent process (i.e. Fe(II)-based photoautotrophy). This results in the conversion of soluble Fe(II) to $Fe(OH)_3$, which is re-reduced by the activity of Fe(III)-respiring microorganisms (labeled "B"). As(V) as well as As(III) strongly adsorb onto $Fe(OH)_3$. Because of this, Fe(III)-reducing bacteria can affect As biogeochemistry by catalyzing the release of As(V) from $Fe(OH)_3$, making it more available for reduction by As(V)-reducing bacteria (labeled "C"). As(V)-reducers, in turn, can promote the release of As(III) into the water column if $Fe(OH)_3$ is not abundant. Finally, the As biogeochemical cycle is completed by As(III)-oxidizing bacteria (labeled "D") that convert As(III) to As(V) coupled to the reduction of oxygen or nitrate.

2.5. Dissecting the Network of Active Microbial Metabolism *in situ*

With the complex combination of microbial metabolisms present and potentially active in nature, predicting the role of each reaction and its impact on As mobilization is an important challenge.

The relative contributions of bacterial arsenate reduction and iron reduction to arsenic mobilization are determined, in part, by the mineralogy present in the environment. Geochemical studies in Bangladesh suggest that the source of arsenic in drinking water originates from surficial sediments that mostly consist of iron (hydr)oxides (Polizzotto et al. 2005). In this setting, both iron and arsenate reduction, along with the oxidation of arsenic-bearing sulfides during dry seasons, mobilize arsenic from these surface sediments and allow it to get transported to the deeper aquifers where well water is drawn. Mineralogical studies at well depth in Bangladesh (~30 m), corresponding also to the highest concentration of aqueous arsenic, reveal only low levels of Fe(III) (hydr)oxides. Here, the majority of arsenic partitioning is determined by silicate and carbonate minerals, both of which interact only weakly with arsenic and displace it even in the presence of deionized water. Thus, the upstream reduction of arsenate and iron mobilizes arsenic that then gets transported to well-depth where sorption is less efficient.

In California, Haiwee Reservoir is the site of deposition of As(V)-sorbed iron hydroxides resulting from water treatment. Naturally occuring arsenic is removed from

water by the addition of ferric chloride, which precipitates at the inlet channel of Haiwee due to decreased water flow. Characterization of the pore water in these anoxic sediments shows a correlated increase in dissolved iron and arsenic concentrations with depth (Kneebone et al. 2002). XANES spectra show that sediments are composed mainly of arsenite below 2.5 cm depth, revealing that the original arsenate is reduced. To test if the reduction was due to microbial activity, microcosm studies of these sediments were performed. Reduction of arsenate was observed, but, unlike in the porewater studies, iron reduction and arsenate reduction were not coupled, suggesting that one metabolism might be more important than another. Addition of antibiotics to these samples partially inhibited arsenate mobilization, suggesting that the effect was biological, but the inhibition was not complete and the effect of the antibiotics was not completely known.

Characterizing the contribution of each of the microbial metabolisms involved in As mobilization is further complicated by the fact that several of the isolated arsenate-respiring strains are found alongside microbes that are capable of other forms of respiration such as iron respiration, or they themselves are capable of respiring on other alternative electron acceptors (Newman et al. 1997; Huber et al. 2000; Macy et al. 2000; Niggemyer et al. 2001; Liu et al. 2004; Santini et al. 2004). The predominance of these different pathways seems to be controlled by the amount of energy that can be harvested from each available electron acceptor (Dowdle et al. 1996; Harvey et al. 2002). However, the differential localization of enzymes, kinetic factors, and signals involved in gene expression must also play a role. Enzymes located at the periphery of cells may be able to access substrates before more internally localized enzymes can. Or, enzymes with faster turnover rates may be preferred over slower enzymes. Because of the metabolic

diversity present in these organisms, laboratory studies of isolated metabolisms such as As(V) respiration are necessary but not completely sufficient. Linking laboratory studies to real-world conditions requires the exploration of molecular tools to identify As(V)-respiratory activity *in situ* and an understanding of the environmental conditions that determine when this metabolism is upregulated on a transcriptional and post-transcriptional level. Studies of interactions between simultaneously occuring metabolic reactions such as As(V) respiration and Fe(III) reductive dissolution are also necessary.

2.6. References

Afkar, E., J. Lisak, et al. (2003). "The respiratory arsenate reductase from *Bacillus selenitireducens* strain MLS10." FEMS Microbiol Lett **226**(1): 107-12.

Ahmann D, K. L., Hemond HF, Lovley DR, Morel FMM (1997). "Microbial mobilization of arsenic from sediments of the Aberjona Watershed." Environ Sci Technol **31**(10): 2923-30.

Ahmann, D., A. L. Roberts, et al. (1994). "Microbe grows by reducing arsenic." Nature **371**(6500): 750.

Anderson, G. L., J. Williams, et al. (1992). "The purification and characterization of arsenite oxidase from *Alcaligenes faecalis*, a molybdenum-containing hydroxylase." J Biol Chem **267**(33): 23674-82.

Armienta, M. A., G. Villasenor, et al. (2001). "The role of arsenic-bearing rocks in groundwater pollution at Zimapan Valley, Mexico." Environ Geol **40**(4-5): 571-81.

Aterman, K. (1999). "From Horus the child to Hephaestus who limps: a romp through history." Am J Med Genet **83**(1): 53-63.

Bennett, M. S., Z. Guan, et al. (2001). "Bacillus subtilis arsenate reductase is structurally and functionally similar to low molecular weight protein tyrosine phosphatases." Proc Natl Acad Sci U S A **98**(24): 13577-82.

Broer, S., G. Ji, et al. (1993). "Arsenic efflux governed by the arsenic resistance determinant of *Staphylococcus aureus* plasmid pI258." J Bacteriol **175**(11): 3480-5.

Butcher, B. G., S. M. Deane, et al. (2000). "The chromosomal arsenic resistance genes of *Thiobacillus ferrooxidans* have an unusual arrangement and confer increased arsenic and antimony resistance to *Escherichia coli*." Appl Environ Microbiol **66**(5): 1826-33.

Cullen, W. R. and K. J. Reimer (1989). "Arsenic Speciation in the Environment." Chemical Reviews **89**(4): 713-764.

Cummings DE, C. F., Fendorf S, Rosenzweig RF (1999). "Arsenic mobilization by the dissimilatory Fe(III)-reducing bacterium *Shewanella alga* BrY." Environ Sci Technol **33**(5): 723-29.

Dey, S. and B. P. Rosen (1995). "Dual mode of energy coupling by the oxyanion-translocating ArsB protein." J Bacteriol **177**(2): 385-9.

Dowdle, P. R., A. M. Laverman, et al. (1996). "Bacterial Dissimilatory Reduction of Arsenic(V) to Arsenic(III) in Anoxic Sediments." Appl Environ Microbiol **62**(5): 1664-1669.

Ellis, P. J., T. Conrads, et al. (2001). "Crystal structure of the 100 kDa arsenite oxidase from *Alcaligenes faecalis* in two crystal forms at 1.64 A and 2.03 A." Structure (Camb) **9**(2): 125-32.

Francesconi, K. A. and D. Kuehnelt (2002). Arsenic Compounds in the Environment. Environmental Chemistry of Arsenic. J. Frankenberger, W. T. New York, Basel, Marcel Dekker, Inc.**:** 51-94.

Gihring, T. M. and J. F. Banfield (2001). "Arsenite oxidation and arsenate respiration by a new *Thermus* isolate." FEMS Microbiol Lett **204**(2): 335-40.

Harvey, C. F., C. H. Swartz, et al. (2002). "Arsenic mobility and groundwater extraction in Bangladesh." Science **298**(5598): 1602-6.

Hedges, R. W. and S. Baumberg (1973). "Resistance to arsenic compounds conferred by a plasmid transmissible between strains of *Escherichia coli*." J Bacteriol **115**(1): 459-60.

Huber, R., M. Sacher, et al. (2000). "Respiration of arsenate and selenate by hyperthermophilic archaea." Syst Appl Microbiol **23**(3): 305-14.

Ilyaletdinov, A. N. and S. A. Abdrashitova (1981). "Autotrophic oxidation of arsenic by a culture of *Pseudomonas arsenitoxidans*." Microbiology **50**(2): 135-140.

Ji, G. and S. Silver (1992). "Reduction of arsenate to arsenite by the ArsC protein of the arsenic resistance operon of *Staphylococcus aureus* plasmid pI258." Proc Natl Acad Sci U S A **89**(20): 9474-8.

Kashyap, D. R., L. M. Botero, et al. (2006). "Complex regulation of arsenite oxidation in *Agrobacterium tumefaciens*." J Bacteriol **188**(3): 1081-8.

Kaur, P. and B. P. Rosen (1992). "Plasmid-encoded resistance to arsenic and antimony." Plasmid **27**(1): 29-40.

Kisker, C., H. Schindelin, et al. (1997). "Molybdenum-cofactor-containing enzymes: structure and mechanism." Annu Rev Biochem **66**: 233-67.

Klein, C. (2002). Mineral Science. New York, John Wiley and Sons, Inc.

Kneebone, P. E., P. A. O'Day, et al. (2002). "Deposition and fate of arsenic in iron- and arsenic-enriched reservoir sediments." Environ Sci Technol **36**(3): 381-6.

Krafft, T. and J. M. Macy (1998). "Purification and characterization of the respiratory arsenate reductase of *Chrysiogenes arsenatis*." Eur J Biochem **255**(3): 647-53.

Liu A, G.-D. E., Rhine ED, Young LY (2004). "A novel arsenate respiring isolate that can utilize aromatic substrates." FEMS Microbiol Eco **48**(3): 323-32.

Lovley, D. R. (1993). "Dissimilatory metal reduction." Annu Rev Microbiol **47**: 263-90.

Macur, R. E., C. R. Jackson, et al. (2004). "Bacterial populations associated with the oxidation and reduction of arsenic in an unsaturated soil." Environ Sci Technol **38**(1): 104-11.

Macy, J. M., K. Nunan, et al. (1996). "*Chrysiogenes arsenatis* gen nov, sp nov; a new arsenate-respiring bacterium isolated from gold mine wastewater." International Journal of Systematic Bacteriology **46**(4): 1153-1157.

Macy, J. M., J. M. Santini, et al. (2000). "Two new arsenate/sulfate-reducing bacteria: mechanisms of arsenate reduction." Arch Microbiol **173**(1): 49-57.

Mazumder, D. N., J. Das Gupta, et al. (1998). "Chronic arsenic toxicity in west Bengal--the worst calamity in the world." J Indian Med Assoc **96**(1): 4-7, 18.

Mobley, H. L., C. M. Chen, et al. (1983). "Cloning and expression of R-factor mediated arsenate resistance in *Escherichia coli*." Mol Gen Genet **191**(3): 421-6.

Muller, D., D. Lievremont, et al. (2003). "Arsenite oxidase aox genes from a metal-resistant beta-proteobacterium." J Bacteriol **185**(1): 135-41.

Murphy, J. N. and C. W. Saltikov (2007). "The cymA gene encoding a tetraheme c-type cytochrome is required for arsenate respiration in *Shewanella* species." J Bacteriol.

Newman, D. K., D. Ahmann, et al. (1998). "A Brief Review of Microbial Arsenate Respiration." Geomicrobiology **15**: 255-68.

Newman, D. K., E. K. Kennedy, et al. (1997). "Dissimilatory arsenate and sulfate reduction in Desulfotomaculum auripigmentum sp. nov." Arch Microbiol **168**(5): 380-8.

Newman, D. K. and R. Kolter (2000). "A role for excreted quinones in extracellular electron transfer." Nature **405**(6782): 94-7.

Neyt, C., M. Iriarte, et al. (1997). "Virulence and arsenic resistance in *Yersiniae*." J Bacteriol **179**(3): 612-9.

Nickson, R., J. McArthur, et al. (1998). "Arsenic poisoning of Bangladesh groundwater." Nature **395**(6700): 338.

Niggemyer, A., S. Spring, et al. (2001). "Isolation and characterization of a novel As(V)-reducing bacterium: implications for arsenic mobilization and the genus *Desulfitobacterium*." Appl Environ Microbiol **67**(12): 5568-80.

Nriagu, J. (2002). Arsenic poisoning through the ages. Environmental Chemistry of Arsenic. J. Frankenberger, W. T. New York, Basel, Marcel Dekker, Inc.**:** 1-26.

Oremland, R. S., P. R. Dowdle, et al. (2000). "Bacterial dissimilatory reduction of arsenate and sulfate in meromictic Mono Lake, California." Geochimica et Cosmochimica Acta **64**(18): 3073-3084.

Oremland, R. S., S. E. Hoeft, et al. (2002). "Anaerobic oxidation of arsenite in Mono Lake water and by facultative, arsenite-oxidizing chemoautotroph, strain MLHE-1." Appl Environ Microbiol **68**(10): 4795-4802.

Oremland, R. S. and J. F. Stolz (2003). "The ecology of arsenic." Science **300**(5621): 939-44.

Philips, S. E. and M. L. Taylor (1976). "Oxidation of arsenite to arsenate by *Alcaligenes faecalis*." Appl Environ Microbiol **32**(3): 392-9.

Polizzotto, M. L., C. F. Harvey, et al. (2005). "Processes conducive to the release and transport of arsenic into aquifers of Bangladesh." Proc Natl Acad Sci U S A **102**(52): 18819-23.

Romao, M. J., J. Knablein, et al. (1997). "Structure and function of molybdopterin containing enzymes." Prog Biophys Mol Biol **68**(2-3): 121-44.

Rosen, B. P. (2002). "Transport and detoxification systems for transition metals, heavy metals and metalloids in eukaryotic and prokaryotic microbes." Comp Biochem Physiol A Mol Integr Physiol **133**(3): 689-93.

Salmassi, T. M., K. Venkateswaran, et al. (2002). "Oxidation of arsenite by *Agrobacterium albertimagni*, AOL15, sp nov., isolated from Hot Creek, California." Geomicrobiology Journal **19**(1): 53-66.

Saltikov, C. W., A. Cifuentes, et al. (2003). "The ars detoxification system is advantageous but not required for As(V) respiration by the genetically tractable *Shewanella* species strain ANA-3." Appl Environ Microbiol **69**(5): 2800-9.

Saltikov, C. W. and D. K. Newman (2003). "Genetic identification of a respiratory arsenate reductase." Proc Natl Acad Sci U S A **100**(19): 10983-8.

Saltikov, C. W., R. A. Wildman, Jr., et al. (2005). "Expression dynamics of arsenic respiration and detoxification in *Shewanella* sp. strain ANA-3." J Bacteriol **187**(21): 7390-6.

Sanders, O. I., C. Rensing, et al. (1997). "Antimonite Is acculmulated by the glycerol facilitator GlpF in *Escherichia coli*." J Bacteriol **179**(10): 3365-3367.

Santini, J. M., L. I. Sly, et al. (2000). "A new chemolithoautotrophic arsenite-oxidizing bacterium isolated from a gold mine: phylogenetic, physiological, and preliminary biochemical studies." Appl Environ Microbiol **66**(1): 92-7.

Santini, J. M., I. C. Streimann, et al. (2004). "*Bacillus macyae* sp. nov., an arsenate-respiring bacterium isolated from an Australian gold mine." Int J Syst Evol Microbiol **54**(Pt 6): 2241-4.

Santini, J. M. and R. N. vanden Hoven (2004). "Molybdenum-containing arsenite oxidase of the chemolithoautotrophic arsenite oxidizer NT-26." J Bacteriol **186**(6): 1614-9.

Sato, T. and Y. Kobayashi (1998). "The *ars* operon in the skin element of *Bacillus subtilis* confers resistance to arsenate and arsenite." J Bacteriol **180**(7): 1655-61.

Schindelin, H., C. Kisker, et al. (1996). "Crystal structure of DMSO reductase: redox-linked changes in molybdopterin coordination." Science **272**(5268): 1615-21.

Senn, D. B. and H. F. Hemond (2002). "Nitrate controls on iron and arsenic in an urban lake." Science **296**(5577): 2373-6.

Shi, J., A. Vlamis-Gardikas, et al. (1999). "Reactivity of glutaredoxins 1, 2, and 3 from *Escherichia coli* shows that glutaredoxin 2 is the primary hydrogen donor to ArsC-catalyzed arsenate reduction." J Biol Chem **274**(51): 36039-42.

Silver, S., K. Budd, et al. (1981). "Inducible plasmid-determined resistance to arsenate, arsenite, and antimony (III) in *Escherichia coli* and *Staphylococcus aureus*." J Bacteriol **146**(3): 983-96.

Silver, S., L. T. Phung, et al. (2002). Arsenic Metabolism: Resistance, Reduction, and Oxidation. Environmental Chemistry of Arsenic. J. Frankenberger, W. T. New York, Basel, Marcel Dekker, Inc.**:** 247-272.

Sofia, H. J., V. Burland, et al. (1994). "Analysis of the *Escherichia coli* genome. V. DNA sequence of the region from 76.0 minutes to 81.5 minutes." Nucleic Acids Research **22**(13): 2576-2586.

Spliethoff, H. M. and H. F. Hemond (1996). "History of toxic metal discharge to surface waters of the Aberjona Watershed." Environ Sci Technol **30**(1): 121-28.

Tisa, L. S. and B. P. Rosen (1990). "Molecular characterization of an anion pump. The ArsB protein is the membrane anchor for the ArsA protein." J Biol Chem **265**(1): 190-4.

vanden Hoven, R. N. and J. M. Santini (2004). "Arsenite oxidation by the heterotroph *Hydrogenophaga* sp. str. NT-14: the arsenite oxidase and its physiological electron acceptor." Biochim Biophys Acta **1656**(2-3): 148-55.

Weeger, W., D. Lievremont, et al. (1999). "Oxidation of arsenite to arsenate by a bacterium isolated from an aquatic environment." Biometals **12**(2): 141-9.

Wilkie, J. A. and J. G. Hering (1998). "Rapid oxidation of geothermal arsenic(III) in streamwaters of the eastern Sierra Nevada." Environ Sci Technol **32**(5): 657-62.

Willsky, G. R. and M. H. Malamy (1980). "Characterization of two genetically separable inorganic phosphate transport systems in *Escherichia coli*." J Bacteriol **144**(1): 356-365.

World Health Organization. Environmental Health Criteria, No. 224: Arsenic. Environmental Health Criteria Series.

World Health Organization. (2000). Assessing Human Health Risks of Chemicals. Hazardous Chemicals in Human and Environmental Health, World Health Organization.

Wu, J. and B. P. Rosen (1991). "The ArsR protein is a trans-acting regulatory protein." Mol Microbiol **5**(6): 1331-6.

Wu, J. and B. P. Rosen (1993). "The *arsD* gene encodes a second trans-acting regulatory protein of the plasmid-encoded arsenical resistance operon." Mol Microbiol **8**(3): 615-23.

Xu, C., W. Shi, et al. (1996). "The chromosomal *arsR* gene of *Escherichia coli* encodes a trans-acting metalloregulatory protein." J Biol Chem **271**(5): 2427-32.

Chapter 3

arrA is a Reliable Marker for As(V)-respiration in the Environment

This chapter includes sections from:

Malasarn, D., C. W. Saltikov, K.M. Campbell, J. M. Santini, J. G. Hering, D. K. Newman. 2004. "*arrA* is a Reliable Marker for As(V)-respiration." Science 306: 455.

3.1. Abstract

Arsenate [As(V)]-respiring bacteria affect the speciation and mobilization of arsenic in the environment. This can lead to arsenic contamination of drinking water supplies and deleterious consequences for human health. Using molecular genetics, we show that the functional gene for As(V)-respiration, *arrA*, is highly conserved, that it is required for As(V) reduction to arsenite when arsenic is sorbed onto iron minerals and that it can be used to identify the presence and activity of As(V)-respiring bacteria in arsenic-contaminated iron-rich sediments. The expression of *arrA* thus can be used to monitor sites in which As(V)-respiring bacteria may be controlling arsenic geochemistry.

3.2. Introduction

The critical role microorganisms play in controlling the geochemistry of arsenic has become well-appreciated (Akai et al. 2004). Metabolic oxidation or reduction of arsenic affects its speciation and mobilization in a variety of low-temperature environments (Ahmann et al. 1997; Harrington et al., 1998; Oremland et al. 2000; Kneebone et al. 2002; Senn and Hemond 2002; Macur 2004). A well known example is the case of Bangladesh, where studies of arsenic fate and transport in aquifers have implicated microbial respiration in the release of arsenic into drinking water supplies (Akai et al. 2004; Harvey et al. 2002; Nickson et al. 1998) and exposure of millions of people to chronic arsenic poisoning (Smith et al. 2000). Arsenate [As(V)] respiration (i.e. the oxidation of organic carbon coupled to As(V) reduction to arsenite [As(III)]) is one of the microbial processes that can contribute to arsenic mobilization in Bangladesh and other environments throughout the world (Ahmann et al. 1997; Harrington et al. 1998; Oremland et al. 2000).

Historically, it has been difficult to assess the extent to which As(V)-respiring bacteria control the arsenic geochemistry of a particular environment due to the lack of a specific marker for this activity. Because the phylogenetic diversity of As(V)-respiring strains is enormous and this metabolic capability is not consistently present within any given clade (Oremland and Stolz 2003; Saltikov et al. 2003), taxonomic genes (e.g. the 16S ribosomal RNA gene) are ineffectual as molecular markers for this activity (Figure

3.1.A.). In light of this, we sought to determine whether a conserved functional gene for As(V) respiration could be used to detect As(V)-respiratory activity in the environment.

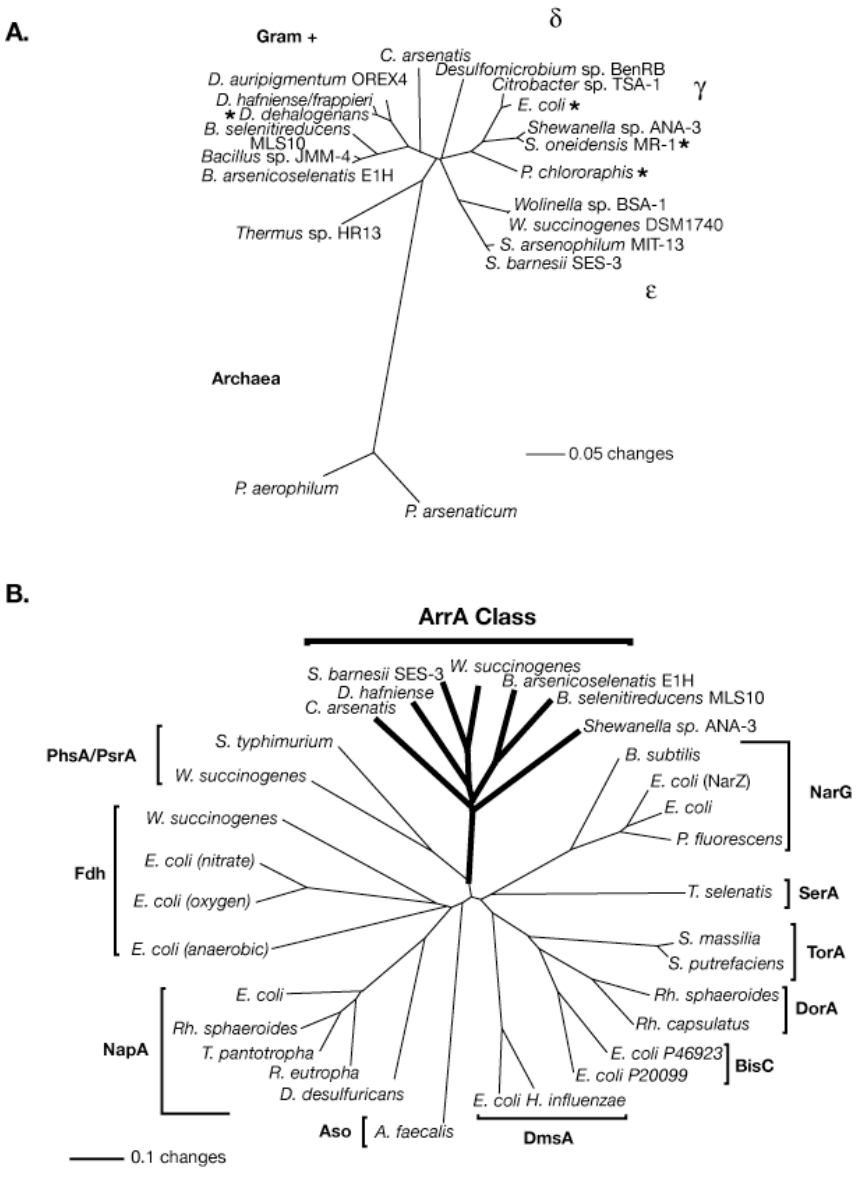

Figure 3.1. ArrA, the respiratory As(V) reductase, is highly conserved amongst a phylogenetically diverse group of As(V)-respiring microorganisms. A. Neighbor-joining tree showing the phylogenetic diversity of 16S rDNA sequences from strains used in this study. Strains marked with an asterisk cannot respire on As(V), and served as negative

controls in Figure 3.3. B. Phylogenetic diversity of ArrA and other members of the DMSO reductase family, showing that ArrA forms a unique branch within this family. Phs/Psr represent polysulfide reductases, Fdh: formate dehydrogenases, NapA and NarG: nitrate reductases, Aso: arsenite oxidase, DmsA and DorA: dimethyl sulfoxide reductase, BisC: biotin sulfoxide reductase, TorA: trimethylamine N-oxide reductase, and SerA: selenate reductase.

3.3. Materials and Methods

3.3.1. *arrA* sequences

Sequences for *C. arsenatis* were obtained by PCR amplification of genomic DNA using degenerate primers based on N-terminal sequencing (Macy et al. 1996). Primers used were CHArrAfwd (5'- GARGCNGARGGNAARTGGAT-3') and CHArrArev (5'-ATCCAYTTNCCYTCNGCYTC-3'). Sequences for *S. barnesii* and *B. arsenicoselenatis* were obtained by PCR amplification of genomic DNA using multiple sets of degenerate primers based on regions conserved among strain ANA-3, *B. selenitireducens*, and *D. hafniense* (Rose et al. 2003).

3.3.2. Phylogenetic tree generation

Figure 3.1.A.: 16SrDNA sequences were aligned using ClustalX and phylogenetic analyses were performed using PAUP* 4.0b10. 1,127 nucleotides were included in the phylogenetic analysis. Figure 3.1.B.: Phylogenetic analysis of ArrA was performed as previously described (Saltikov and Newman 2003). 463 amino acid residues were included in the phylogenetic analysis. Figure 3.5.A.: ArrAfwd and ArrA rev PCR product sequences were aligned using ClustalX and phylogenetic analyses were

performed using PAUP* 4.0b10. ~160-200 nucleotides were included in the phylogenetic analysis.

3.3.3. PCR using ArrAfwd and ArrArev.

Primer ArrAfwd anneals to the strain ANA-3 respiratory As(V) reductase gene from bp 869-902 while primer ArrArev anneals to the gene from bp 1015 to 1043 in the reverse direction. Together, these primers amplify a ~160-200 bp fragment that specifically identifies *arrA*. The degeneracy of these primers is 18 for ArrAfwd and 48 for ArrArev. The optimized PCR conditions include incubation at 95˚C for 10 minutes, followed by 40 cycles of 95˚C for 15 seconds, 50˚C for 40 seconds, and 72˚C for one minute. The concentration of each primer in a single reaction was 0.5 μM.

3.3.4. Heterologous Complementation Experiment

arrAB from *D. hafniense* was cloned into pBBR1-MCS2, creating pDHarrAB, and introduced into strain ANA-3Δ*arrA*. This heterologously complemented mutant was grown in arsenate medium alongside ANA-3 (WT) or *Shewanella* sp. strain ANA-3Δ*arrA* with vector only. Data are presented as the mean of three parallel samples with error bars showing the standard deviation.

3.3.5. Synthesis of As(V)-sorbed poorly crystalline iron hydroxide

$Fe(OH)_3$ was synthesized according to the protocol of Schwertmann and Cornell (Schwertmann and Cornell 1991). Briefly, 0.5 M NaOH was added to a 0.05 M $Fe(NO_3)_3$

solution to precipitate the iron hydroxide. The mineral was centrifuged at 7000 x g for 10 minutes and washed three times with sterile water. The mineral was then incubated overnight in a sterile 0.05 M As(V) solution to allow complete saturation of the iron surface sites. The specific surface area was assumed to be 600 m^2/g (Dzombak and Morel 1990), resulting in 0.0015 mol As(V)/g Fe. The mineral was washed, resuspended in anoxic medium containing 0.5 mM phosphate, 12.9 mM lactate and 50 mM bicarbonate buffer, divided into nine 200-mL aliquots and incubated for 24-36 hours at 30˚C to allow it to equilibrate with the medium. Total As(V) concentration was 2.6 mM or 0.0016 mol/g iron oxide, total Fe concentration was 24.3 mM, and each sample contained 2.1 g As(V)-sorbed iron oxide/liter. 10^5 cells were added to each sample at the start of the experiment.

3.3.6. Sampling during the time course experiment

At each time point, the samples were shaken in the chamber, and 4.02 mL were withdrawn with sterile pipettes for analysis. For nucleic acid extractions, 3 mL samples were centrifuged at 4˚C for ~5-10 minutes, then iron was dissolved by adding 0.3 M oxalic acid (pH=3) and mixed with the sample resting on ice. The samples were spun again to pellet the cells. The supernatant was removed and pellets were frozen at –80˚C until processing. Upon thawing, the samples were divided into two. RNA was extracted from one half of the sample using the TRIzol Reagent. Contaminating DNA was removed using the RQ1 DNase kit (Promega). Reverse transcription was performed using TaqMan Reverse Transcriptase Reagents (Applied Biosystems). DNA was

extracted from the other half using the DNeasy Tissue Kit (Qiagen). Quantitative PCR was performed on an Applied Biosystems 7300 Real Time PCR System. To determine gene expression, the absolute quantity, normalized by cell number, of the *arrA* fragment in the DNA and cDNA fraction was determined at each time point based on a standard curve. Data are presented as the ratio of cDNA quantity to DNA quantity. To confirm that the observed effect was not due to PCR inhibition by iron in samples taken after inoculation, known concentrations of DNA were added to the nucleic acid samples, and quantitative PCR was repeated. No inhibition was observed in RNA samples, and a constant level of inhibition was observed on all DNA samples, ruling out the possibility of PCR-bias. The PCR protocol was the same as described above with an additional 1 minute step at 60˚C added at the end of each cycle for measurement of fluorescence.

As(V), As(III), lactate and acetate were measured by high pressure liquid chromatography (HPLC) using a Hamilton PRP-X300 column in series with a Bio-Rad Aminex HPX-87H column. Both columns were heated to 50˚C and run at a rate of 0.6 mL/min with 30 mM phosphoric acid as the mobile phase. Samples were measured by UV absorbance at 210 nm.

Iron was measured using a Synergy HT Multi-Detection Microplate Reader using the ferrozine assay (Stookey 1970).

3.3.7. Nucleic acid extractions from Haiwee Reservoir

Total nucleic acid was extracted according to the protocol of Hurt et al. (Hurt et al. 2001) Briefly, ~2 g frozen sediment was amended with 1g sterile sand and 1 mL

denaturing solution. The sample was then frozen in liquid nitrogen and ground with a mortar and pestle. This was repeated three times. The sample was then moved to a conical tube and 9 mL extraction buffer was added. The sample was incubated at 65˚C for 30 minutes with occasional shaking followed by centrifugation at 1,800 x g for 10 minutes at 4˚C. The supernatant was removed and added to 20 mL of 24:1 chloroform-isoamyl alcohol. This was centrifuged again and the supernatant was transferred to a new conical tube. 0.6 volumes of isopropyl alcohol was added and the sample was incubated at room temperature for 30 minutes. The sample was centrifuged at 1,600 x g for 20 minutes at room temperature. The supernatant was removed, and the remaining nucleic acid pellet was resuspended in DEPC-treated water. RNA and DNA were separated with a Qiagen Tip 100 RNA-DNA purification system before performing DNase treatment, reverse transcription PCR, and/or PCR. Amplified fragments were TOPO-cloned and sequenced by Laragen using M13 forward primer.

For isolating As(V)-respiring strains, 5 mL of a cored Haiwee sediment slurry was inoculated into 125 mL bottles containing N_2-sparged enrichment medium consisting of the following in g/L: 1.5 NH_4Cl, 0.6 NaH_2PO_4, 0.1 KCl, and buffered with 10 mM HEPES at pH 7. The medium was supplemented with 20 mM sodium lactate, 10 mM Na_2HAsO_4, and 10 mL/L each of Wolfe's trace element and vitamin solutions. After several days of incubation at 30˚C, the enrichments were aseptically transferred to fresh anaerobic medium (10% inoculum) and incubated for 2 more days. The enrichments were plated on medium solidified with 2% agar and incubated either aerobically or anaerobically at 30˚C. Putative As(V)-respiring strains were confirmed to grow in the

presence of As(V) under anaerobic conditions, and one (HAR-4), was selected for further characterization.

3.4. Results and Discussion

3.4.1. Conservation of *arrA*

Recently, the *arrA* gene from the gram-negative γ-Proteobacterium*, Shewanella* species strain ANA-3, was shown to be required for respiratory As(V) reduction (Saltikov and Newman 2003). It is predicted to encode a large molybdenum-containing subunit of a respiratory As(V) reductase, and is 56.7% identical on a nucleotide level and 46% identical and 63% similar on an amino acid level to a homolog from the As(V)-respiring low-GC Gram-positive bacterium, *Bacillus selenitireducens* strain MLS10 (Saltikov and Newman 2003; Afkar et al. 2003). Given the high degree of conservation between *arrA* genes from such phylogenetically distant As(V)-respiring strains, we hypothesized that *arrA* might also be present and conserved in other As(V)-respiring bacteria.

BLAST (Altschul et al. 1990) searches using *arrA* from ANA-3 identified two additional gene sequences from *Desulfitobacterium hafniense* strain DCB-2 (low-GC Gram-positive) and *Wolinella succinogenes* (ε-Proteobacterium) that showed high amino acid similarity; both *D. hafniense* (Niggemyer et al. 2001) and *W. succinogenes* (Lovley et al. 1999) were previously identified as As(V)-respiring strains. To verify As(V)-reductase function, we cloned the *arrA* homolog from *D. hafniense* and used it to

complement a Δ*arrA* mutant of strain ANA-3 that cannot respire on As(V) (strain ANA-3Δ*arrA*), (Saltikov and Newman 2003). When provided with the *D. hafniense arrA* gene, strain ANA-3Δ*arrA* reduced 1.2 mM As(V) within 5 days and oxidized 0.79 mM lactate to acetate (Figure 3.2.). This 1.5:1 ratio of As(V) reduced to lactate oxidized, though less than the stoichiometric 2:1 ratio predicted by the equation $CH_3CHOHCOO^- + 2HAsO_4^{2-} + 3H^+ \rightarrow CH_3COO^- + 2HAsO_2 + 2H_2O + HCO_3^-$, was close to the 1.6:1 ratio observed with strain ANA-3. Cell number also doubled during this time, showing that the cells were using As(V) as the terminal electron acceptor for growth (data not shown). Strain ANA-3 reduced 8 mM As(V) in 5 days, which is significantly more than the complemented strain ANA-3Δ*arrA*, but the reduced efficiency of the *D. hafniense* reductase is not surprising because we would not expect it to interact as well as the native ArrA protein with the other components of the *Shewanella* respiratory chain.

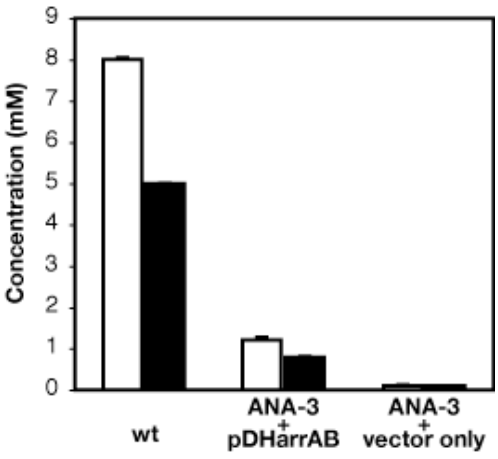

Figure 3.2. As(V) reduction (white) and acetate production (black) after 5 days by wild-type strain ANA-3, strain ANA-3Δ*arrA* with *arrAB* from *D. hafniense*, and strain ANA-3Δ*arrA* with vector only. Data is presented as the mean of three parallel samples with error bars showing the standard deviation.

We also obtained *arrA* gene sequence from *Chrysiogenes arsenatis* strain BAL-1 (the type strain of the phylum *Chrysiogenetes*) (Macy et al. 1996), *Sulfurospirillum barnesii* strain SES-3 (ε-Proteobacterium) (Laverman et al. 1995) and *Bacillus arsenicoselenatis* strain E1H (Gram-positive) (Blum et al. 1998). The seven sequences ranged from 43-100% identity at the nucleotide level and 47-100% identity and 61-100% similarity at the amino acid level. Additionally, biochemical and genetic studies confirmed that the gene sequences from strain ANA-3 (Saltikov and Newman 2003), *B. selenitireducens* (Afkar et al 2003), *D. hafniense* (this study) and *C. arsenatis* (Krafft and Macy 1998) could be associated with As(V) reductase activity. Alignment of these genes shows that they form a unique clade within the DMSO reductase family of molybdenum-containing enzymes, which includes other terminal reductases such as polysulfide reductase, nitrate reductase, formate dehydrogenase, and dimethyl sulfoxide reductase, among others (Figure 3.1.B.).

3.4.2. Design of degenerate primers

Because of the high degree of conservation within the ArrA protein subfamily, we designed degenerate PCR primers that would allow us to amplify a diagnostic region of *arrA* in any given As(V)-respiring bacterium, regardless of its phylogeny. All of the nearly complete *arrA* sequences were aligned using Clustal X and conserved regions were identified using Block Maker (Rose et al. 2003). Regions that shared similarity with other genes within the DMSO family were eliminated, and two of the remaining

three regions flanked a gene fragment of ~160-200 bp. From these two regions, we designed COnsensus-DEgenerate Hybrid Oligonucleotide Primers (CODEHOP) (Rose et al. 2003), ArrAfwd (5'-AAGGTGTATGGAATAAAGCGTTTgtbgghgaytt-3') and ArrArev (5'-CCTGTGATTTCAGGTGCCcaytyvggngt-3'), by inspection of the gene sequences.

To determine whether these primers would specifically amplify *arrA*, we tested them on 13 phylogenetically diverse As(V)-respiring bacteria, 1 As(V)-respiring archaeon, and 5 negative control strains that cannot respire As(V) but which possess other genes within the DMSO reductase family. Fragments ranging from ~160-200 bp were amplified from 12 of the 13 As(V)-respiring bacteria, while no fragments were amplified from the As(V)-respiring archaeon or negative control strains (Figure 3.3.). All positive fragments were sequenced to confirm amplification of the correct gene. The only As(V)-respiring bacterium that did not test positive in the PCR was *Desulfosporosinus auripigmentum* strain OREX-4 (Newman et al. 1997; Stackebrandt et al. 2003), which suggests the presence of a highly divergent gene, or possibly a novel system of respiration in this organism. The fact that every other As(V)-respiring bacterium tested positive indicates that ArrAfwd and ArrArev are reliable markers for the respiratory As(V)-reductase gene (i.e. *arrA*) for the majority of As(V)-respiring bacteria.

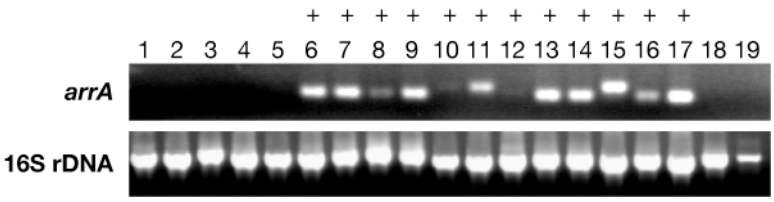

Figure 3.3. Degenerate primers specifically amplify *arrA* fragments. (Top row) PCR products from genomic DNA samples using primers ArrAfwd and ArrArev. Positive amplification by these primers is also marked by a "+" sign above the lane number. (Bottom row) PCR products from the same samples using universal 16S rDNA primers 8F and 1492R as positive controls. Lane designations: 1. *Shewanella* sp. strain ANA-3Δ*arrA*, 2. *S. oneidensis* strain MR-1, 3. *Desulfitobacterium dehalogenens* strain JW/IU-DC1, 4. *E. coil* strain DH10β, 5. *Pseudomonas chlororaphis* strain PCL1391, 6. *Shewanella* sp. strain ANA-3, 7. *D. hafniense* strain DCB-2, 8. *D. frappieri* strain PCP-1, 9. *D.* sp. strain GBFH, 10. *Wolinella* sp. strain BSA-1, 11. *W. succinogenes*, 12. *Citrobacter* sp. strain TSA-1, 13. *Bacillus arsenicoselenatis* strain E1H, 14. *B. selenitireducens* strain MLS10, 15. *Sulfurospirillum barnesii* strain SES-3, 16. *Shewanella* sp. strain HAR-4 (see Figure 3.5.B.), 17. *Chrysiogenes arsenatis* strain BAL1^T, 18. *Desulfosporosinus auripigmentum* strain OREX-4, 19. *Pyrobaculum arsenaticum*.

3.4.3. *arrA* expression dynamics in microcosm experiments

Having designed a specific set of primers for *arrA*, we could test the hypothesis that *arrA* is required for arsenic transformations under anaerobic conditions and that its expression is correlated with the reduction of As(V) in the environment. Because many sediments where arsenic-contamination is a problem are also iron-rich, we designed our first experiment to test this hypothesis using poorly crystalline ferric [Fe(III)] (hydr)oxide [$Fe(OH)_3$], which has been shown to be the most critical sedimentary phase in controlling arsenic mobility in a variety of locales, including sediments of the Haiwee Reservoir in

Olancha, CA, USA (Kneebone et al. 2002) and Bengal delta aquifers (Akai et al. 2004; Nickson et al. 1998). Accordingly, we prepared As(V)-saturated $Fe(OH)_3$ for experiments with strain ANA-3 and the mutant strain ANA-3Δ*arrA* (Schwertmann and Cornell 1991). Both strain ANA-3 and strain ANA-3Δ*arrA* are capable of respiratory Fe(III) reduction and As(V) reduction for the purpose of detoxification using the ArsC As(V) reductase, but only ANA-3 is capable of respiratory As(V) reduction using ArrA (Saltikov and Newman 2003). Over the course of 373 hours, *arrA* expression, organic substrate transformations, dissolved and total arsenic [As(V) + As(III)], and dissolved and total iron (Fe(III) + ferrous [Fe(II)]) were followed for both strains and an uninoculated control (Figure 3.4.A-F.).

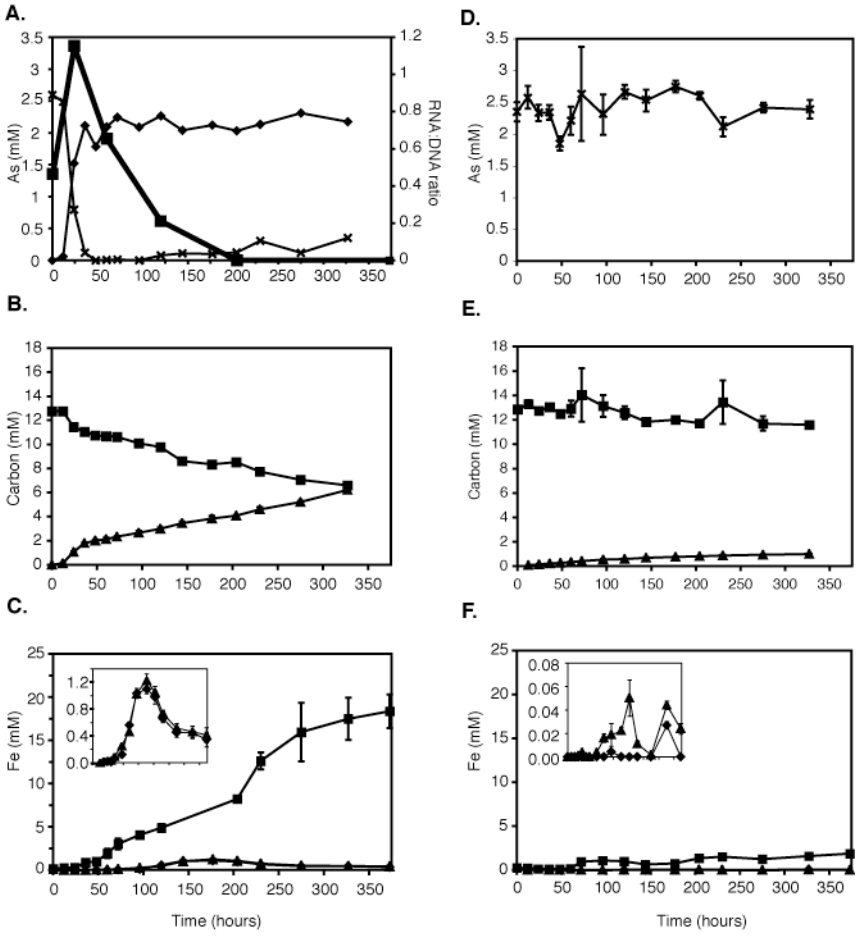

Figure 3.4. *arrA* is required for As(V) reduction to As(III) under anoxic conditions in which As(V) is sorbed onto $Fe(OH)_3$. Initial conditions: 12.9 mM lactate, 2.6 mM As(V), 24.3 mM total Fe(III) where all Fe(III) is present as 2.1 g/L $Fe(OH)_{3(s)}$ and all As(V) is sorbed onto the solid. Top row: Concentrations of As(V) (✕) and As(III) (♦) over time in samples containing *Shewanella* sp. strain ANA-3 (A) and ANA-3Δ*arrA* (D) and ratio of strain ANA-3 *arrA* mRNA transcript per *arrA* gene copy number (bold line, ■). Middle row: Concentrations of lactate (■) and acetate (▲) in samples containing strain ANA-3 (B) and ANA-3Δ*arrA* (E). Bottom row: Total Fe(II) (■), total dissolved iron (▲) and dissolved Fe(II) (♦) species in samples containing strain ANA-3 (C) and ANA-3Δ*arrA* (F). The insets in (C) and (F) show a magnified view of the total dissolved iron and dissolved Fe(II). Arsenic and iron species are presented as millimoles/liter for comparative purposes, although both species are primarily bound to the solid phase and thus not in homogeneous solution. Data represent the average and standard deviation of triplicate samples, except in the case for the RNA:DNA ratio, where a representative data set is shown.

Reduction of As(V) occurred in samples incubated with strain ANA-3 (Figure 3.4.A.), but not in the uninoculated samples (data not shown) or samples inoculated with strain ANA-3Δ*arrA* (Figure 3.4.D.), showing that As(V) reduction is not mediated abiotically or in the absence of *arrA*, even when *arsC* is present. With strain ANA-3, the ratio of *arrA* mRNA transcripts to chromosomal gene copy number increased from 0.55 prior to inoculation (t=0) to 1.15 at 24 hours. The RNA:DNA ratio then decreased to 0.65 at 60 hours and steadily continued to decrease until no expression was detected at 200 hours (Figure 3.4.A.). The time when *arrA* expression was highest corresponded to the fastest rate of As(V) reduction. mRNA transcripts of *arrA* were detected prior to inoculation, when the cells were growing anaerobically in rich medium without arsenic, but no transcripts were detected after 200 hours (Figure 3.4.A.). This effect cannot be explained by cell death in the later time points as oxidation of lactate to acetate continued beyond 200 hours, showing that the cells were alive throughout the experiment (Figure 3.4.B., 3.4.E.). This suggests that the decrease in *arrA* gene expression was regulated by the cell. Repression of *arrA* may be induced by limiting substrates or a metabolic product of As(V) reduction [e.g. As(III)].

Interestingly, Fe(III) reduction did not begin until As(V) reduction had nearly reached completion in samples inoculated with strain ANA-3 (Figure 3.4.A., 3.4.C.). In samples incubated in the presence of strain ANA-3Δ*arrA*, Fe(III) reduction occurred at a slower rate than in samples containing strain ANA-3 (Figure 3.4.C., 3.4.F.). Because both the wild-type and mutant reduce $Fe(OH)_3$ at equal rates when As(V) is not sorbed onto the mineral (Saltikov and Newman 2003), the slower reduction of As(V)-saturated

$Fe(OH)_3$ by strain ANA-3Δ*arrA* compared to strain ANA-3 cannot be due to defects in Fe(III) respiration. Instead, two explanations are possible. First, the ability to gain energy from As(V) could have allowed more cells to grow in samples containing strain ANA-3, resulting in faster bulk Fe(III) reduction yet similar rates of Fe(III) reduction per cell compared to strain ANA-3Δ*arrA*. Another possibility is that sorption of As(V) onto $Fe(OH)_3$ limits access to Fe(III) by cells lacking *arrA* activity.

To determine how *arrA* activity affects arsenic mobilization in an iron-rich context such as this, we measured the amounts of dissolved and total arsenic and iron. Although the cells reduced 87% of As(V) and 72% of Fe(III) (Figure 3.4.A., 3.4.C.), almost all the As(III) and Fe(II) remained associated with the solid phase, with dissolved arsenic concentrations remaining close to the detection limit (50 μM) throughout the experiment (data not shown). Furthermore, while total Fe(II) increased throughout the experiment, the concentration of total dissolved iron reached 1.2 mM and that of dissolved Fe(II) reached 1.1 mM at 160 hr, then decreased over the remaining span of the experiment (Figure 3.4.C., inset). This decrease in dissolved iron [Fe(III)+Fe(II)] correlated with the production of a black magnetic mineral, presumably the mixed valence iron oxide magnetite, Fe_3O_4, but other reduced iron mineral phases were also present. Thus, although As(V) respiration clearly affects arsenic speciation, it does not necessarily result in arsenic mobilization in the absence of changes in iron mineralogy or other environmental conditions that would facilitate its release (Harvey et al. 2002; Bostick and Fendorf 2003; Dixit and Hering 2003). From these experiments, we concluded that *arrA* is required to catalyze the conversion of As(V) to As(III) in iron-rich systems and that ArrAfwd and ArrArev can be used to track *arrA* expression.

3.4.4. *arrA* expression in Haiwee Reservoir

To extend these results to natural environments, we focused on sediments from the Haiwee Reservoir, which is subject to deposition of arsenic associated with a poorly crystalline Fe(III) (hydr)oxide floc (Kneebone et al. 2002). Sediment analysis by X-ray absorption spectroscopy (XAS) has shown that this association persists in the sediments and that arsenic occurs in the solid phase primarily as As(III) (Kneebone et al. 2002). Further XAS studies of sediments collected at several locations in Haiwee Reservoir confirm that As(V) is present only in the most surficial sediments and that As(III) is predominant in the sediments below a few centimeters (O'Day, pers. comm.).

DNA and total RNA were extracted from a 32 cm core taken from Haiwee sediments. After reverse transcription of the mRNA fraction to produce cDNA, we performed PCR using ArrAfwd and ArrArev. PCR products from both the DNA fraction and the cDNA fraction were successfully amplified, while no products were amplified from the mRNA fraction in which no RT PCR was performed. To confirm that these PCR products were *bona fide arrA* gene fragments, we purified and cloned 7 representative DNA fragments and 14 cDNA fragments (Figure 3.5.A.). These fragments ranged from ~62-97% identity to *arrA* sequences from *B. selenitireducens*, *C. arsenatis* and strain ANA-3, suggesting that the microbial community contained As(V)-respiring bacteria of these types. The presence of As(V)-respiratory activity was also supported by the isolation of several As(V)-respiring strains from Haiwee sediments. One of these, HAR-4, was characterized in detail (Figure 3.5.B.). Based on 16S rDNA sequence

analysis (1,286 nucleotides considered), this strain is most closely related to *S. oneidensis* strain MR-1 (99% sequence identity). As expected, using ArrAfwd and ArrArev, we were able to amplify the *arrA* homolog from HAR-4 using PCR (Figure 3.3.). Partial sequence of the HAR-4 *arrA* gene displayed 92% nucleotide identity (851 nucleotides considered) and its product 94% amino acid identity to the ANA-3 As(V) reductase. These results show that the *arrA* gene is not only present, but expressed in Haiwee sediments. This suggests that bacterial As(V)-respiration is contributing to the prevalence of As(III) that has been observed at this site.

It is striking that the *arrA* gene is so well conserved amongst such phylogenetically different clades, implying that it may have a deep evolutionary root, and/or may have been transferred horizontally. Regardless of its evolutionary history, the fact that *arrA* is so well conserved now enables a simple molecular assay to be used to determine whether respiratory As(V) reduction is contributing to the speciation and mobilization of arsenic in a variety of environments. Although the entry of arsenic into drinking water supplies typically involves a complex set of physical, chemical and biological factors, knowing whether As(V)-respiring bacteria are active at any given site should help in the design of more effective remediation strategies.

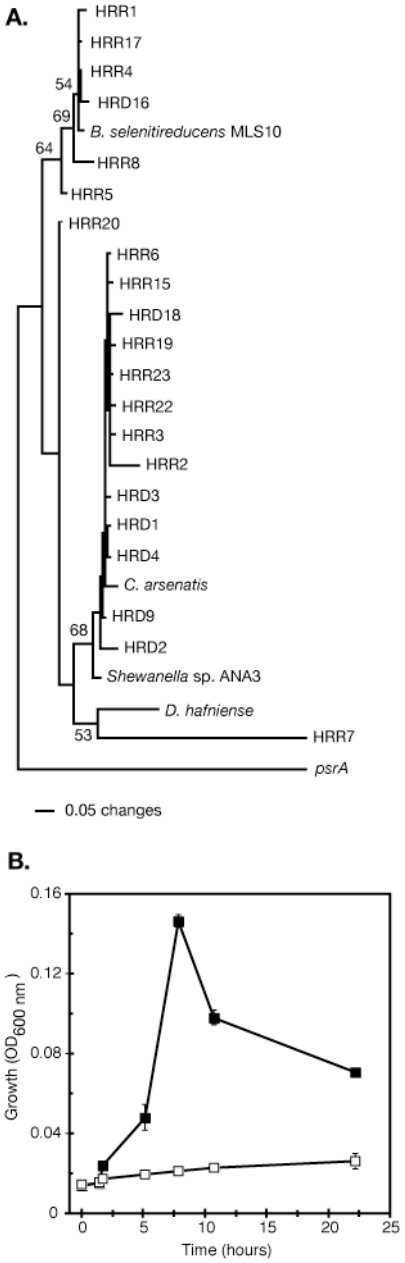

Figure 3.5. *arrA* is present and expressed in Haiwee sediments, as evidenced by culture independent studies and by isolation of As(V)-respiring bacteria. (A) Phylogenetic diversity of DNA and RNA clones from Haiwee Reservoir nucleic acid extractions. Haiwee Reservoir DNA (HRD) and Haiwee Reservoir RNA (HRR) samples are shown relative to the four known functional sequences of *arrA*, along with the polysulfide reductase, *psrA*, from *Wolinella succinogenes* as an outgroup. (B) Representative growth curve of *Shewanella* sp. strain HAR-4, one of the As(V)-respiring bacteria isolated from Haiwee sediments. Growth is measured by optical density (600 nm) in the

presence of 20 mM lactate and 10 mM As(V) (■). No growth is measured under the same conditions in the absence of As(V) (□).

3.5. Acknowledgements

All new arrA gene sequences have been deposited in Genbank. This work was supported by the Luce and Packard Foundations (D. K. N.) and NSF awards BES-0201888 (J. G. H.) and DBI-0200145 (C. W. S.). We thank P. O'Day for permission to cite her unpublished work, and F. Rosenzweig, R. Oremland, and C. House for sending us strains.

3.6. References

Afkar, E., J. Lisak, et al. (2003). "The respiratory arsenate reductase from *Bacillus selenitireducens* strain MLS10." FEMS Microbiol Lett **226**(1): 107-12.

Ahmann, D., L. R. Krumholz, et al. (1997). "Microbial mobilization of arsenic from sediments of the Aberjona Watershed." Environ Sci Technol **31**(10): 2923-2930.

Akai, J., K. Izumi, et al. (2004). "Mineralogical and geomicrobiological investigations on groundwater arsenic enrichment in Bangladesh." Applied Geochemistry **19**(2): 215-230.

Altschul, S. F., W. Gish, et al. (1990). "Basic local alignment search tool." J Mol Biol **215**(3): 403-10.

Blum, J. S., A. B. Bindi, et al. (1998). "*Bacillus arsenicoselenatis*, sp nov, and *Bacillus selenitireducens*, sp nov: two haloalkaliphiles from Mono Lake, California that respire oxyanions of selenium and arsenic." Arch Microbiol **171**(1): 19-30.

Bostick, B. C. and S. Fendorf (2003). "Arsenite sorption on troilite (FeS) and pyrite (FeS2)." Geochim Cosmochim Ac **67**(5): 909-921.

Dixit, S. and J. G. Hering (2003). "Comparison of Arsenic(V) and Arsenic(III) Sorption onto Iron Oxide Minerals: Implications for Arsenic Mobility." Environ Sci Technol **37**(18): 4182-4189.

Dzombak, D. A. and F. M. M. Morel (1990). Surface Complexation Modeling: Hydrous Ferric Oxide. New York, John Wiley & Sons.

Harrington, J. M., S. E. Fendorf, et al. (1998). "Biotic generation of arsenic(III) in metal(loid)-contaminated freshwater lake sediments." Environ Sci Technol **32**(16): 2425-2430.

Harvey, C. F., C. H. Swartz, et al. (2002). "Arsenic mobility and groundwater extraction in Bangladesh." Science **298**(5598): 1602-6.

Hurt, R. A., X. Qiu, et al. (2001). "Simultaneous recovery of RNA and DNA from soils and sediments." Appl Environ Microbiol **67**(10): 4495-503.

Kneebone, P. E., P. A. O'Day, et al. (2002). "Deposition and fate of arsenic in iron- and arsenic-enriched reservoir sediments." Environ Sci Technol **36**(3): 381-6.

Krafft, T. and J. M. Macy (1998). "Purification and characterization of the respiratory arsenate reductase of *Chrysiogenes arsenatis*." Eur J Biochem **255**(3): 647-53.

Laverman, A. M., J. S. Blum, et al. (1995). "Growth of Strain SES-3 with Arsenate and Other Diverse Electron Acceptors." Appl Environ Microbiol **61**(10): 3556-3561.

Lovley, D. R., J. L. Fraga, et al. (1999). "Humics as an electron donor for anaerobic respiration." Environ Microbiol **1**(1): 89-98.

Macur, R. E., C. R. Jackson, et al. (2004). "Bacterial populations associated with the oxidation and reduction of arsenic in an unsaturated soil." Environ Sci Technol **38**(1): 104-11.

Macy, J. M., K. Nunan, et al. (1996). "*Chrysiogenes arsenatis* gen nov, sp nov; a new arsenate-respiring bacterium isolated from gold mine wastewater." Inter J Sys Bacteriol **46**(4): 1153-1157.

Newman, D. K., E. K. Kennedy, et al. (1997). "Dissimilatory arsenate and sulfate reduction in *Desulfotomaculum auripigmentum* sp. nov." Arch Microbiol **168**(5): 380-8.

Nickson, R., J. McArthur, et al. (1998). "Arsenic poisoning of Bangladesh groundwater." Nature **395**(6700): 338.

Niggemyer, A., S. Spring, et al. (2001). "Isolation and characterization of a novel As(V)-reducing bacterium: implications for arsenic mobilization and the genus *Desulfitobacterium*." Appl Environ Microbiol **67**(12): 5568-80.

Oremland, R. S., P. R. Dowdle, et al. (2000). "Bacterial dissimilatory reduction of arsenate and sulfate in meromictic Mono Lake, California." Geochim Cosmochim Ac **64**(18): 3073-3084.

Oremland, R. S. and J. F. Stolz (2003). "The ecology of arsenic." Science **300**(5621): 939-44.

Rose, T. M., J. G. Henikoff, et al. (2003). "CODEHOP (COnsensus-DEgenerate Hybrid Oligonucleotide Primer) PCR primer design." Nucleic Acids Res **31**(13): 3763-6.

Saltikov, C. W. and D. K. Newman (2003). "Genetic identification of a respiratory arsenate reductase." Proc Natl Acad Sci USA **100**(19): 10983-8.

Schwertmann, U. and R. M. Cornell (1991). Iron Oxides in the Laboratory. Weinheim, Wiley-VCH.

Senn, D. B. and H. F. Hemond (2002). "Nitrate controls on iron and arsenic in an urban lake." Science **296**(5577): 2373-6.

Smith, A. H., E. O. Lingas, et al. (2000). "Contamination of drinking-water by arsenic in Bangladesh: a public health emergency." Bull World Health Organ **78**(9): 1093-103.

Stackebrandt, E., P. Schumann, et al. (2003). "Reclassification of *Delsulfotomaculum auripigmentum* as *Desulfosporosinus auripigmenti* corrig., comb. nov." Inter J Sys Evol Microbiol **53**: 1439-1443.

Stookey, L. L. (1970). "Ferrozine-A new spectophotometric reagent for iron." Analytical Chemistry **42**(7): 779-781.

Chapter 4

Microbial Reduction of Iron(III) and Arsenic(V) in Suspensions of Hydrous Ferric Oxide

This chapter is adapted from:

Campbell, K. M., D. Malasarn, C. W. Saltikov, D. K. Newman, and J. G. Hering. "Simultaneous Microbial Reduction of Iron (III) and Arsenic (V) in Suspensions of Hydrous Ferric Oxide" published in Environmental Science and Technology **40**(19): 5950-5955 (2006).

4.1. Abstract

Bacterial reduction of arsenic(V) and iron(III)-oxides influences the redox cycling and partitioning of arsenic (As) between solid and aqueous phases in sediment-porewater systems. Two types of anaerobic bacterial incubations were designed to probe the relative order of As(V) and Fe(III)-oxide reduction and to measure the effect of adsorbed As species on the rate of iron reduction, using hydrous ferric oxide (HFO) as the iron substrate. In one set of experiments, HFO was pre-equilibrated with As(V) and inoculated with fresh sediment from Haiwee Reservoir (Olancha, CA), an As-impacted field site. The second set of incubations consisted of HFO (without As), As(III)- and As(V)-equilibrated HFO incubated with *Shewanella* sp. ANA-3 wild-type (WT) and ANA-3Δ*arrA*, a mutant unable to produce the respiratory As(V) reductase. Of the two pathways for microbial As(V) reduction (respiration and detoxification), the respiratory

pathway was dominant under these experimental conditions. In addition, As(III) adsorbed onto the surface of HFO enhanced the rate of microbial Fe(III) reduction. In the sediment and ANA-3 incubations, As(V) was reduced simultaneously or prior to Fe(III), consistent with thermodynamic calculations based on the chemical conditions of the ANA-3 WT incubations.

4.2. Introduction

Arsenic (As) causes severe health effects when ingested, and evidence for this type of poisoning is apparent in countries such as Bangladesh, where millions of people are affected by drinking As-contaminated groundwater (NRC 1999; NRC 2001; Nordstrom 2002; Smedley and Kinniburgh 2002). In Bangladesh and many other As-impacted areas, As commonly co-occurs with iron (Fe) minerals in sediments as an adsorbed species, and the fate of Fe and As are often closely linked (McGeehan and Naylor 1994; Dixit and Hering 2003; Akai et al. 2004). Arsenic mobility can be affected by redox chemistry (i.e., the cycling between the +III and +V oxidation states), and also by sediment transformations, particularly the reductive dissolution of Fe(III) (hydr)oxides.

Microorganisms can mediate redox cycling of both As and Fe (Newman et al. 1998; Nickson et al. 2000; Oremland and Stolz 2003). Microbially-driven As redox transformations have been observed in laboratory and field studies (Ahmann et al., 1997; Zobrist et al. 2000; Oremland and Stolz 2003; Islam et al. 2004). There are two known microbial pathways for reduction of As(V) to As(III). The respiratory pathway (*arrA*

pathway) couples the oxidation of an organic substrate to As(V) reduction resulting in cell growth (Cervantes et al. 1994; Laverman et al. 1995; Dowdle et al. 1996; Newman et al. 1998; Malasarn et al. 2004). The detoxification pathway (*arsC* pathway) is used by the cell to convert As(V) to As(III), which is actively transported out of the cell; this process requires ATP (Cervantes et al. 1994).

Dissimilatory Fe reducing bacteria (DIRB) are widespread and considered to be the primary agent in the reductive dissolution of Fe minerals in sedimentary environments (Lovley et al. 1991; Smedley and Kinniburgh 2002; Akai et al. 2004). Less crystalline Fe phases with higher surface areas are more susceptible to biological reduction (Roden and Zachara 1996; Jones et al. 2000; Roden 2003; Hansel et al. 2004; Roden 2004). Furthermore, rates of reductive dissolution are affected by Fe mineralogy and accumulation of Fe(II) reaction products. As the parent mineral is reduced, reaction products, including sorbed or precipitated Fe(II), accumulate on the mineral surface, slowing the reduction rate (Urrutia and Roden 1998; Urrutia et al. 1999; Hansel et al. 2004; Roden 2004; Royer et al. 2004). The observed rates and products of these microbial reactions depend on experimental conditions such as bacterial strain, initial Fe mineral, and flow-through or batch incubation.

The amount of As released into solution due to the bacterial reductive dissolution of Fe (hydr)oxides has been shown to depend on As oxidation state and Fe mineralogy (Ahmann et al. 1997; Langner and Inskeep 2000; Zobrist et al. 2000; Islam et al. 2004; van Geen et al. 2004; Herbel and Fendorf 2005). The oxidation state of As at the onset of Fe reduction is crucial to As mobility, since As(V) and As(III) sorption and complexation can be significantly different at environmentally relevant pH values when competing

sorbates, such as phosphate, are present (Dzombak and Morel 1990; Dixit and Hering 2003). As a result, whether As(V) is reduced prior to Fe(III) may partially determine As mobilization. In addition, while the rates of Fe(III) and As(V) reduction are affected by Fe mineralogy, the effect of adsorbed As species on rates of Fe reduction has not been investigated.

This study addresses the relative order of microbial As(V) and Fe(III) reduction as well as the effect of sorbed As species on rates of Fe reduction. Two microcosm studies were performed with a synthetic iron oxyhydroxide slurry, and incubated with bacteria from two types of microbial inocula. One inoculum was fresh sediment containing its ambient microbial community from Haiwee Reservoir (Olancha, CA, USA), where Fe- and As-rich sediment have been deposited as a result of *in situ*, full-scale water treatment (Kneebone 2000; Kneebone et al. 2002). Arsenic in Haiwee sediment is primarily adsorbed to a poorly crystalline Fe(III) oxyhydroxide phase. Iron and As in the sediment porewaters are strongly correlated, consistent with reductive dissolution. In the solid phase, As(V) was detectible only in the surficial sediment with As present as As(III) throughout the sediment column (Kneebone et al. 2002; Malasarn et al. 2004). The other type of inoculum was a well-studied laboratory strain, *Shewanella* sp. strain ANA-3 wild-type (WT), and a mutant strain with a deletion of the *arrA* gene. ANA-3 WT is capable of both Fe and arsenate reduction. ANA-3 is a reasonable model organism since an isolate of native arsenate-reducing bacteria from Haiwee Reservoir sediments was found to be a strain of *Shewanella* bacteria, also capable of Fe and As reduction (Malasarn et al. 2004).

Inocula of Haiwee sediment or ANA-3 were incubated with hydrous ferric oxide (HFO), an amorphous Fe(III) oxyhydroxide similar to the Fe phase in Haiwee reservoir sediments (Kneebone et al. 2002; Cooper et al. 2005). For experiments with Haiwee sediment inoculum, HFO was equilibrated with As(V) prior to inoculation and experiments were conducted with varying organic substrates (lactate, acetate or no added organic carbon). For experiments with ANA-3, HFO was equilibrated with either As(V) or As(III) before inoculation or used without exposure to As. The order of microbial As(V) and Fe(III) reduction, the effects of organic substrates on As(V) and Fe(III) reduction, and the effect of adsorbed As(V) and As(III) on microbial Fe(III) reduction were examined.

4.3. Materials and Methods

4.3.1. Reagents

All chemicals used were reagent grade and used without further purification. Solutions were prepared with 18 MΩ-cm deionized water (Barnstead, Nanopure infinity) and stored in plastic containers that had been washed in 10% oxalic acid. For bacterial incubations, all solutions were autoclaved before use with the exception of the bicarbonate buffer, which was filter sterilized (0.2 μm pore size) and added to the autoclaved medium. The bacterial minimal growth medium (Tables 4.1 and 4.2) was buffered with 50 mM bicarbonate and had a total phosphate concentration of 50 μM and an ionic strength of 0.06 M.

Chemical Formula	Concentration	Brand and Purity
K_2HPO_4	0.05 g/L	Mallinckrodt, AR-ACS, 100.0%
KH_2PO_4	0.035 g/L	Mallinckrodt, AR-ACS, 99.8%
NaCl	0.46 g/L	Mallinckrodt, AR-ACS, 100.1%
$(NH_4)_2SO_4$	0.225 g/L	Mallinckrodt, AR-ACS
$MgSO_4 \cdot 7H_2O$	0.117 g/L	Allied Chemical, 99.5%
$NaHCO_3$	8.4%	Mallinckrodt, AR-ACS, 100.2%
NaOH	1 M	Mallinckrodt, AR-ACS, 99%
HCl	1 M	Mallinckrodt, ACS reagent grade
$NaC_3H_5O_3$	60% syrup	Sigma
Vitamin Mix	5 mL	See Table 4.2.
Mineral Mix	5 mL	See Table 4.2.

Table 4.1. Chemical constituents of the bacterial minimal medium

Vitamin Mix	
Biotin	2 mg/L
Folic acid	2 mg/L
Pyridoxine HCl	10 mg/L
Riboflavin	5 mg/L
Thiamine	5 mg/L
Nicotinic acid	5 mg/L
Pantothenic acid	5 mg/L
B-12	0.1 mg/L
p-aminobenzoic acid	5 mg/L
Thioctic acid	5 mg/L

Mineral Mix	
NTA	1.5 g/L
$MgSO_4$	3.0 g/L
$MnSO_4 \cdot H_2O$	0.5 g/L
NaCl	1.0 g/L
$FeSO_4 \cdot 7H_2O$	0.1 g/L
$CaCl_2 \cdot 2H_2O$	0.1 g/L
$CoCl_2 \cdot 6H_2O$	0.1 g/L
$ZnCl_2$	0.13 g/L
$CuSO_4 \cdot 5H_2O$	0.01 g/L
$AlK(SO_4) \cdot 12H_2O$	0.01 g/L
H_3BO_3	0.01 g/L
Na_2MoO_4	0.025 g/L
$NiCl_2 \cdot 6H_2O$	0.024 g/L
$Na_2WO_4 \cdot 2H_2O$	0.025 g/L

Table 4.2. Vitamin and minerals used in bacterial minimal medium

4.3.2. Preparation of HFO and As-equilibrated HFO.

HFO was prepared by the drop-wise addition of 0.5 M NaOH to 0.05 M $Fe(NO_3)_3$ until the solution stabilized at pH 8 (Schwertmann and Cornell 1991). The suspension was equilibrated for >3 h under constant stirring, adjusting any pH drift as necessary with 0.5 M NaOH. The HFO was then washed three times with sterile water and centrifuged at 7000×g for 10 minutes. The HFO was not autoclaved after synthesis to avoid changes in mineralogy.

After the final wash, the HFO was resuspended in an As solution, and equilibrated overnight with constant stirring. For the sediment incubations, 15 g of HFO was resuspended in 1 L of 0.05 M Na_2HAsO_4 (Sigma) at pH 7.2. For the ANA-3 incubations, 5 g of HFO was suspended in 0.5 L of 0.02 M Na_2HAsO_4 and 3 g of HFO was suspended in 0.5L of 0.02 M $NaAsO_2$ (Sigma) at pH 8.0. These conditions ensured that all available surface sites for As sorption were saturated with As at the given pH. In all cases, the HFO was washed twice with sterile water to remove excess As that was not sorbed and resuspended in bacterial minimal medium to a final slurry composition summarized in Table 4.3. The pH was adjusted to 7.2 for the sediment incubations, and pH 8 for the ANA-3 incubations with 0.5 M NaOH prior to inoculation. In the case of HFO without any adsorbed As, the solid was resuspended directly in bacterial medium after the initial washing and adjusted to pH 8. Uninoculated controls were maintained over the course of the experiment to ensure that no contamination was introduced in the synthesis, washing, distribution, and sampling of the HFO slurries.

Inoculum	Solid	mol_{As}/g_{HFO}	Solid-to-Solution Ratio (g/L)	pH	Carbon Source	Carbon (mM)
Haiwee Sediment	HFO/As(V)	0.002	2.0	7.2	Lactate	19
	HFO/As(V)	0.002	2.0	7.2	Acetate	17
	HFO/As(V)	0.002	2.0	7.2	No carbon amendment	0
Shewanella sp. strain ANA-3 WT	HFO/As(V)	0.001	2.8	8.0	Lactate	14
	HFO/As(III)	0.003	2.7	8.0	Lactate	14
	HFO/no As	—	1.9	8.0	Lactate	14
Shewanella sp. strain ANA-3 *ΔarrA*	HFO/As(V)	0.001	2.8	8.0	Lactate	14

Table 4.3. Summary of experimental conditions

4.3.3. Incubation Experiments

The HFO suspension was transferred under sterile conditions to acid-washed and autoclaved plastic bottles with a screw-cap lid; 200 mL of HFO slurry was added to each bottle. The bottles were transferred to an anaerobic chamber (80% N_2, 15% CO_2, 5% H_2) and equilibrated for 24 h with the lid loosely covering the bottle mouth to allow for passive gas exchange before inoculation. The bottles were inoculated in the anaerobic chamber and then incubated in the dark at 30°C in the anaerobic chamber for the remainder of the experiment. The bottles were not stirred during incubation, but were shaken vigorously prior to each sampling. All experiments were repeated in triplicate. In

each experiment, an additional bottle was left uninoculated as a control, and sampled in an identical manner.

Incubations with Haiwee Sediment. Bacterial minimal medium was amended with lactate, acetate, or left unamended (no added carbon source). The slurry consisted of HFO pre-equilibrated with As(V). The bottles were inoculated with fresh sediment from Haiwee Reservoir (2 g wet sediment/200 mL slurry), extracted from a core (5-10 cm depth) and homogenized in the anaerobic chamber. Control bottles consisted of inoculation with pasteurized sediment or autoclaved sediment, but both controls showed both As and Fe reduction. Formaldehyde prevented further reduction in autoclaved sediment control bottles (data not shown), suggesting that the reduction was microbially catalyzed. Uninoculated bottles did not show evidence of growth. Aliquots were taken from the bottles approximately every 12 h for 112 h, and analyzed as described below.

Incubations with ANA-3. Incubations were also performed using a laboratory isolate, *Shewanella* sp. strain ANA-3 WT, and mutant ANA-3Δ*arrA*, which has a deletion of the respiratory *arrA* gene (Saltikov and Newman 2003). Slurries were prepared with HFO with adsorbed As(V), HFO with adsorbed As(III), or HFO only (no As). ANA-3 WT was inoculated into bottles with HFO/As(V), HFO/As(III) and HFO. The ANA-3Δ*arrA* mutant was inoculated into bottles containing HFO/As(V), as a control for respiratory arsenate reduction. Lactate was included in all bottles as the electron donor. Bottles were inoculated to 10^5 total cells initially, corresponding to 500 cells/mL. Samples were taken approximately every 12 h for 131 h. The pH was monitored with pH indicator strips (EM, ColorpHast) at the time of each sampling.

At each time point, samples were removed from the bottles and processed as follows. For determination of dissolved concentrations, 1 mL of sample was filtered through a microcentrifuge filter with a 0.2 μm pore size (Costar, nylon Spin-x) in the glove box; filtered samples were analyzed for lactate, acetate, As(III), As(V), Fe(II) and total dissolved Fe. For determination of total concentrations, 20 μL of concentrated phosphoric acid was added to 1 mL of sample to dissolve the HFO. Ten μL of sample was added to 90 μL of 1 M HCl in a 96-well plate for total Fe(II) analysis and the remainder of the sample was analyzed for lactate, acetate, As(III), and As(V). At the first and last time point, an additional 0.375 mL of slurry was removed and acidified for total Fe analysis. Total and dissolved Fe(II) and total Fe (Fe(II) + Fe(III)) were measured by the ferrozine method (Stookey 1970) on a 96-well plate prepared in the anaerobic chamber, and analyzed immediately. The limit of detection for all iron analysis was 10μM. All other samples were frozen at -80°C until analysis by high performance liquid chromatography (HPLC, Waters 2487 detector, 715plus autosampler, 515 HPLC pump). HLPC analysis was conducted using a Hamilton PRP-X300 column in series with a BioRad Aminex HPX-87H column, heated to 50°C, with a 30 mM phosphate mobile phase at 0.6 mL/min flow rate. As(V), As(III), lactate and acetate were detected by absorbance at 210 nm. The detection limit for As(III) and As(V) was 100 μM.

A sediment core was sectioned anoxically and dried at 70°C for 2 days. The dry sediment was fumigated with HCl in a desiccator for 8 hours to remove inorganic carbon. The residue was then analyzed for organic carbon by CHN analysis (University of California Davis Stable Isotope Facility).

The thermodynamic driving force (ΔG) for both arsenate reduction and Fe reduction coupled to lactate oxidation was calculated based on experimental conditions observed in the ANA-3 WT/HFO/As(V) time course. The coupled reactions of arsenate or iron reduction to lactate oxidation were obtained from the appropriate redox half reactions with dominant dissolved species at pH 8 (Table 4.4.).

Table 4.4. Reactions and constants used for thermodynamic calculations. Constants were taken from reference (Latimer 1952).

	log K	**ΔG^0 (kJ/mol)**
Redox Half Reactions		
$CH_3CHOHCOO^- + 2H_2O = 5H^+ + CH_3COO^- + HCO_3^- + 4e^-$	-5.81	
$am\text{-}Fe(OH)_{3(s)} + e^- + 3H^+ = Fe^{2+} + 3H_2O$	16.2	
$HAsO_4^{2-} + 4H^+ + 2e^- = H_3AsO_3 + H_2O$	28.21	
Coupled Reactions		
$CH_3CHOHCOO^- + 2\ HAsO_4^{2-} + 3H^+ = CH_3COO^- + HCO_3^- + 2H_3AsO_3$	50.41	-287.2
$4\ am\text{-}Fe(OH)_{3(s)} + CH_3CHOHOO^- + 7H^+ = 4\ Fe^{2+} + CH_3COO^- + HCO_3^- + 10H_2O$	58.99	-336.24

Values of ΔG at 25°C were calculated from the expression:

$$\Delta G = \Delta G^0 + RT(\ln 10) \log Q = \Delta G^0 + 5.7081 \log Q$$

where

$$Q_1 = \frac{[CH_3COO^-][HCO_3^-][H_3AsO_3]^2}{[CH_3CHOCHOO^-][HAsO_4^{2-}]^2\{H^+\}^3}$$

for the arsenate reduction reaction, and

$$Q_2 = \frac{[CH_3COO^-][HCO_3^-][Fe^{2+}]^4}{[CH_3CHOCHOO^-]\{H^+\}^7}$$

for the HFO reduction reaction, where the activity of HFO is assumed to be 1, and $\{H^+\}$ corresponds to the measured pH. Total concentrations (dissolved plus adsorbed) of As(V), As(III), lactate, acetate, and Fe(II) were measured at each time point. Total lactate and acetate concentrations were directly substituted into the equations, since their total and dissolved concentrations were approximately equal. The pH was maintained between 7.9-8.1 for the entire incubation, and therefore $\{H^+\}$ was assumed to be 10^{-8} for all time points. The bicarbonate concentration was assumed to be constant and in equilibrium with the $CO_{2(g)}$ present in the glove box gas mixture at pH 8. The ionic strength was 0.06 M.

Since dissolved concentrations of H_3AsO_3, $HAsO_4^{2-}$, and Fe^{2+} were below the detection limits of the analytical methods, MINEQL+ was used to calculate these concentrations based on experimental measurements.

Fe_T was determined at t=0. Fe(III) at each time point was determined by:

$$Fe(III) = Fe_T - Fe(II)$$

From Dzombak and Morel (Dzombak and Morel 1990), $[\equiv Fe^{wk}OH] = 0.2\ Fe_T$ and $[\equiv Fe^{st}OH] = 0.005\ Fe_T$ and the specific surface area for HFO is assumed to be 600 m^2/g. The value of $0.2 mol_{sites}/mol_{Fe}$ is a general average, with values for arsenic sorption between 0.05-0.18 mol_{sites}/mol_{Fe}. Based on isotherm studies with HFO synthesized identically to this study, $0.12 mol_{sites}/mol_{Fe}$ more accurately describes the sorption site capacity for arsenic in this system. Assuming that the ratio of strong-to-weak sites is the

same as the general value from Dzombak and Morel (i.e., [≡$Fe^{st}OH$] / [≡$Fe^{wk}OH$] = 0.025), the site density is:

[≡$Fe^{wk}OH$] = 0.117 Fe_T

[≡$Fe^{st}OH$] = 0.0029 Fe_T

Only ferrihydrite was allowed to precipitate in the model. The ionic strength was calculated from the bacterial medium salts concentration, and was found to be 0.06M. The double-layer FeOH sorption model was used to calculated the amount of sorbed and dissolved As(V), As(III), and Fe(II) species at each time point. The intrinsic surface complexation constants used in the model are given in Table 4.5. Activity coefficients were calculated in MINEQL+, using the Davies equation correction for ionic strength. The contribution of lactate and acetate complexation are neglected in these calculations since complexation with As(III), As(V), and Fe(II) species is weak (Urrutia and Roden 1998). Concentrations of species used in thermodynamic calculations are given in Table 4.6.

Table 4.5. Intrinsic Surface Complexation Constants used in MINEQL+ model

Surface Reaction	**log K** (I = 0 M, 25°C)	**Reference**
As(V) reactions		
≡$FeOH + AsO_4^{3-} + 3H^+ = ≡FeH_2AsO_4 + H_2O$	29.31	(Dzombak and Morel 1990)
≡$FeOH + AsO_4^{3-} + 2H^+ = ≡FeHAsO_2^- + H_2O$	23.51	(Dzombak and Morel 1990)
≡$FeOH + AsO_4^{3-} = ≡FeOHAsO_4^{3-}$	10.58	(Dzombak and Morel 1990)

As(III) reactions		
$\equiv FeOH + AsO_3^{3-} + 3H^+ = \equiv FeH_2AsO_3 + H_2O$	38.76	(Dzombak and Morel 1990)
Fe(II) reactions		
$\equiv Fe^{wk}OH + Fe^{2+} = \equiv Fe^{wk}OFe^+ + H^+$	-2.98	(Appelo, Van der Weiden et al. 2002)
$\equiv Fe^{st}OH + Fe^{2+} = \equiv Fe^{st}OFe^+ + H^+$	-0.95	(Appelo, Van der Weiden et al. 2002)
$\equiv Fe^{wk}OH + Fe^{2+} = \equiv Fe^{wk}OFeOH + 2H^+$	-11.55	(Appelo, Van der Weiden et al. 2002)

Table 4.6. Concentrations of species used in thermodynamic calculations (pH = 8.0)

As(V)		As(III)		Fe(II)		Lactate	Acetate	HCO_3^-	H^+
As^V_{total} measured (M)	$H_2AsO_4^-{}_{(aq)}$ calculated (M)	As^{III}_{total} measured (M)	$H_3AsO_{3(aq)}$ calculated (M)	Fe^{II}_{total} measured (M)	$Fe^{2+}_{(aq)}$ calculated (M)	measured (M)	measured (M)	calculated (M)	measured (M)
2.1×10^{-3}	5.0×10^{-4}	2.3×10^{-4}	6.5×10^{-7}	2×10^{-4}	1.4×10^{-7}	1.4×10^{-2}	2.2×10^{-4}	1.0×10^{-1}	1×10^{-8}
5.0×10^{-4}	1.1×10^{-6}	1.8×10^{-3}	3.2×10^{-6}	1.3×10^{-3}	8.2×10^{-6}	1.2×10^{-2}	1.8×10^{-3}	1.0×10^{-1}	1×10^{-8}
4.1×10^{-4}	1.7×10^{-8}	1.9×10^{-3}	4.4×10^{-6}	1.9×10^{-3}	2.7×10^{-5}	1.2×10^{-2}	2.3×10^{-3}	1.0×10^{-1}	1×10^{-8}

4.4. Results

The two experimental time courses in this study were designed to investigate the effects of organic substrates on As(V) and Fe(III) reduction and adsorbed As species on the rate of Fe(III) reduction. Dissolved concentrations of Fe and As were undetectable throughout the course of both microcosm experiments. Thus, Fe(II), As(V) and As(III) were predominantly associated with the solid phase.

4.4.1. Incubations with Haiwee Sediment.

Both As(V) and Fe(III) were reduced in all of the incubations inoculated with Haiwee sediment (Figure 4.1.). Reduction of As(V) began before Fe(III) reduction and ceased after 40-60 h in the lactate- and acetate-amended bottles. Even though the rate and extent of reduction varied with carbon amendment, the onset of As(V) reduction preceded Fe(III) reduction in all cases. For part of the time course, reduction of As(V) and Fe(III) proceeded simultaneously, after which As(V) reduction ceased and Fe(III) reduction continued until the termination of the experiment.

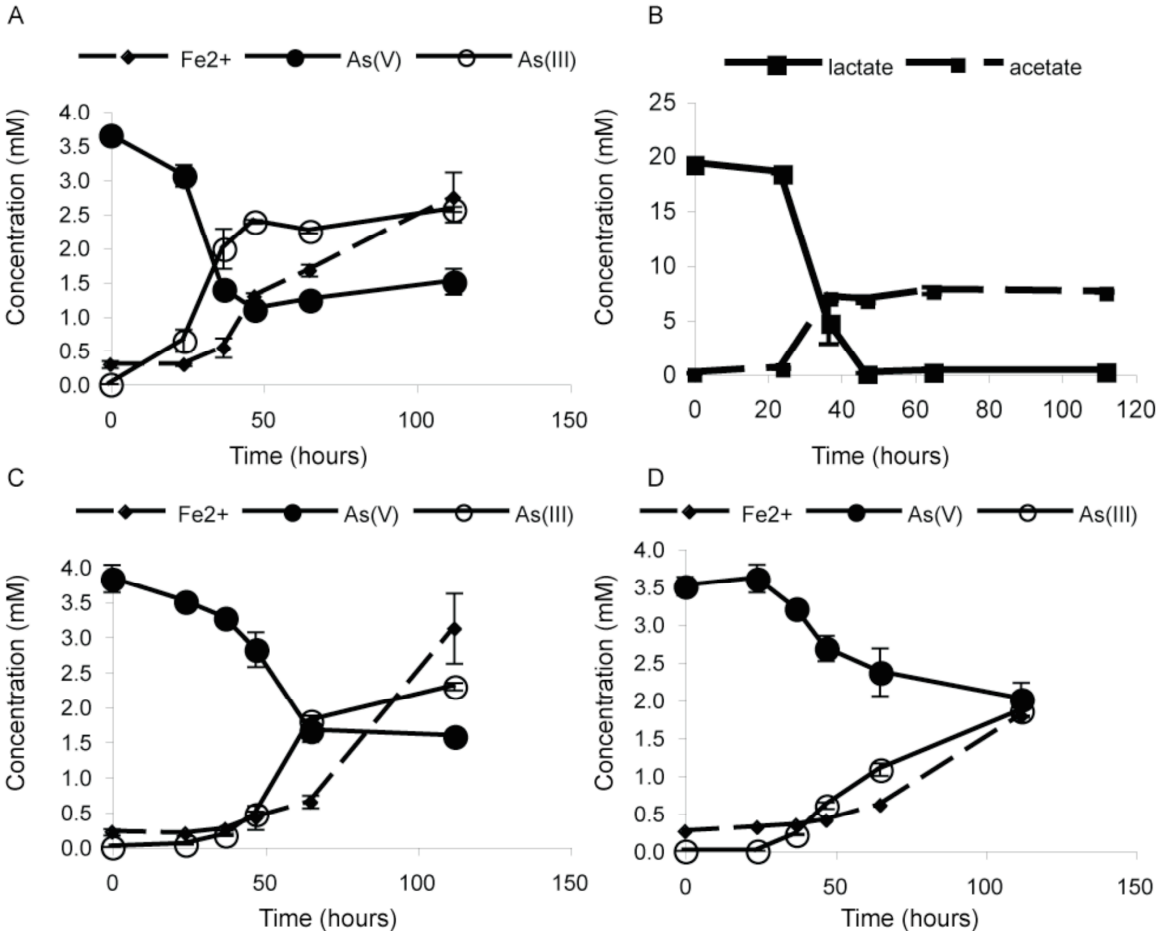

Figure 4.1. Measured total concentrations of As(III), As(V), Fe(II) and organic carbon for sediment incubations A. and B. amended with lactate, C. amended with acetate, and

D. without a carbon amendment. The HFO was pre-equilibrated with As(V), and inoculated with fresh sediment from Haiwee reservoir, introducing a natural bacterial community to the slurry. The error bars represent one standard deviation of measured concentrations of triplicate samples, and if not visible, are smaller than the symbol. For experimental conditions, see Table 4.3.

The rate and extent of As(V) and Fe(III) reduction depended on the type of organic substrate, with the greatest amount of reduction occurring in the lactate-amended bottles. As(V) reduction occurred within 50 h with lactate, 70 h with acetate, and proceeded from 20 h until the termination of the experiment in the unamended bottles. Although As(V) was not completely reduced, the termination of As(V) reduction in the lactate-amended bottles occurred concurrently with the complete consumption of lactate (~45 h). Fe(III) reduction continued even after the lactate was exhausted, but as the experiments with the unamended bottles show, some As(V) and Fe(III) reduction can occur without organic carbon amendment. About 13-14% of the Fe(III) was reduced in the lactate- and acetate-amended bottles, while 8% of the Fe(III) was reduced in the unamended bottles.

In the lactate-amended bottles, the changes in lactate and acetate concentration exceeded the values expected based on the stoichiometry of Fe(II) and As(III) production. Since the sediment inoculum introduced a mixed microbial community, it is possible that some consumption of lactate proceeded through alternative pathways not involving Fe(III) or As(V) reduction, such as nitrate or manganese reduction.

Reduction of As(V) and Fe(III) was observed in the unamended microcosm inoculated with Haiwee reservoir sediment, indicating that the bacteria were able to

utilize the ambient carbon from the small amount of sediment introduced with the inoculum. The carbon content of the sediment is 2.8% on a dry weight basis.

4.4.2. Incubations with ANA-3

As(V) and Fe(III) were simultaneously reduced in the incubations with ANA-3 WT with HFO/As(V) (Figure 4.2.A.). As(V) reduction occurred within 40 h of incubation, although it was not completely converted to As(III). HFO reduction continued throughout the course of the experiment. No As(V) reduction was observed in the ANA-3Δ*arrA* mutant incubation on HFO/As(V), and acetate production (Figure 4.2.C.) was coupled to Fe(III) reduction (Figure 4.3.). As(III) concentrations remained constant over time in experiments where ANA-3 WT was incubated with HFO/As(III). In all incubations with ANA-3, conversion of lactate to acetate was observed consistent with previous observations (Saltikov et al. 2003). Although acetate concentrations were less than expected, lactate was consumed stoichiometrically based on As(III) and Fe(II) production (Table 4.7.). Fe(III) reduction was observed in all incubations with ANA-3 but the rates of Fe(III) reduction varied in the different incubations (Figure 4.3.). The mutant ANA-3Δ*arrA* showed the lowest rate of Fe(III) reduction. With ANA-3 WT, more Fe(III) reduction was observed with HFO was pre-equilibrated with either As(V) or As(III) than with HFO alone.

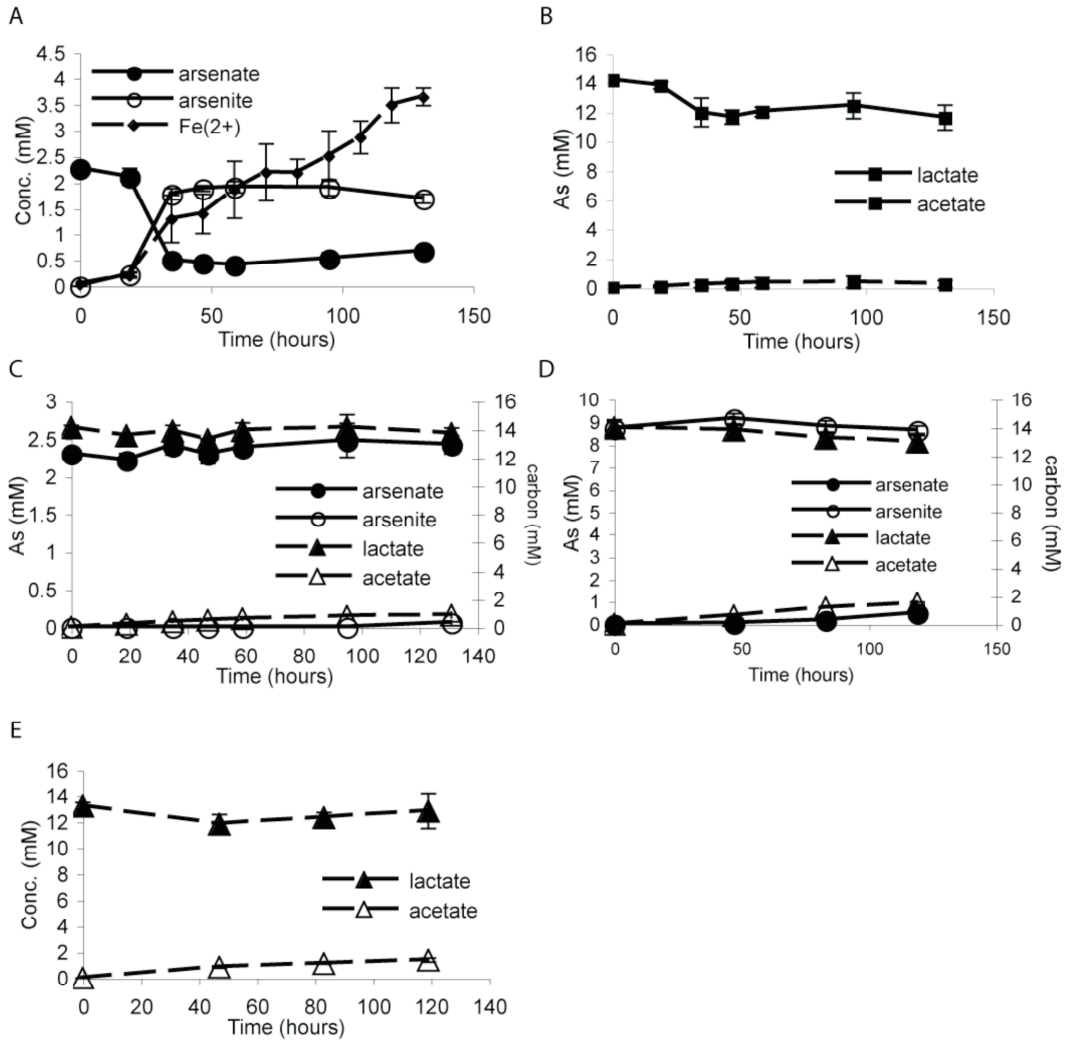

Figure 4.2. Measured total concentrations of As(V), As(III), Fe(II), lactate and acetate in incubations with A., B. ANA-3 WT incubated with As(V)-equilibrated HFO, C. ANA-3 Δ*arrA* mutant incubated with As(V)-equilibrated HFO, D. ANA-3 WT incubated with As(III)-equilibrated HFO, E. ANA-3 WT incubated with HFO (no As). ANA-3 WT or Δ*arrA* mutant was inoculated into the appropriate HFO slurry at a final cell density of 500 cells/mL slurry. For experimental conditions, see Table 4.3.

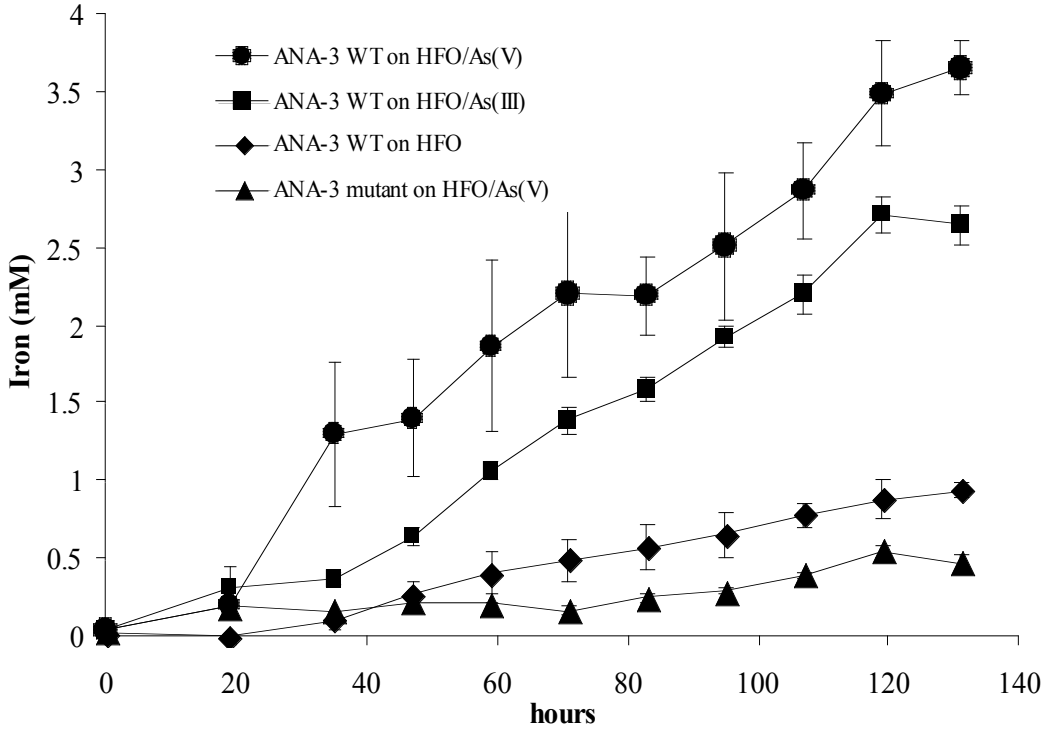

Figure 4.3. Measured total concentrations of Fe(II) for ANA-3 WT grown on HFO pre-equilibrated with As(V), As(III), or HFO only (no As), and ANA-3Δ*arrA* mutant on HFO pre-equilibrated with As(V). The rates of Fe(II) production after 40 h of incubation are 0.024 mM Fe/h for ANA-3 WT on HFO/As(V), 0.028 mM Fe/h for ANA-3 WT on HFO/As(III), 0.009 mM Fe/h for ANA-3 WT on HFO only, and 0.003 mM Fe/h for ANA-3Δ*arrA* mutant. The presence of As(III) adsorbed onto HFO enhances the rate of Fe(III) reduction.

	HFO/As(V)			HFO/As(III)			HFO only		
	initial mol	final mol	Δequiv.	initial mol	final mol	Δequiv.	initial mol	final mol	Δequiv.
lactate	2.8×10^{-3}	2.2×10^{-3}	-2.4×10^{-3}	2.8×10^{-3}	2.6×10^{-3}	-8.0×10^{-4}	2.8×10^{-3}	2.6×10^{-3}	-8.0×10^{-4}
acetate	0	6.0×10^{-5}	2.4×10^{-4}	0.0	3.0×10^{-4}	1.2×10^{-3}	0.0	2.8×10^{-4}	1.1×10^{-3}
HFO (as Fe(III)	6.4×10^{-3}	--	--	6.1×10^{-3}	--	--	4.2×10^{-3}	--	--
Fe(II)	0.0	7.2×10^{-4}	7.2×10^{-4}	0.0	5.2×10^{-4}	5.2×10^{-4}	0.0	1.8×10^{-4}	1.8×10^{-4}
As(V)	4.6×10^{-4}	1.4×10^{-4}	-6.4×10^{-4}	0.0	8.0×10^{-5}	1.6×10^{-4}	0.0	0.0	0.0
As(III)	0.0	3.4×10^{-4}	6.8×10^{-4}	1.74×10^{-3}	1.72×10^{-3}	-4.0×10^{-5}	0.0	0.0	0.0

Table 4.7. Comparison of initial and final concentrations in ANA-3 microcosm experiments. Changes in concentration are expressed in equivalents to normalize for stoichiometry (1 Fe equiv./mol; 2 As equiv./mol; 4 lactate or acetate equiv./mol).

4.5. Discussion

4.5.1. Utilization of terminal electron acceptors

In both sediment and ANA-3 microcosm experiments, As(V) reduction occurs concurrently or even prior to Fe(III) reduction. In the ANA-3 WT microcosms, the utilization of As(V) as a terminal electron acceptor prior to or concurrently with Fe(III) is consistent with calculations of the thermodynamic driving force for As(V) and Fe(III) reduction coupled with lactate oxidation. For conditions where the reactant As(V) and the products As(III) and Fe(II) are predominantly sorbed to HFO, As(V) reduction is more favorable than Fe(III) reduction throughout the course of the experiment (Table 4.8.) even as ΔG becomes less favorable for both reactions as they progress. Decreased driving force (less negative ΔG) has been calculated in other Fe systems, where Fe(II)

accumulation decreases the driving force for bacterial reduction of hematite over time (Royer et al., 2004). In the ANA-3 microcosms, As(V) was not reduced completely to As(III), indicating that the residual As(V) may have been limited by kinetic factors such as inaccessibility of residual As(V) rather than thermodynamic considerations.

Time (hours)	**$\Delta G_{As(V)}$ (kJ/mol)**	**ΔG_{HFO} (kJ/mol)**
19	-200	-189
35	-144	-143
59	-133	-130

Table 4.8. Thermodynamic driving force calculation results for ANA-3 WT microcosm.

Thermodynamics alone do not always predict the utilization of TEAs in these types of reactions, since other factors such as enzyme kinetics may influence the rates and extent of TEA consumption. However, the thermodynamic calculations presented here show that the effects of chemical reactions such as adsorption can greatly affect the energetics of the system.

Our study illustrates the importance of considering the speciation of As and Fe associated with the solid phase both in assessing the full extent of As(V) and Fe(III) reduction and in comparing the energetics of As(V) and Fe(III) reduction. In other studies where As and Fe were measured only in the dissolved phase, Fe(II) either accumulated in solution prior to the increase in dissolved As(III), or As and Fe(II) were released simultaneously into solution (McGeehan and Naylor 1994; Ahmann et al. 1997;

Zobrist et al. 2000; Islam et al. 2004). However, the amount of Fe and As in solution is dependent not only on the extent of reduction of each element but also the extent to which they are sorbed onto the solid phase. Therefore, measurement of both dissolved and solid phase redox speciation is necessary to follow the energetics of the reactions.

Although the bicarbonate, As, and Fe concentrations used in the microcosms are higher than would be generally found in natural systems, the HFO used in this study is a reasonable laboratory model for the Fe floc deposited in Haiwee sediments. Thus, the observed order of terminal electron acceptor utilization may be expected for Haiwee sediment. Our laboratory results are consistent with field observations at Haiwee reservoir, where As(V) was converted to As(III) in the surficial sediments and Fe(III) reduction occurred deeper in the sediment column (Kneebone et al. 2002). In addition, the *arrA* gene was identified in Haiwee sediments (Malasarn et al. 2004) indicating that the respiratory pathway of As(V) reduction may be important. This suggests that the redox transitions observed in Haiwee sediments are due to microbial As(V) and Fe(III) reduction.

	HFO/As(V)			HFO/As(III)			HFO only		
	initial mol	final mol	Δequiv.	initial mol	final mol	Δequiv.	initial mol	final mol	Δequiv.
ctate	2.8×10^{-3}	2.2×10^{-3}	-2.4×10^{-3}	2.8×10^{-3}	2.6×10^{-3}	-8.0×10^{-4}	2.8×10^{-3}	2.6×10^{-3}	-8.0×10^{-4}
etate	0	6.0×10^{-5}	2.4×10^{-4}	0.0	3.0×10^{-4}	1.2×10^{-3}	0.0	2.8×10^{-4}	1.1×10^{-3}
s Fe(III))	6.4×10^{-3}	--	--	6.1×10^{-3}	--	--	4.2×10^{-3}	--	--
e(II)	0.0	7.2×10^{-4}	7.2×10^{-4}	0.0	5.2×10^{-4}	5.2×10^{-4}	0.0	1.8×10^{-4}	1.8×10^{-4}
s(V)	4.6×10^{-4}	1.4×10^{-4}	-6.4×10^{-4}	0.0	8.0×10^{-5}	1.6×10^{-4}	0.0	0.0	0.0
s(III)	0.0	3.4×10^{-4}	6.8×10^{-4}	1.74×10^{-3}	1.72×10^{-3}	-4.0×10^{-5}	0.0	0.0	0.0

Table 4.9. Comparison of initial and final concentrations in ANA-3 microcosm experiments. Changes in concentration are expressed in equivalents to normalize for stoichiometry (1 Fe equiv./mol; 2 As equiv./mol; 4 lactate or acetate equiv./mol).

4.5.2. Respiratory and Detoxification Pathways

The ANA-3Δ*arrA* mutant in an HFO/As(V) slurry did not reduce any As(V) (Figure 3.2.C.), although both ANA-3 WT and ANA-3Δ*arrA* mutant are capable of As(V) reduction for the purpose of detoxification using the ArsC reductase. Therefore, the detoxification pathway did not play a significant role in this incubation. The threshold for expressing the *ars* detoxification genes is >100 μM As(V), while the *arr* respiratory genes are expressed at As(V) concentrations of 100 nM (Saltikov et al., 2005). Dissolved concentrations of As(V) were below the detection limit of 100 μM, below the threshold for *ars* expression. Thus, detoxification should not be a significant pathway for As(V) reduction, consistent with the experimental observations.

In the sediment microcosms, the reduction of arsenate ceased around 40 h of incubation in lactate-amended bottles, which corresponds to the complete consumption of lactate. The correlation between As(V) reduction and lactate consumption is indicative of the respiratory pathway, and suggests it may be dominant in the sediment microcosms as well. This is consistent with previous studies that suggest that rates of As(V) reduction via the detoxification pathway may be slower than the respiratory pathway in other bacterial strains (Jones et al. 2000).

It is evident that bacteria can reduce As(V) for respiration or detoxification even under conditions where As(V) is predominantly adsorbed to or associated with an Fe mineral matrix (Ahmann et al. 1997; Jones et al. 2000; Langner and Inskeep 2000; Zobrist et al. 2000; Herbel and Fendorf 2005). The arsenate reductase ArrA is thought to

be located in the periplasm of the bacterial cell on the basis of genetic similarities to other known proteins (Krafft and Macy 1998; Saltikov and Newman 2003) and to require a phosphate transporter to translocate dissolved As (i.e., after desorption from the solid) into the periplasm. This would imply that the dissolved As(V) in our experiments, although below the detection limit, was sufficient to support the observed microbial reduction. However, the question remains as to whether a bacterial cell can directly utilize adsorbed As(V) or requires desorption of As(V) from the solid phase.

4.5.3. Effect of sorbed As on Fe(III) reduction

The presence of adsorbed As(III) increased the rate of Fe reduction in the ANA-3 WT microcosm experiments. In the incubations with HFO/As(V), sorbed As(V) was reduced to As(III) within approximately 40 h. Once most of the As(V) was reduced (>40 h) and As(III) was the dominant species adsorbed onto the HFO, the rate of Fe reduction was comparable to the HFO/As(III) case (0.024 mM Fe/h for HFO/As(V) microcosm and 0.028 mM Fe/h for the HFO/As(III) microcosm) from 40 h to 130 h. The HFO only and HFO/As(V)/mutant incubations show substantially less Fe reduction (0.009 and 0.003 mM Fe/h, respectively) than observed in the HFO/As(V) and HFO/As(III) microcosms, which indicates that sorbed As(III) enhances the bacterial reduction of HFO.

The rate of microbial reduction of Fe(III) oxyhydroxides depends on the surface area and crystallinity of the oxide mineral (Jones et al. 2000; Zobrist et al. 2000; Hansel et al. 2004). Changes in these properties could be related to the observed differences in rates of Fe reduction. The time scale of this experiment (~4 days) is considerably less

than the timescale of ~15 days over which substantial re-crystallization of HFO, with or without adsorbed As, was observed in abiotic batch experiments (Ford 2002). In flow-through experiments, however, a transition from HFO to lepidocrocite has been observed within 2 days of incubation with bacteria (Benner et al. 2002; Hansel et al. 2003). The absence of dissolved As in our study suggests that surface area did not decrease substantially over the course of the experiment.

The enhancement of microbial Fe reduction observed when As(III) was adsorbed on the HFO substrate was unexpected and may have significant environmental implications. Bacterial reduction of As(V) to As(III) may increase the rate of reductive dissolution of poorly crystalline Fe hydroxides, possibly leading to an increase in As mobility into groundwater in sediment systems.

4.6. Acknowledgements

This work was done in collaboration with Dr. Kate Campbell, Dr. Chad Saltikov, and Dr. Janet Hering. As lead author, Kate helped in all field sample collection and time course analyses and performed all of the thermodynamic calculations. Chad helped collect field samples and assisted with HPLC analysis.

4.7. References

Ahmann, D., L. R. Krumholz, et al. (1997). "Microbial mobilization of arsenic from sediments of the Aberjona Watershed." Environ Sci Technol **31**(10): 2923-2930.

Akai, J., K. Izumi, et al. (2004). "Mineralogical and geomicrobiological investigations on groundwater arsenic enrichment in Bangladesh." Appl Geochem **19**: 215-230.

Appelo, C. A. J., M. J. J. Van der Weiden, et al. (2002). "Surface Complexation of Ferrous Iron and Carbonate on Ferrihydrite and the Mobilization of Arsenic." Environ Sci Technol **36**(14): 3096-3103.

Benner, S. C., C. M. Hansel, et al. (2002). "Reductive dissolution and biomineralization of iron hydroxide under dynamic flow conditions." Environ Sci Technol **36**(8): 1705-1711.

Cervantes, C., G. Ji, et al. (1994). "Resistance to arsenic compounds in microorganisms." FEMS Microbiol Rev **15**: 355-367.

Cooper, D. C., A. L. Neal, et al. (2005). "Effects of sediment iron mineral composition on microbially mediated changes in divalent metal speciation: Importance of ferrihydrite." Geochim Cosmochim Ac **69**(7): 1739-1754.

Dixit, S. and J. G. Hering (2003). "Comparison of Arsenic(V) and Arsenic(III) Sorption onto Iron Oxide Minerals: Implications for Arsenic Mobility." Environ Sci Technol **37**(18): 4182-4189.

Dowdle, P. R., A. M. Laverman, et al. (1996). "Bacterial Dissimilatory Reduction of Arsenic(V) to Aresnic(III) in Anoxic Sediments." Appl Environ Microbiol **62**(5): 1664-1669.

Dzombak, D. A. and F. M. M. Morel (1990). Surface Complexation Modeling: Hydrous Ferric Oxide. New York, John Wiley & Sons.

Ford, R. G. (2002). "Rates of Hydrous Ferric Oxide Crystallization and the Influence on Coprecipitated Arsenate." Environ Sci Technol **36**(11): 2459-2463.

Hansel, C. M., S. G. Benner, et al. (2003). "Secondary mineralization pathways induced by dissimilatory iron reduction of ferrihydrite under advective flow." Geochim Cosmochim Ac **67**(16): 2977-2992.

Hansel, C. M., S. G. Benner, et al. (2004). "Structural constraints of ferric (hydr)oxides on dissimilatory iron reduction and the fate of Fe(II)." Geochim Cosmochim Ac **68**(15): 3217-3229.

Herbel, M. and S. Fendorf, Eds. (2005). "Transformation and Transport of As within Ferric Hydroxide Coated Sands upon Dissimilatory Reducing Bacterial Activity." Advances in Arsenic Research: Integration of Experimental and Observational Studies and Implications for Mitigation, ACS Symposium Series.

Islam, F. S., A. G. Gault, et al. (2004). "Role of metal-reducing bacteria in arsenic release from Bengal delta sediments." Nature **430**: 68-71.

Jones, C. A., H. W. Langner, et al. (2000). "Rates of microbially mediated arsenate reduction and solubilization." Soil Sci Soc Am J **64**: 600-608.

Kneebone, P. (2000). Arsenic geochemistry in a geothermally impacted system: The Los Angeles Aqueduct. Environmental Engineering Science. Pasadena, California Institute of Technology**:** 210.

Kneebone, P. E., P. A. O'Day, et al. (2002). "Deposition and Fate of Arsenic in Iron- and Arsenic-Enriched Reservoir Sediments." Environ Sci Technol **36**(3): 381-386.

Krafft, T. and J. M. Macy (1998). "Purification and characterization of hte respiratory arsenate reductase of *Chrysiogenes arsenatis*." Eur J Biochem **255**: 647-653.

Langner, w. and W. P. Inskeep (2000). "Microbial Reduction of Arsenate in the Presence of Ferrihydrite." Environ Sci Technol **34**(15): 3131-3136.

Latimer, W. M. (1952). The Oxidation States of the Elements and their Potentials in Aqueous Solutions. Englewood Cliffs, Prentice-Hall.

Laverman, A. M., J. S. Blum, et al. (1995). "Growth of Strain SES-3 with Arsenate and other diverse electron acceptors." Appl Environ Microbiol **61**(10): 3556-3561.

Lovley, D. R., E. J. P. Phillips, et al. (1991). "Enzymatic versus nonenzymating mechanisms for Fe(III) reduction in aquatic sediments." Environ Sci Technol **25**: 1062-1067.

Malasarn, D., C. W. Saltikov, et al. (2004). "arrA is a reliable marker for As(V) respiration." Science **306**(5695): 455.

McGeehan, S. L. and D. V. Naylor (1994). "Sorption and Redox Transformation of Arsenite and Arsenate in Two Flooded Soils." Soil Sci Soc Am J **58**: 337-342.

Newman, D. K., D. Ahmann, et al. (1998). "A Brief Review of Microbial Arsenate Respiration." Geomicrobiol J **15**: 255-268.

Nickson, R. T., J. M. McArthur, et al. (2000). "Mechanism of arsenic release to groundwater, Bangladesh and West Bengal." Appl Geochem **15**: 403-413.

Nordstrom, D. K. (2002). "Worldwide Occurrences of Arsenic in Groundwater." Science **296**.

NRC (1999). Arsenic in Drinking Water. Washington, DC, National Academy Press.

NRC (2001). Arsenic in Drinking Water Update. Washington, DC, National Academy Press.

Oremland, R. S. and J. F. Stolz (2003). "The Ecology of Arsenic." Science **300**: 393-944.

Roden, E. E. (2003). "Fe(III) Oxide Reactivity Toward Biological versus Chemical Reduction." Environ Sci Technol **37**: 1319-1324.

Roden, E. E. (2004). "Analysis of long-term bacterial vs. chemical Fe(III) oxide reduction kinetics." Geochim Cosmochim Ac **68**(15): 3205-3216.

Roden, E. E. and J. M. Zachara (1996). "Microbial Reduction of Crystalline Iron (III) Oxides: Influence of Oxide Surface Area and Potential for Cell Growth." Environ Sci Technol **30**(5): 1618-1628.

Royer, R. A., B. A. Dempsey, et al. (2004). "Inhibition of Biological Reductive Dissolution of Hematite by Ferrous Iron." Environ Sci Technol **38**(1): 187-193.

Saltikov, C. W., A. Cifuentes, et al. (2003). "The *ars* Detoxification System is Advantageous but not Required for As(V) Respiration by the Genetically Tractable *Shewanella* Species Strain ANA-3." Appl Environ Microbiol **69**(5): 2800-2809.

Saltikov, C. W. and D. K. Newman (2003). "Genetic identitfication of a respiratory arsenate reductase." PNAS.

Saltikov, C. W., R. A. Wildman, Jr., et al. (2005). "Expression dynamics of arsenic respiration and detoxification in Shewanella sp. strain ANA-3." J Bacteriol **187**(21): 7390-6.

Schwertmann, U. and R. M. Cornell (1991). Iron Oxides in the Laboratory. Weinheim, Wiley-VCH.

Smedley, P. L. and D. G. Kinniburgh (2002). "A review of the source, behaviour and distribution of arsenic in natural waters." Appl Geochem **17**: 517-568.

Stookey, L. L. (1970). "Ferrozine-A new spectophotometric reagent for iron." Analytical Chemistry **42**(7): 779-781.

Urrutia, M. M. and E. E. Roden (1998). "Microbial and Surface Chemistry Controls on Reduction of Synthetic Fe(III) Oxide Minerals by the Dissimilatory Iron-Reducing Bacterium *Shewanella alga*." Geomicrobiol **15**: 269-291.

Urrutia, M. M., E. E. Roden, et al. (1999). "Influence of Aqueous and Solid-Phase Fe(II) Complexants on Microbial Reduction of Crystalline Iron(III) Oxides." Environ Sci Technol **33**: 4022-4028.

van Geen, A., J. Rose, et al. (2004). "Decoupling of As and Fe Release to Bangladesh groundwater under reducing condiditons. Part II: Evidence from sediment incubations." Geochim Cosmochim Ac **68**(17): 3475-3486.

Zobrist, J., P. R. Dowdle, et al. (2000). "Mobilization of Arsenite by dissimiliatory reduction of adsorbed arsenate." Environ Sci Technol **34**(22): 4747-4753.

Chapter 5

Characterization of the Arsenate Respiratory Reductase from *Shewanella* sp. strain ANA-3

5.1. Abstract

Arsenic contamination of alluvial aquifers exposes tens of millions of people to arsenic poisoning. Microbial arsenate respiration has been implicated as an important metabolism contributing to the mobilization of arsenic from the solid to the soluble phase. To begin to understand the extent to which As(V) respiration impacts arsenic geochemical cycling, we characterized the expression and activity of the arsenate respiratory reductase (ARR), the key enzyme involved in this metabolism. ARR is expressed at the beginning of exponential phase and persists through stationary phase, at which point it is released from the cell. In intact cells, the enzyme is localized to the periplasm. ARR requires anaerobic conditions and molybdenum for activity. Elemental analysis of pure protein determined that molybdenum, iron and inorganic sulfur were all associated with the protein. ARR functions as a heterodimer consisting of 2 subunits. It has a K_m of 5 μM and a V_{max} of 11,111 μmol As(V) reduced · min^{-1} · mg $protein^{-1}$. It reduces arsenate and shows no activity in the presence of other alternative electron acceptors.

5.2. Introduction

Arsenic contamination of alluvial aquifers that supply drinking water to Bangladesh and West Bengal exposes tens of millions of people to chronic arsenic poisoning annually (Nickson et al. 1998; Smith et al. 2000). Field and microcosm studies of environments where arsenic contamination occurs determined that microbial activity is responsible for arsenic partitioning from the solid sediment to the aqueous phase (Harvey et al. 2002). In particular, microbial respiratory reduction of arsenate, As(V), to arsenite, As(III), is thought to prevent the sorption of arsenic onto sediment surfaces (Ahmann et al. 1994; Newman et al. 1997). This unique metabolism is dependent on the arsenate respiratory reductase, or ARR (Saltikov and Newman 2003).

To understand the contribution of As(V) respiration to arsenic geochemical cycling and mobilization, details about ARR expression and activity must be characterized. In initial biochemical studies, native ARR from *Chrysiogenes arsenatis* (Krafft and Macy 1998) and *Bacillus selenitireducens* (Afkar et al. 2003) was purified and characterized. In both studies, ARR was isolated as a heterodimer containing molybdenum (Mo) and iron (Fe) cofactors, and basic enzyme kinetics were determined. The enzyme was found to be localized in the periplasm of *C. arsenatis* and associated with the membrane fraction in *B. selenitireducens*. Because both of these strains are obligate anaerobes with little available genomic data, however, additional biochemical analysis and genetic manipulations that could complement biochemical studies were difficult to perform.

To circumvent this limitation, a new model arsenate-respiring strain, *Shewanella* sp. strain ANA-3, was isolated that could also respire on oxygen and grow on agar plates (Saltikov et al. 2003). These capabilities allowed for easier laboratory manipulation of the strain and the application of standard genetic techniques. Using ANA-3, As(V) respiration was shown to be independent of the well-characterized *ars* detoxification system that includes a small cytoplasmic arsenate reductase, ArsC (Saltikov et al. 2003). Two genes, *arrA* and *arrB*, were required for As(V) respiration (Saltikov and Newman 2003). They were predicted to encode a *bis*-molybdopterin guanine dinucleotide (MGD)-containing member of the DMSO reductase family that directly interacts with As(V). Using these gene sequences, it was determined that *arrA* is well-conserved among almost all of the isolated bacterial As(V) respirers, and a set of degenerate PCR primers was designed and applied to show that *arrA* was expressed in Haiwee Reservoir, a site of arsenic contamination (Malasarn et al. 2004). In microcosm studies using a sediment analog that consisted of hydrous ferric oxide sorbed with As(V), the *arr* system was required for the reduction of As(V) while the *ars* system was not (Malasarn et al. 2004). Additionally, studies of *arrAB* regulation revealed that these genes are upregulated upon the shift to anaerobic conditions and in the presence of low micromolar concentrations of As(V) or nanomolar concentrations of As(III) (Saltikov et al. 2005).

The knowledge that *arrA* is required for As(V) reduction in environmental contexts and that it is expressed in arsenic-contaminated field sites prompts the investigation of post-transcriptional details of As(V) respiration that will eventually allow us to quantify and predict its contribution to the arsenic geochemical cycle. Here, we

present the characterization of ARR expression and activity in ANA-3 and in a heterologous over-expression system.

5.3. Materials and Methods

5.3.1. Bacterial Strains and plasmids.

Bacterial strains and plasmids used in this study are presented in Table 5.1.

Table 5.1. Bacterial strains and plasmids used in this study.

Bacterial strain or plasmid	Genotype or markers and characteristics and uses	Source
Shewanella sp. strain ANA-3	As(V)-respiring gram-negative bacterium isolated from a wooden pier in Eel Pond, Woods Hole, Mass.	(Saltikov et al., 2003)
E. coli		
UQ950	DH5α λ(pir) lysogen of DH5α used for cloning	D. Lies, Caltech
C43	Mutant of overexpression strain BL21 optimized for expression of membrane and toxic proteins.	(Miroux and Walker, 1996)
plasmids		
pET32H	Modified version of pET32H (Novagen) in which sequences encoding S-tag and enterokinase cleavage site were removed.	(Tochio et al., 2001)
pET32H Xa-2	Modified version of pET32H in which sequence encoding thrombin cleavage site was replaced with Factor Xa cleavage site and His_6 tag was replaced with His_9 tag.	This study
pET32HP	Modified version of pET32H in which sequence encoding thrombin cleavage site was replaced with Prescission Protease cleavage site.	L. Dietrich, Caltech

5.3.2. Activity Assays.

Respiratory As(V) reduction activity was quantified with a colorimetric assay. A reaction mix containing 120 μM methyl viologen (MV), 90 μM dithionite, 50 mM MOPS buffer at pH 7, and 0.15 M NaCl was placed into a plastic cuvette in an anaerobic

chamber. The solution was allowed to equilibrate for several seconds, then enzyme samples and electron acceptors were added. The cuvettes were stoppered before they were removed from the anaerobic chamber, and MV oxidation was measured by following loss of blue color at 600 nm using a DU7400 or a DU800 spectrophotometer (both from Beckman Coulter). Electron acceptors used in this assay include As(V), As(III), selenate, antimonate, nitrate, and dimethyl sulfoxide (DMSO) at 50 mM each. Malate dehydrogenase activity was measured by reacting 5 µL sample with 1 mL 0.1 M potassium phosphate at pH 7.5, 1 µL oxaloacetate, and 10 µL 27 mM NADH in a cuvette. NADH oxidation was followed by measuring optical density at 340 nm over 10 minutes. Alkaline phophatase activity was measured by mixing 90 µL of sample with 10 µL of 4% p-Nitrophenyl Phosphate, Disodium Salt (Sigma) in a microtiter plate. The appearance of p-Nitrophenol was followed by measuring optical density at 405 nm over 3 hours using a Synergy HT Multi-Detection Microplate Reader (BIO-TEK).

5.3.3. Protein expression dynamics.

To measure ARR expression in bacterial cultures over various phases of growth, ANA-3 cultures were grown anaerobically at 30˚C in medium containing LB Miller Broth (25 g/L), 10 mM lactate, and 10 mM As(V) at pH 7. At each time point, 50 µL of sample were withdrawn from cultures and used in activity assays in the presence and absence of As(V) to determine As(V)-dependent reduction activity. Optical density of the cultures was measured by placing 1 mL of culture into a cuvette and measuring optical density using the DU7400 spectrophotometer reading at 600 nm.

5.3.4. Filtrate Analysis.

Samples from early and late phase cultures of ANA-3 growing in As(V) medium were withdrawn and filtered through a nylon microcentrifuge filter with a 0.2 μm pore size (Costar Spin-x column) by centrifugation at 14,000 rpm for 1 min. Activity was measured simultaneously in samples that had and had not been filtered. Heat denaturation was carried out by heating the samples to 95˚C for 10 minutes.

5.3.5. Localization.

Initial fractionation separated soluble proteins from membrane bound proteins in 50 mM Tris buffer at pH 8, 50 mM PIPES buffer at pH 7, and 50 mM PIPES buffer + 0.3 M NaCl at pH 7 to account for possible differences in protein interaction due to buffer choice. Cell cultures were homogenized using a Mini-Beadbeater 8-cell Disrupter (Biospec Products, Inc.) and 0.1 mm zirconia/silica beads for 60 seconds to release the cytoplasmic contents. Additional cycles in the beadbeater did not result in increasing concentrations of protein measured by the BioRad protein assay. Unbroken cells were removed by centrifugation at 8,000 x g. Activity was measured in the remaining fraction before and after ultracentrifugation as well as in resuspended membrane fractions.

To separate the periplasmic contents from the cytoplasmic contents, cells were centrifuged and washed once in buffer containing 50 mM Tris at pH 8 and resuspended in 50 mM Tris with sucrose. EDTA was added to a final concentration of 500 μM, and lysozyme was added to a concentration of 0.3 mg/mL. The mix was allowed to sit on ice for 30 min, which corresponded to the time required for the formation of sphaeroplasts,

visualized under a light microscope. The sample was centrifuged at 10,000 x g for 10 minutes to separate the supernatant containing the periplasmic contents from the pellet containing sphaeroplasts. The sphaeroplasts were homogenized using the beadbeater. Both the periplasmic fraction and the cytoplasmic fraction were ultracentrifuged to remove contaminating membrane components.

5.3.6. Construction of over-expression vectors.

Initial attempts to over-express ARR with a C-terminal His_6 tag resulted in low affinity binding to TALON Superflow Metal Affinity Resin (Clontech). As an alternative, a truncated version of ArrA was expressed, in which the first 41 amino acids, corresponding to a predicted TAT signal cleavage, were deleted to prevent loss of the affinity tag during protein processing. Truncated *arrA* and full-length *arrB* were amplified together or individually using primers NcoarrA5-2 (5'-CAT GCC ATG GGT GCT GAA TTA CCC GCG CCT CTA-3'), XhoarrA3-2 (5'-CCG CTC GAG TCA CAC TTT CTC AAC ACG AAC-3'), NcoarrB5 (5'-CCA TGG GTA TGA GAT TAG GAA TGG TGA TT-3'), and XhoarrB3 (5'-CCG CTC GAG TTA ATA AGC GGT TTT AAC ACC-3'). The PCR protocol is as follows: 1 cycle at 95˚C for 5 minutes, followed by 33 cycles at 95˚C for 35 seconds, 58˚C for 40 seconds, and 72˚C for 2 minutes, and finishing with 1 cycle at 72˚C for 10 minutes. The Fail Safe PCR system using PreMix D (Epicentre) was used in all PCR reactions. Products were digested with Nco I and Xho I (New England Biolabs) and ligated to similarly digested vectors.

Two derivatives of the pET32H over-expression vector (Tochio et al. 2001) were used in this study: pET32H Xa-2 encodes a thioredoxin fused to a His_9 tag upstream of

the protein of interest. A Factor Xa protease cleavage site is located between the His_9 and the N-terminus of the protein of interest, however, no cleavage was performed using this construct. The presence of the His_9 tag resulted in stronger binding of the fusion protein to cobalt resin compared to a His_6 tag. This allowed higher imidazole washes and rapid partial purification of ARR, ArrA, and ArrB for some of the studies presented here. For the final purification of ARR used in kinetic studies, pET32HP (provided by Lars Dietrich, Caltech) was created in which the thrombin protease cleavage site in pET32 BamHind was replaced by a Prescission Protease (GE Healthcare Life Sciences) cleavage site. This allowed the efficient cleavage of the affinity tag from the protein at 4˚C, resulting in pure enzyme.

All constructs were sequenced to confirm that no mutations were introduced during PCR or other genetic manipulations.

5.3.7. Heterologous expression of ARR.

Over-expression of ARR was based on a previous protocol for the expression of sulfite oxidase (Temple et al. 2000). Cells were initially grown overnight aerobically in Miller LB at 37˚C. To induce, cultures were diluted 1 to 25 in fresh aerobic Miller LB supplemented with 20 mM lactate and 1 mM sodium molybdate at 30˚C and grown with shaking until they reached an optical density of 1.0 (OD 600 nM) in a standard 1 cm cuvette. The culture was then diluted 1 to 25 to anaerobic medium containing LB, 20 mM lactate, 1 mM sodium molybdate, 40 μM IPTG, and 14 mM DMSO as a terminal electron acceptor. These cultures were grown at room temperature for 18 hours, during

which time the enzyme was expressed. Cells were harvested by centrifugation at 10,000 x g for 15 minutes at 4˚C, and the resulting pellet was frozen at -80˚C until further use.

5.3.8. Purification.

Cells from 8 L of medium were resuspended in 30 mL of 50 mM Tris, 0.3 M NaCl, pH 7.0 and amended with 2 tablets of protease inhibitor cocktail. To lyse the cells, 1.26 g of CelLytic Powder (Sigma) was added to the solution, and the mix was passed through a French Press once. The crude lysate was clarified by centrifugation at 15,000 x g for 10 minutes. The resulting supernatant was added to 2 mL of washed Cobalt resin slurry and incubated on ice with gentle rocking for 2 hrs. Resin was collected by centrifugation at 500 x g for 5 minutes and washed two times with 20 mL buffer containing 5 mM imidazole followed by two washes with 10 mM imidazole. The sample was then eluted in 3 mL buffer containing 200 mM imidazole. 80 U of Prescission protease was added to the sample and allowed to cleave off the thioredoxin and His-tag for 2 hours at 4˚C. The sample was then incubated with 1 mL of gluthathione sepharose for 30 min., desalted, and incubated with 2 mL cobalt resin for 1 hr. Sample was collected using a gravity flow column and was concentrated in a Microcon Centrifugal Filter Device with a MWCO of 10 kDa centrifuged at 4˚C.

5.3.9. Size exclusion chromatography.

Size exclusion chromatography was performed on an AKTA FPLC using a 16/60 XK column prepacked with Superdex 200 Prep Grade Resin. The mobile phase

contained 50 mM Tris with 0.15 M NaCl at pH 7.0 and was run at a flow rate of 0.5 mL/minute. Protein concentration was measured using UV absorbance at 280 nm. Elution volumes were plotted against the log of the molecular weight for the standards and the best fit line was found. From this line, an equation was derived and used to calculate MW based on elution volume.

5.3.10. Protein Gel Electrophoresis.

SDS PAGE was done using a precast 12% denaturing gel (Bio-Rad). Unstained broad range standards (Bio-Rad) were used. Gel images were acquired with a Chemidoc XRS gel imager (Bio-Rad) with epi illumination.

5.3.11. Elemental Analysis.

Elemental analysis was performed with an Agilent 7500ce ICP-MS at the Molecular Instrumentation Center (MIC) at the University of California, Los Angeles.

5.4. Results

5.4.1. ARR expression dynamics.

To characterize the expression dynamics of ARR over various phases of growth, As(V)-dependent MV oxidation by ANA-3 cultures was followed (Figure 5.1.). Activity was first detected at 4 hours. This coincided with the beginning of exponential phase. Activity increased past 8 hours, at which time the OD of the culture began to decrease

dramatically from 0.25 to 0.03 at 13.5 hours. At 12 hours, activity begin to taper, although it persisted at significant levels throughout the 24-hour experiment.

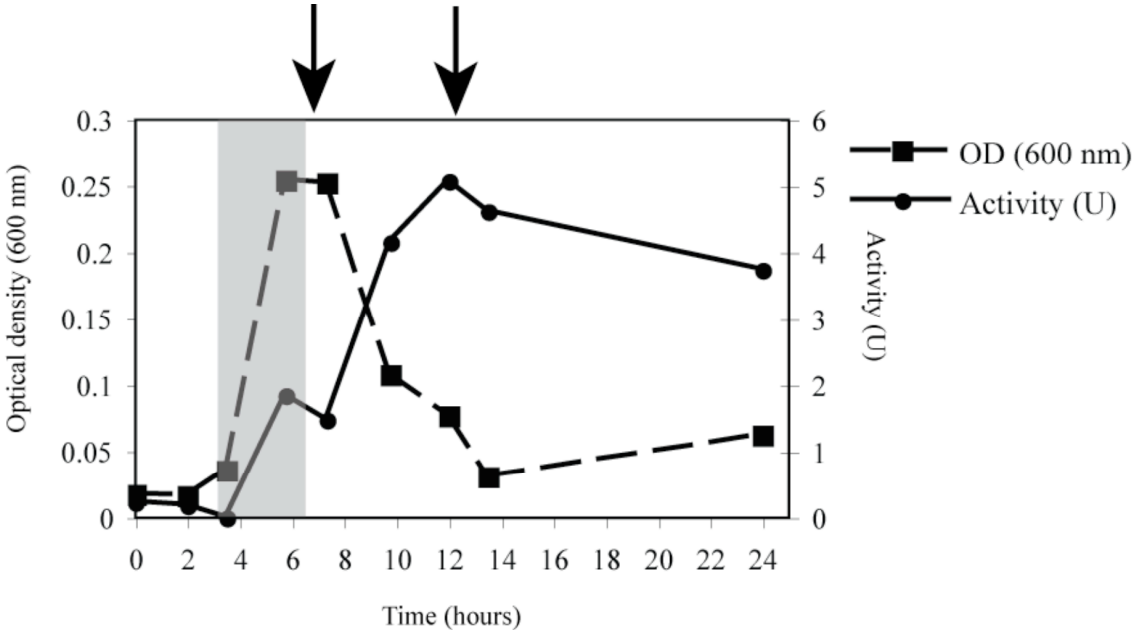

Figure 5.1. ARR expression dynamics. ARR activity (circles) and culture optical density (squares) over different growth phases for ANA-3 respiring on As(V). Gray box indicates the period at which *arrA* mRNA transcripts are expressed (based on Saltikov et al. 2003). Arrows indicate time points analyzed for release of ARR (see below).

5.4.2. Extracellular Release of ARR.

The decrease in OD in late-phase cultures was not observed when cells were growing aerobically or in the presence of other electron acceptors. To determine the fate of cells after this decrease in OD, samples from late-phase As(V)-respiring cultures were stained with 4',6-diamidino-2-phenylindole (DAPI) and visualized under fluorescence

microscopy. While a small population of normal-sized cells were seen, the majority of cells appeared to be reduced in size to ~1 μm length (Figure 5.2.A.).

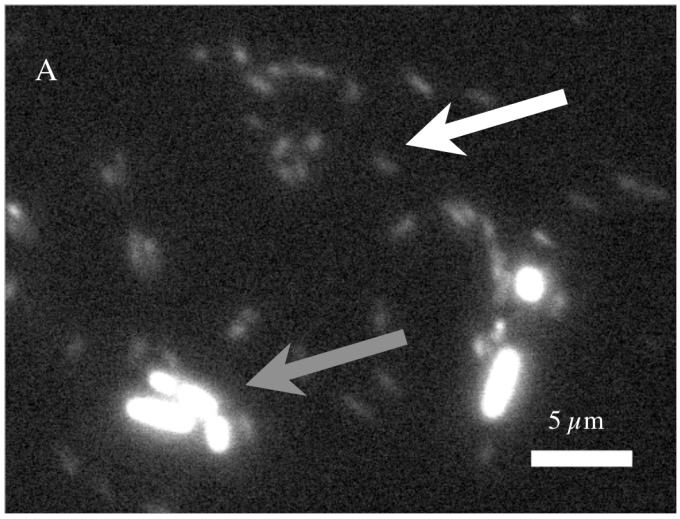

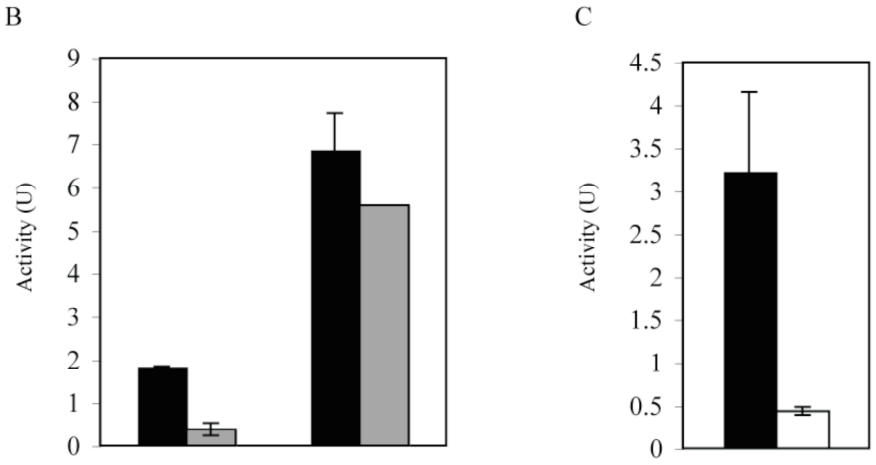

Figure 5.2. Cell dwarfing and release of ARR in late phase cultures. A. Light microscope picture of late phase As(V)-respiring cultures. Gray arrow indicates typical-sized cell. White arrow indicates dwarf. B. At 7 hours and 12.5 hours samples were collected and analyzed for ARR activity with and without filtration. Black bars indicate

total activity. Gray bars indicate filtrate activity. C. Activity in 12.5-hour filtrate without heat denaturation (black) and with heat denaturation (white).

To determine if the disparity between activity and OD was due simply to the dwarfing of cells, or if the enzyme was released into the medium, samples were taken during exponential growth (7 hours) and after the decrease in OD (12.5 hours) and assayed before and after passage through a 0.2 μm filter. At 7 hours, only 20.8% of the total activity was retained after filtration. At 12.5 hours, 81% of the activity was retained (Figure 5.2.B.). Filtrates were observed under a microscope to confirm that no cells were able to pass through the filter. Incubation of filtrates at 95˚C for 10 minutes resulted in 86% loss of the activity (Figure 5.2.C.).

5.4.3. Localization of the arsenate respiratory reductase.

To determine where the arsenate reductase is localized within intact ANA-3 cells, native activity was measured in different subcellular fractions of cells growing anaerobically in the absence of As(V) (Table 5.2.). Soluble and membrane fractions were analyzed first. To account for changes in protein-protein interactions due to buffer and salt conditions, cell samples from anaerobic cultures were washed and resuspended in three different buffers: 50 mM Tris, 50 mM PIPES, and 50 mM PIPES amended with 0.3 M NaCl. The resuspended cells were homogenized, centrifuged at 8000 x g to remove unbroken cells, and then ultracentrifuged to separate soluble and membrane fractions. With all three buffers, nearly 100% of the arsenate reductase activity was determined to be soluble. Washes were also assayed for activity to determine if the reductase was

loosely bound to the outside of the cell. Under all three conditions, no activity was found in the outer fractions. We concluded that the reductase was soluble and present on the inside of the cell.

Table 5.2. Localization of ARR in ANA-3

Enzyme	Fraction	Total Activity (%)
Fractionation 1		
Arsenate Reductase	Outer membrane-associated	0
	Soluble	100
	Membrane	0
Fractionation 2		
Arsenate Reductase	Periplasm	90
	Cytoplasm	10
Alkaline phosphatase	Periplasm	73
	Cytoplasm	27
Malate dehydrogenase	Periplasm	23
	Cytoplasm	77

In a second fractionation, the periplasmic contents were separated from the cytoplasmic fractions by incubating anaerobic cells in EDTA, lysozyme, and sucrose on ice until sphaeroplasts were formed. Samples were centrifuged to separate the periplasmic contents from the sphaeroplasts. The sphaeroplasts were then homogenized to release the cytoplasmic contents, and both the periplasm and cytoplasmic fractions were ultracentrifuged to remove contamination from membrane components. Malate dehydrogenase served as a cytoplasmic marker, and alkaline phosphatase served as a marker for the periplasm. 77% of the malate dehydrogenase activity was found in the cytoplasmic fraction. 73% of the alkaline phosphatase activity was found in the

periplasmic fraction. Under these conditions, 90% of the arsenate reductase activity was found in the periplasmic fraction compared to the cytoplasmic fraction.

5.4.4. Heterologous expression of the arsenate respiratory reductase.

Members of the DMSO reductase family all possess a molybdopterin cofactor assembled by the anaerobically expressed *moa* and *mod* operons. At the center of this cofactor is either a Mo or W atom that serves as the electron donor or acceptor in the catalyzed redox reaction. To characterize the conditions required for the assembly of active arsenate reductase, *arrA* and *arrB* were inserted into an overexpression vector, introduced into C43 *E. coli* cells, and cells were induced under different conditions (Figure 5.3.). Under all conditions tested, both ArrA and ArrB were expressed at similar levels relative to background proteins. Cultures grown in the presence of oxygen and molybdate showed 55.28 ± 14.29 μmol As(V) reduced · min^{-1} · mg $protein^{-1}$ activity. This rate increased to 152.54 ± 52.54 μmol As(V) reduced · min^{-1} · mg $protein^{-1}$ activity when cells were induced under anaerobic conditions still in the presence of molybdate. No activity was found when tungstate was added nor in the presence of no supplemental metal.

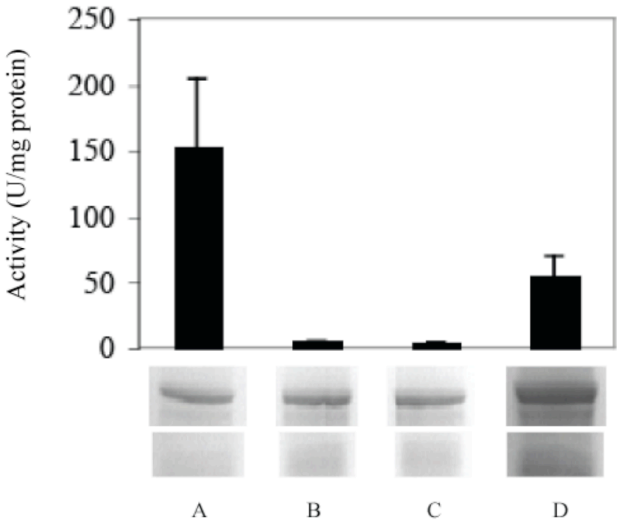

Figure 5.3. Expression of ARR under varying conditions. Activity in crude lysates was measured after cells were induced under (A) anaerobic conditions with 1mM sodium molybdate, (B) anaerobic conditions with 1 mM sodium tungstate, (C) anaerobic conditions with no metal supplement, and (D) aerobic conditions with sodium molybdate.

5.4.5. Purification of ArrAB, ArrA, and ArrB.

Overexpressed ArrAB was purified with affinity chromatography (Figure 5.4.). Two subunits were present when the purified sample was run on an SDS PAGE gel, one with a molecular weight of 95 kDa and one at 27 kDa. Mass spectrometry showed that each of the visible bands only consisted of a single protein and confirmed that the identity of these subunits were ArrA and ArrB from *Shewanella* sp. strain ANA-3, respectively. 17 fragments of ArrA were identified, which covered 32% of the protein sequence. 5 fragments of ArrB were identified, which covered 16% of the protein sequence. Size exclusion chromatography using a 16/60 gel filtration column and Superdex 200 prep

grade resin determined the molecular size of the reductase to be 131 kDa, consistent with the reductase being a heterodimer composed of one ArrA and one ArrB subunit. Overexpressed ArrA and ArrB were also partially purified individually to ~50% purity for activity assays and reconstitution experiments.

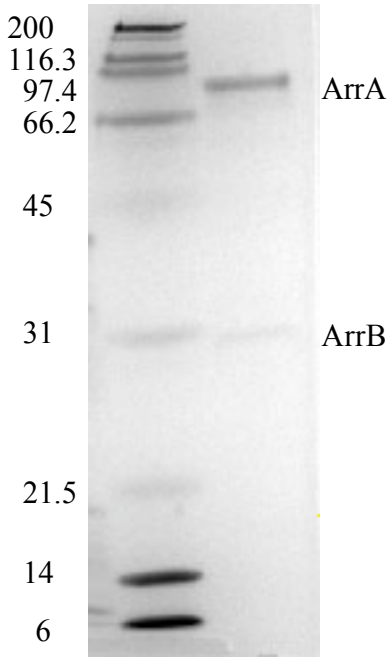

Figure 5.4. SDS PAGE of purified ARR. Protein was stained with Bio-Safe Coomassie dye (Bio-Rad). Lane A: Bio-Rad SDS-PAGE Standards, Broad Range (Myosin, 200 kDa; ß-Galactosidase, 116.25 kDa; Phosphorylase b, 97.4 kDa; Bovine serum albumin, 66.2 kDa; Ovalbumin, 45 kDa; Carbonic anhydrase, 31 kDa; Trypsin inhibitor, 21.5 kDa; Lysozyme 14.4 kDa; Aprotinin, 6.5 kDa). Lane B: Purified ARR from C43 overexpression cells.

5.4.6. Cofactor Composition.

Elemental analysis of the purified active ARR revealed a stoichiometry of 1.35 mol Mo: 23.5 mol inorganic S: 16.5 mol Fe per mole of enzyme. Analysis of the ARR induced in the presence of W revealed a stoichiometry of 0.15 mol W per mol enzyme, suggesting that the metal was not incorporated into the protein.

5.4.7. Activity.

Arsenate respiratory reductase activity was measured using a colorimetric assay that couples MV oxidation to As(V) reduction. No activity was measured when ArrA or ArrB were heterologously expressed alone or when they were combined after expression (Figure 5.5.). However, when ArrA and ArrB were expressed together, a K_m of 5μM and a V_{max} of 11,111 μmol As(V) reduced · min^{-1} · mg $protein^{-1}$ were measured (Figure 5.6.). The presence of 50 mM As(III) or 50 mM phosphate in addition to As(V) did not affect activity. Additionally, ARR showed no activity in the presence of arsenite, selenate, sulfate, nitrate, dimethyl sufoxide (DMSO), or antimonate.

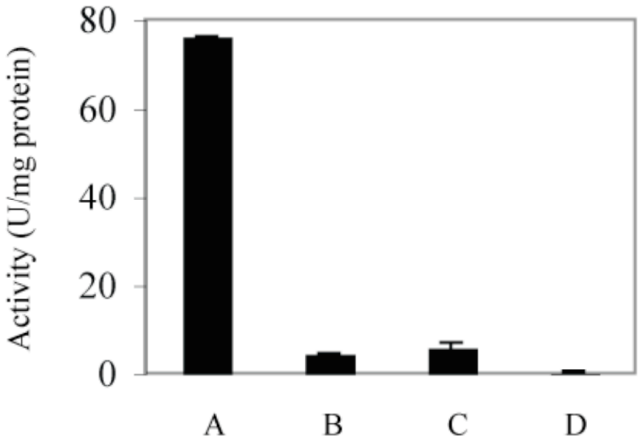

Figure 5.5. Activity of individual subunits. Activity in crude lysates from C43 cells expressing (A) ARR heterodimer, (B) ArrA alone, (C) ArrB alone, or (D) ArrA mixed with ArrB after independent induction of each subunit.

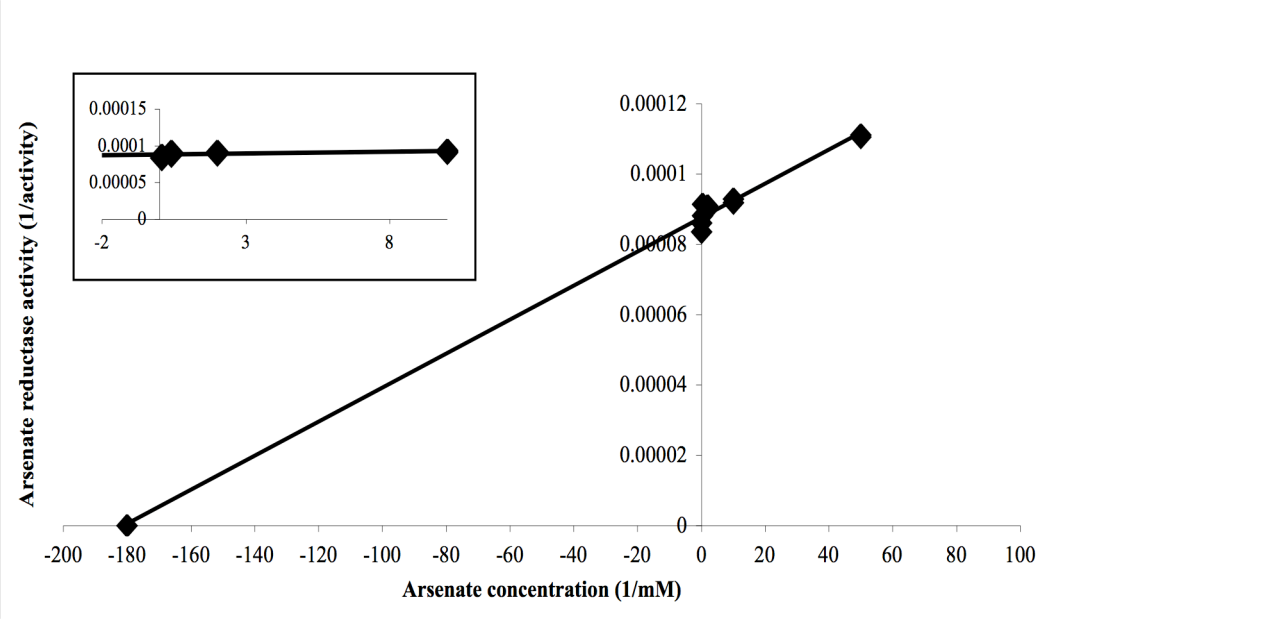

Figure 5.6. Lineweaver Burk Plot of ARR activity. ARR activity was calculated by following MV oxidation in an anaerobic colorimetric assay. Inset shows magnified view of larger plot between -2 and 10 1/mM As(V).

5.5. Discussion

Characterization of the properties of ARR is required to predict and quantify the contribution of the enzyme to the arsenic geochemical cycle. Here we present work focused on ARR expression and activity from the genetically tractable bacterium *Shewanella* sp. strain ANA-3. This study includes the heterologous over-expression of ARR in *E. coli*, which will facilitate future crystallographic studies.

In a previous study of gene expression during growth of ANA-3 in As(V) medium, *arrA* was upregulated at the beginning of exponential phase, reached maximal expression before the peak in optical density was attained, and decreased significantly

upon the onset of exponential phase and the following decrease in optical density (Saltikov et al. 2005). Our observation of ARR activity during growth determined that enzyme activity also began at the start of exponential growth, suggesting the lack of additional extracellular signals required for post-transcriptional upregulation. The persistence of ARR activity beyond the time point at which *arrA* transcripts are detectable suggests that the enzyme has a half life of at least several hours and does not require constant regeneration. Thus, in the environment, the identification of *arrA* mRNA transcripts implies the activity of ARR, however, ARR may also be active when *arrA* mRNA transcripts cannot be detected. The presence of proteases may shorten the lifetime of the enzyme.

In late phase cultures, cells growing on As(V) shrunk and/or lysed and released ARR into the medium. Once released, the enzyme retained activity for several hours, showing that it is relatively stable in solution at 30˚C. The release of enzyme into the medium suggests that the properties of ARR in both whole cells and pure enzyme samples may be directly relevant to environmental studies. And, though, to our knowledge, supernatant filtrates of other isolated As(V) respirers have not been studied, the drop in optical density of cultures growing on As(V) was observed when multiple species of As(V)-respiring bacteria were grown in our laboratory for other studies, suggesting that this phenomenon is not specific only to ANA-3. The presence of cell-free ARR in the environment may be relevant if electron donors with sufficiently low redox potentials are present to allow the enzyme to catalyze As(V) reduction. Small molecules such as phenazines (Price-Whelan et al. 2006) or humic substances (Hernandez and Newman 2001) may serve this purpose, though this hypothesis needs to be tested.

Within intact cells, the periplasmic localization of ARR allows the cell to couple As(V) reduction to energy production before As(V) can be transported to the cell cytoplasm and enter the *ars* detoxification pathway, an energy-requiring process. In environmental contexts where As(V) is present at micromolar or nanomolar concentrations, the activity of ARR may be sufficient to reduce all of the available As(V) without requiring the activity of ArsC at all. Consistent with this, our previous studies of ANA-3 with or without ArrA suggest that the ArsC arsenate reductase does not contribute significantly to total As(V) reduction when soluble As(V) concentrations are low (Malasarn et al. 2004; Campbell et al. 2006).

The periplasmic localization of ARR also corroborates the idea that As(V) must desorb from sediments prior to reduction. This transient dissociation may be responsible for arsenic mobilization if water flow transports the As(III) as soon as it exits the cell from environments capable of sequestering it, such as Fe rich sediments, to environments that cannot sequester it, such as those dominated by aluminum oxides, manganese oxides, or silicate and carbonate minerals (Polizzotto et al. 2005). Such a model has been proposed for sediments in Bangladesh, in which the source of contaminating arsenic is thought to be Fe-rich surface sediments where As(V) respiration and Fe reductive dissolution are active. The resulting As(III) is thought to avoid readsorption and flow to sediments dominated by silicate and carbonate minerals present at well-depth in subsurface aquifers (Polizzotto et al. 2005).

Metal cofactors associated with ARR are essential to its activity. Other members of the DMSO reductase family are characterized as having a tungsten or molybdenum atom coordinated to the sulfur atoms of the molybdenum guanine dinucleotide cofactors.

The ability of an enzyme to use Mo or W is thought to depend on metal availability under which the enzyme is assembled and other currently unidentified factors involved in insertion of the metal into the enzyme active site (Johnson et al. 1996). Early studies predicted that the tungstoenzyme members were adapted for low redox potential reactions such as the conversion of formate to CO_2, which has a redox potential of -432 mV (Johnson et al. 1996). Molybdoenzymes, on the other hand, were thought to be more tolerant to oxygen and involved in reactions that have higher redox potentials. Recently, however, both the tungsto- and molybdo- forms of the same enzyme have been purified in various studies. The TMAO reductase from *E. coli* showed increased activity upon replacement of the native molybdenum atom with tungsten; this form was also capable of reducing DMSO coupled to growth (Buc et al. 1999). In *Rhodobacter capsulatus*, the DMSO reductase is active with either tungsten or molybdenum in its active site, although only the molybdenum-substituted form is capable of catalyzing the reverse reaction of oxidizing DMS (Stewart et al. 2000). These cells required nanomolar concentrations of molybdenum to produce active tungstoenzyme, and this phenomenon was thought to have arisen due to (1) the requirement for Mo to be involved in the biosynthesis of the molybdopterin cofactor or (2) the requirement for Mo to activate the molybdate/tungstate transporter repressor, ModE, that would prevent tungsten from accumulating to toxic levels inside the cell. In our studies, induction of ARR in the presence of 1 mM tungstate resulted in inactive protein that did not incorporate tungsten, but the inactive form does not seem to be inhibited by either of the processes mentioned above. Because induction was allowed to occur for 18 hours in cells growing with DMSO as an electron acceptor, active DMSO reductase was required, suggesting that the assembly of the molybdopterin

cofactor proceeded normally and tungsten did not accumulate to high enough levels to inhibit growth. Thus, other mechanisms must be involved in the exclusion of W from ARR.

The inhibition of ARR by oxygen can be explained by two possibilities. First, oxygen may inactivate properly expressed protein by degrading or converting essential Fe-S clusters (Beinert et al. 1997) or by affecting the thiolate ligands in the molybdenum cofactor (Adams et al. 1999; Bray et al. 2000). Alternatively, assembly of ARR may require enzymes that are only expressed under anaerobic conditions. Such a requirement has been observed for other DMSO reductase family members. The assembly of the molybdopterin cofactor, for example, is known to be dependent on the *moa* and *mod* operons, both of which are expressed under anaerobic conditions. Regardless of the mechanism involved, the inhibition of activity in the presence of oxygen is relevant in environmental settings where sediments are frequently exposed to open air. Such a situation was observed in Haiwee Reservoir, where water levels frequently drop below the surface level of sediments (Kneebone et al. 2002). The suggestion that contaminating arsenic originates in surface sediments in Bangladesh (Polizzotto et al. 2005) may also mean that As(V)-respiring bacteria are exposed to oxygen. The extent to which these aeration events decrease the level of As(V) reduction presents an important area of study; aeration may also serve as an effective inhibitor of As(V) reduction.

Characterization of the purified enzyme determined that it is a heterodimeric protein consisting of one large A subunit and one small B subunit. These characteristics are identical to ARR from *C. arsenatis* and differ from ARR in *B. selenitireducens* only in that the *B. selenitireducens* enzyme is associated with membrane fractions prior to

solubilization with detergent (Table 5.3.). *C. arsenatis* ARR has a K_m of 0.3 mM and a V_{max} of 7,013 μmol As(V) reduced · min^{-1} · mg $protein^{-1}$. Mo, Fe, acid-labile sulfur, and zinc were all found to be associated with the enzyme. ARR from *B. selenitireducens* has a K_m of 34 μM and a V_{max} of 2.5 μmol As(V) reduced · min^{-1} · mg $protein^{-1}$. Molybdenum and iron were also found to be associated with it, but stoichiometry was low, suggesting that a significant amount of metal was lost during purification. Kinetic characterization of the heterologously expressed protein from ANA-3 showed that it has the lowest K_m and the highest V_{max} of the three studied enzymes. Interestingly, the K_m of 5 μM As(V) is within the concentration range of 1-10 μM As(V) required to upregulate *arr* gene expression in anaerobically growing ANA-3 cells (Saltikov et al. 2005), suggesting that these concentrations are physiologically relevant. The stoichiometry of the metal cofactors associated with ANA-3 ARR is consistent with each enzyme molecule having 1 Mo atom, 4 S atoms associated with the *bis*-MGD cofactor, and 4-5 [4Fe-4S] clusters, 4 associated with ArrB and possibly one associated with ArrA, as is present in other members of the DMSO reductase family.

Table 5.3. Summary of properties of ARR

	Shewanella sp. strain ANA-3	*Chrysiogenes arsenatis*	*Bacillus selenitireducens*
K_m (μM)	5	300	34
V_{max} (U/mg protein)	11,111	7,013	2.5
Stoichiometry	$\alpha_1\beta_1$	$\alpha_1\beta_1$	$\alpha_1\beta_1$
Localization	Periplasm	Periplasm	Membrane associated
Metal stoichiometry per mole enzyme	1.3 Mo: 16.5 Fe: 23.5 inorg. S	0.89 Mo: 14 Fe: 16.4 inorg. S: 0.67 Zn	0.18 Mo: 9 Fe
Substrate specificity	Arsenate only	Arsenate only	Arsenate, arsenite, selenate, selenite

Unlike ARR from *B. selenitireducens*, which could reduce As(III), selenate, and selenite, in addition to As(V), ARR from ANA-3 was not able to reduce any of the alternate substrates assayed here. Such variations in substrate specificity have been observed for other members of the DMSO reductase family (Ridge et al. 2002). An understanding of the active site environment and mechanism of substrate binding will help to determine the amino acid sequence involved in these differences in substrate specificity.

Heterologous expression of the independent subunits ArrA and ArrB resulted in no As(V) reductase activity. Taken together with the facts that (1) the two genes encoding these proteins are found adjacent to one another in all of the sequenced As(V) respirers (Saltikov and Newman 2003; Murphy and Saltikov 2007) and (2) ArrA and ArrB are associated with one another in every purification to date (Krafft and Macy 1998; Afkar et al. 2003), this provides substantive evidence that the two subunits function together *in vivo*. The lack of activity upon mixing the subunits together may suggest that ArrA and ArrB are also dependent on each other for proper assembly. Such a requirement has been observed in other molybdoenzymes such as nitrogenase, in which

the Fe-protein is required for both the maturation of the Fe-Mo cofactor and for maturation of the Mo-Fe protein (Christiansen et al. 1998).

Recently, it has been determined that *cymA*, a gene encoding a membrane-bound c-type cytochrome is required for As(V) respiration in *Shewanella* sp. strain ANA-3 and *Shewanella putrefaciens* strain CN-32 (Murphy and Saltikov 2007). It was suggested that CymA is the site of interaction between ARR and the rest of the electron transport chain. As this cytochrome is also known to participate in other modes of respiration, such as Fe(III)-, Mn(IV)-, and fumarate-respiration, these results suggest that ArrA and ArrB form the minimal set of unique proteins required to confer As(V)-respiring ability among anaerobic bacteria.

To extend the findings reported here to the environment, techniques to detect and quantify the abundance of ARR in the field are required. The purification of ARR may allow the production of antibodies or other probes that can be used identify the enzyme in environmental samples. Additionally, heterologous expression of an affinity tagged version of ARR will allow structural studies that can elucidate the mechanism by which this enzyme functions and possibly result in the development of specific inhibitors for As(V) respiration. Lastly, the differences observed in the properties of ARR from the different bacteria discussed here elicits the need for additional comparitive studies.

5.6. Acknowledgements

We thank Jim Howard, Doug Rees, and Steve Mayo for valuable discussions.

5.7. References

Adams, B., A. T. Smith, et al. (1999). "Reactions of dimethylsulfoxide reductase from Rhodobacter capsulatus with dimethyl sulfide and with dimethyl sulfoxide: complexities revealed by conventional and stopped-flow spectrophotometry." Biochemistry **38**(26): 8501-11.

Afkar, E., J. Lisak, et al. (2003). "The respiratory arsenate reductase from Bacillus selenitireducens strain MLS10." FEMS Microbiol Lett **226**(1): 107-12.

Ahmann, D., A. L. Roberts, et al. (1994). "Microbe grows by reducing arsenic." Nature **371**(6500): 750.

Beinert, H., R. H. Holm, et al. (1997). "Iron-sulfur clusters: nature's modular, multipurpose structures." Science **277**(5326): 653-9.

Bray, R. C., B. Adams, et al. (2000). "Reversible dissociation of thiolate ligands from molybdenum in an enzyme of the dimethyl sulfoxide reductase family." Biochemistry **39**(37): 11258-69.

Buc, J., C. L. Santini, et al. (1999). "Enzymatic and physiological properties of the tungsten-substituted molybdenum TMAO reductase from Escherichia coli." Mol Microbiol **32**(1): 159-68.

Campbell, K. M., D. Malasarn, et al. (2006). "Simultaneous microbial reduction of iron(III) and arsenic(V) in suspensions of hydrous ferric oxide." Environ Sci Technol **40**(19): 5950-5.

Christiansen, J., P. J. Goodwin, et al. (1998). "Catalytic and biophysical properties of a nitrogenase Apo-MoFe protein produced by a nifB-deletion mutant of Azotobacter vinelandii." Biochemistry **37**(36): 12611-23.

Harvey, C. F., C. H. Swartz, et al. (2002). "Arsenic mobility and groundwater extraction in Bangladesh." Science **298**(5598): 1602-6.

Hernandez, M. E. and D. K. Newman (2001). "Extracellular electron transfer." Cell Mol Life Sci **58**(11): 1562-71.

Johnson, M. K., D. C. Rees, et al. (1996). "Tungstoenzymes." Chem Rev **96**(7): 2817-2840.

Kneebone, P. E., P. A. O'Day, et al. (2002). "Deposition and fate of arsenic in iron- and arsenic-enriched reservoir sediments." Environ Sci Technol **36**(3): 381-6.

Krafft, T. and J. M. Macy (1998). "Purification and characterization of the respiratory arsenate reductase of Chrysiogenes arsenatis." Eur J Biochem **255**(3): 647-53.

Malasarn, D., C. W. Saltikov, et al. (2004). "arrA is a reliable marker for As(V) respiration." Science **306**(5695): 455.

Miroux, B. and J. E. Walker (1996). "Over-production of proteins in Escherichia coli: mutant hosts that allow synthesis of some membrane proteins and globular proteins at high levels." J Mol Biol **260**(3): 289-98.

Murphy, J. N. and C. W. Saltikov (2007). "The cymA gene encoding a tetraheme c-type cytochrome is required for arsenate respiration in Shewanella species." J Bacteriol.

Newman, D. K., E. K. Kennedy, et al. (1997). "Dissimilatory arsenate and sulfate reduction in Desulfotomaculum auripigmentum sp. nov." Arch Microbiol **168**(5): 380-8.

Nickson, R., J. McArthur, et al. (1998). "Arsenic poisoning of Bangladesh groundwater." Nature **395**(6700): 338.

Polizzotto, M. L., C. F. Harvey, et al. (2005). "Processes conducive to the release and transport of arsenic into aquifers of Bangladesh." Proc Natl Acad Sci U S A **102**(52): 18819-23.

Price-Whelan, A., L. E. Dietrich, et al. (2006). "Rethinking 'secondary' metabolism: physiological roles for phenazine antibiotics." Nat Chem Biol **2**(2): 71-8.

Ridge, J. P., K. F. Aguey-Zinsou, et al. (2002). "Site-directed mutagenesis of dimethyl sulfoxide reductase from Rhodobacter capsulatus: characterization of a Y114 → F mutant." Biochemistry **41**(52): 15762-9.

Saltikov, C. W., A. Cifuentes, et al. (2003). "The ars detoxification system is advantageous but not required for As(V) respiration by the genetically tractable Shewanella species strain ANA-3." Appl Environ Microbiol **69**(5): 2800-9.

Saltikov, C. W. and D. K. Newman (2003). "Genetic identification of a respiratory arsenate reductase." Proc Natl Acad Sci U S A **100**(19): 10983-8.

Saltikov, C. W., R. A. Wildman, Jr., et al. (2005). "Expression dynamics of arsenic respiration and detoxification in Shewanella sp. strain ANA-3." J Bacteriol **187**(21): 7390-6.

Smith, A. H., E. O. Lingas, et al. (2000). "Contamination of drinking-water by arsenic in Bangladesh: a public health emergency." Bull World Health Organ **78**(9): 1093-103.

Stewart, L. J., S. Bailey, et al. (2000). "Dimethylsulfoxide reductase: an enzyme capable of catalysis with either molybdenum or tungsten at the active site." J Mol Biol **299**(3): 593-600.

Temple, C. A., T. N. Graf, et al. (2000). "Optimization of expression of human sulfite oxidase and its molybdenum domain." Arch Biochem Biophys **383**(2): 281-7.

Tochio, H., M. M. Tsui, et al. (2001). "An autoinhibitory mechanism for nonsyntaxin SNARE proteins revealed by the structure of Ykt6p." Science **293**(5530): 698-702.

Chapter 6

Conclusions

6.1 Summary

The work in this thesis explores bacterial arsenate respiration on a molecular level and an environmental level. Genetic techniques were used to determine if *arrA*, a gene required for As(V) respiration, was conserved among several isolated As(V)-respirers. This information was used to design a set of degenerate PCR primers that could be used as a marker for arsenate respiration in environmental settings. The genetic techniques were combined with chemical and environmental work to determine the relevance of arsenate respiration in Haiwee Reservoir, a site that is dominated by arsenic-sorbed iron sediments. The impact of arsenate respiration on iron reduction was also explored. In a series of microcosm studies using pure strains and natural microbial consortia from Haiwee Reservoir, rates of arsenate respiration on iron reduction were compared. Then, the expression and activity of ARR was characterized using native protein from ANA-3 and heterologously expressed ARR. The knowledge gained from the biochemical work brings us closer to being able to quantify and predict the contribution of this unique metabolism to the geochemistry of arsenic as well as more detailed studies of electron transport through the protein. With the work presented here, the questions posed in chapter 1 can now be revisited.

6.1.1. Is there a molecular marker for respiratory As(V) reduction? If so, can we use this marker to determine if As(V) respiration is active and significant in contaminated environments?

arrA sequence from seven previously identified arsenate-respirers ranged from 43-100% identical at the nucleotide level and 61-100% identical at the amino acid level, suggesting that the gene was highly conserved. This allowed us to develop a set of degenerate primers that could be used to amplify a diagnostic region of the gene from enrichment cultures or naturally occurring bacterial consortia. Using these primers as a marker for gene expression, microcosm studies showed that the gene was required for the reduction of As(V) when it is sorbed onto hydrous ferric oxide sediments. We also determined that the gene was expressed in contaminated sediments located at Haiwee Reservoir.

6.1.2. How does respiratory As(V) reduction impact bacterial dissimilatory iron reduction, another microbial metabolism that may influence arsenic mobilization?

Aside from being important to the reduction of As(V) sorbed onto solid sediments, arsenate respiration increased the rates of iron reduction in microcosm studies. First, using natural microbial consortia from Haiwee Reservoir, we observed that As(V) reduction occurred simultaneously with or prior to iron reduction. This result was reproducible using multiple carbon sources that would have changed microbial

populations, suggesting that it is a common phenomenon, probably resulting from cells wanting to harvest energy from the most thermodynamically favored electron acceptor available. We repeated this experiment with *Shewanella* sp. strain ANA-3 and ANA-3Δ*arrA* in the presence of As(V)/HFO, As(III)/HFO, or HFO alone and showed that the presence of As(III) increased rates of iron reduction. To explain why the sorption of As(III) onto HFO might increase iron reduction, a series of experiments were performed to identify differences in the properties of As(V)/HFO, As(III)/HFO, and HFO alone. Subtle changes in surface morphology and the presence of smaller iron particles in As(III)/HFO were observed, possibly providing cells with a larger amount of sediment surface area by which they can access the iron.

6.1.3. What are the dynamics of post-transcriptional expression of ARR, and what mechanisms are involved in the assembly of active enzyme?

Post-transcriptional expression of ARR occurs under anoxic conditions at the beginning of exponential growth, correlating to the onset of *arrA* gene expression. ARR persists in cells well after *arrA* transcription stops, and, in late phase cultures, ARR is released from the cells and active in the culture medium for several hours. ARR is localized in the periplasm of ANA-3, giving the enzyme access to any imported As(V) before the toxin enters the energy-requiring cytoplasmic detoxification system. ARR is a soluble heterodimer, containing Mo, Fe, and S in stoichiometric ratios that are consistent with it having a *bis*-molybdenum guanine dinucleotide cofactor and 4-5 [4Fe-4S]

clusters. It requires Mo for activity and its assembly is partially inhibited by oxygen. It has a K_m of 5μM and a V_{max} of 11,111 μmol As(V) reduced · min^{-1} · mg $protein^{-1}$.

6.2 Future Directions

The work presented here identifies *arrA* as a key gene involved in As(V) reduction and iron reduction in environmental contexts. With the development of methods for studying ARR on a biochemical level, multiple areas of study can now be pursued to more precisely describe the role of As(V) respiration in the environment. First, structural studies of ARR will help to determine the mechanism by which the enzyme interacts and reduces As(V). These studies may also allow the development of specific inhibitors to ARR. Since ARR is a member of the DMSO reductase family, structural studies and comparative studies of ARR from different microbes will also help to identify the amino acid residues involved in determining substrate specificity and the evolutionary relationships of the members in this interesting class of enzymes. Second, the availability of purified enzyme will allow the production of antibodies or other probes that can be used to visualize ARR in environmental samples. Ideally, researchers will be able to couple measurements of the abundance of ARR with kinetic data to get rough estimates of As(V) reduction in specific field sites. Third, interaction studies and genetic screens can be used to identify regulators and additional components of the electron transport chain used in As(V) respiration. In organisms that can utilize several alternative electron acceptors, such as *Shewanella*, the evolution of modularity in the electron

transport chain and the mechanism by which terminal reductases are regulated offers an exciting and challenging field of study.

To obtain a full understanding of arsenic geochemistry, the integration of work from various disciplines is required. Already, data from hydrological studies, chemical studies, mineralogical studies, and biological studies have been integrated to form our current model for the sources and causes of arsenic mobilization in Bangladesh and other locations. Ultimately, the fastest way to protect the people of Bangladesh from chronic arsenic exposure will probably rely on filtration methods and the provision of cleaner water supplies. But, the knowledge acquired through studies focused on the causes of mobilization may allow us to predict when arsenic contamination will occur in other environments and prevent such a disaster from ever repeating.

Appendix A

Detecting *in situ* Expression of arrA with Degenerate PCR

This appendix includes sections from:

Saltikov, C. W., D. Malasarn. "Arsenic Respiring Bacteria" published in The Manual of Environmental Microbiology, 3rd edition (2006).

A.1. Abstract

A method for determining the presence and expression of the arsenate respiratory reductase gene, *arrA*, using degenerate PCR is presented. This work is an elaboration of the previously published work in Malasarn et al. (Malasarn et al. 2004).

A.2. Introduction

Respiratory As(V) reduction has been implicated in arsenic mobilization around the world. However, As(V)-respiring bacteria are phylogenetically diverse and, therefore, cannot be detected using 16S rRNA gene sequences (Oremland and Stolz 2003). One must turn to functional genes for the detection of this metabolism.

The key gene involved in respiratory arsenate reductase is *arrA* (Saltikov and Newman 2003), and the gene product, ArrA, is highly conserved among several arsenate respiring bacteria. The arsenate respiratory reductase is sufficient to reduce arsenate when it is sorbed onto environmentally relevant substrates such as hydrous ferric oxide, and expression of *arrA* correllate to the observed reductase activity (Malasarn et al. 2004). Here, we present a method for detecting DNA or RNA transcripts of *arrA* using PCR and a set of degenerate primers. This method allows the identification of expressed *arrA* genes without the need for culturing bacterial strains in a laboratory setting.

A.3. Methods

A.3.1. Identification of conserved regions and primer design

To design degenerate primers, sequences for *arrA* genes from *Shewanella* sp. strain ANA-3, *Chrysiogenes arsenatis*, *Bacillus selenitireducens, Bacillus arsenicoselenatis, Wolinella Succinogenes, Desulfitobacterium hafniense*, and *Sulfurospirillum barnesii* were aligned using Clustal X. Conserved regions were identified using Block Maker. Regions that shared similarity with other genes in the DMSO reductase family were eliminated, and two of the remaining three blocks were used to design COnsensus-DEgenerate Hybrid Oligonucleotide Primers (CODEHOP) (Rose et al. 2003) by visual inspection. The resulting primers were ArrAfwd (5'-AAGGTGTATGGAATAAAGCGTTTgtbgghgaytt-3') with a calculated degeneracy of

18 and ArrArev (5'-CCTGTGATTTCAGGTGCCcaytyvggngt-3') with a degeneracy of 48.

A.3.2. Primers and PCR conditions

Primers ArrAfwd and ArrArev were used at 0.5 µM per reaction. The PCR conditions used began with an initial incubation at 95˚C for 10 minutes, followed by 40 cycles of 95˚C for 15 seconds, 50˚C for 40 seconds, and 72˚C for 60 seconds. Taq polymerase was used in all reactions.

The current primer set amplifies a ~160-200 bp fragment and is appropriate for quantitative PCR studies. However, for diversity studies, a larger arrA PCR product is helpful. The development of a second-generation consensus *arrA* primer set should be possible given the high degree of amino acid sequence conservation among known ArrAs.

A.3.3. Nucleic Acid Extraction

A number of DNA and RNA extraction methods have been developed for sediments, soils, and water (Zhou et al. 1996). Companies such as MoBio and Q-Biogene have also developed rapid and reliable nucleic acid extraction kits that have been widely used in environmental microbiological studies. Kits such as these allow the standardization of extraction methods and reduce the technical challenge often associated with environmental nucleic acid work. These kits should be used with caution on low

biomass samples and should be validated for efficiency and reproducibility on each sediment type under investigation.

For laboratory experiments involving HFO, we have developed a modified protocol for dissolving solid iron prior to DNA and RNA extractions. In this method, an HFO suspension is centrifuged and the pellet is dissolved with 0.3 M oxalic acid (pH 3). Cells can then be harvested by centrifugation for nucleic acid extraction using standard techniques, such as the TRIzol reagent (Invitrogen) for RNA extraction and the DNeasy Tissue Kit (Qiagen) for DNA extraction. By dividing samples in half, *arrA* can be quantified in RNA and DNA extracted from the same sample. This procedure should be done rapidly to avoid lysis of cells upon the addition of oxalic acid.

A.3.4. Controls

The high number of PCR cycles required for significant amplification can easily lead to false positives as a result of cross contamination between samples or through other sources. Extreme care must be taken when mixing PCR reactions, such as wearing gloves and using filtered pipette tips. Additionally, PCR tubes can be autoclaved prior to the experiment. A negative control containing all reagents used in the test reactions but lacking DNA or cDNA should be included.

With environmental samples, contaminants such as iron can inhibit PCR reactions. These contaminants can result in false negative results. To control for this, reactions in which the sample to be analyzed is amended with verified copies of the *arrA* gene should be included to ensure that DNA can be successfully amplified. If an inhibitor is present, dilution of the environmental sample may increase amplification.

In some cases, no fragment can be visualized on a standard agarose gel, even when some amplification was successful. Running a positive control alongside samples will identify the gel position where the amplicon should be. Excision of a gel band at this position and cloning the fragments with standards kits such as the TOPO TA Cloning Kit (Invitrogen), even when no band is visible, may still allow the identification of gene fragments.

A.3.5. Characterization of amplified products

Any amplified fragments should be cloned and sequenced to determine their sequence identity to known *arrA* genes. Because the length of the amplicon is relatively short, methods to identify more sequence, such as inverse PCR, can be used based on this initial sequence when sufficiently pure sample is available. Using additonal conserved areas of the gene, new primer sets can be designed to provide additional sequence information. To this end, alternative primer sets have been designed by other researchers (Perez-Jimenez et al. 2005).

It should be noted that, in our sample set, amplified fragments from the epsilon proteobacteria *Wolinella* and *Sulfurospirillum barnesii* were ~40 bp longer than fragments from other phylogenetic groups (Malasarn et al. 2004). Differences between gene products due to this extra sequence have not been studied.

A.4. References

Malasarn, D., C. W. Saltikov, et al. (2004). "*arrA* is a reliable marker for As(V) respiration." Science **306**(5695): 455.

Oremland, R. S. and J. F. Stolz (2003). "The ecology of arsenic." Science **300**(5621): 939-44.

Perez-Jimenez, J. R., C. DeFraia, et al. (2005). "Arsenate respiratory reductase gene (*arrA*) for *Desulfosporosinus* sp. strain Y5." Biochem Biophys Res Commun **338**(2): 825-9.

Rose, T. M., J. G. Henikoff, et al. (2003). "CODEHOP (COnsensus-DEgenerate Hybrid Oligonucleotide Primer) PCR primer design." Nucleic Acids Res **31**(13): 3763-6.

Saltikov, C. W. and D. K. Newman (2003). "Genetic identification of a respiratory arsenate reductase." Proc Natl Acad Sci USA **100**(19): 10983-8.

Zhou, J. Z., M. A. Bruns, et al. (1996). "DNA recovery from soils of diverse composition." Appl Environ Microbiol **62**(2): 316-322.

Appendix B

Homology Modeling and Mutational Analysis of ARR

B.1. Abstract

The arsenate respiratory reductase reduces arsenate, As(V), to arsenite, As(III), as part of the electron transport chain. Structural information of ARR will help us to understand its mechanism and substrate binding characteristics. Homology modeling of ARR identified conserved domains that are shared with the large and small subunits of other members of the DMSO reductase family. Potential ligands to the metal cofactors present in the enzyme were identified. And, mutational analysis of a protein region that was previously determined to be unique to ARR was carried out to show that it was important for enzyme function.

B.2. Introduction

The DMSO family of oxidoreductases are characterized by the presence of a *bis*-molybdenum guanine dinucleotide cofactor containing either a molybdenum (Mo) or tungsten (W) atom that serves as the site at which electrons and an oxygen atom are transferred to or from the substrate. Structures for several members of this family have

been determined through crystallographic studies (Kisker et al. 1997). From these, details about substrate specificity, redox potential, and mechanisms of catalysis have been characterized.

One member of the DMSO reductase family, the arsenate respiratory reductase (ARR) catalyzes the reduction of arsenate, As(V), to arsenite, As(III), at the terminal end of the electron transport chain during anaerobic respiration. This metabolism has been identified as a contributor to arsenic mobilization in contaminated sediments. Structural information of ARR will elucidate information on the mechanism by which the enzyme reacts with As(V) and may allow the development of inhibitors specific to this metabolism. Here, we present homology modeling and preliminary mutational analysis based on the ARR sequence from *Shewanella* sp. strian ANA-3.

B.3. Materials and Methods

B.3.1. Structural Prediction.

Homology modeling of ArrA and ArrB was performed using the First Approach mode on the SWISS-MODEL web server (http://swissmodel.expasy.org) (Schwede et al. 2003). Briefly, this protocol compared the submitted protein sequence to the ExNRL-3D database using BLASTP2. Candidate templates with a sequence identity of greater than 25% and projected model size of greater than 20 amino acid residues were selected. Protein models were generated using ProModII, followed by energy minimization using Gromos96.

B.3.2. Construction of ARR Mutants

Mutant forms of ArrA were generated using primers 1fdonorm (5'-GAA AAC CTG TAT GAT AAG GCG TTT GTA GCG AGC AGA ATT GAG GGT AAA AAC CTG-3'), 1fdorevcomp (5'-TCT GCT CGC TAC AAA CGC CTT ATC ATA CAG GTT TTC AAC TAA GGC CAC ATG GGC AAT AG-3'), 2napAnorm (5'-GAA GAA CTG GAT AAC CCC AGA TTT TGG CAG AGA TAT ATT GAG GGT AAA AAC CTG-3'), 2napArevcomp (5'-ATA TCT CTG CCA AAA TCT GGG GTT ATC CAG TTC TTC AAC TAA GGC CAC ATG GGC AAT AG-3'), 1e60Cnorm (5'-GAA GAT CTG TAT GAT AAG GAT TTT ATT GCG AAC TAT ATT GAG GGT AAA AAC CTG-3'), 1e60Crevcomp (5'-ATA GTT CGC AAT AAA ATC CTT ATC ATA CAG ATC TTC AAC TAA GGC CAC ATG GGC AAT AG-3'), W293norm (5'-GTT GAA GGT GTA GCG CAT AAG CCC TTT-3'), W293revcomp (5'-AAA GGG CTT ATG CGC TAC ACC TTC AAC-3'), K295norm (5'-GGT GTA TGG CAT GCG CCC TTT GTT GGA-3'), K295revcomp (5'-TCC AAC AAA GGG CGC ATG CCA TAC ACC-3'), NcoarrA5-2 (5'-CAT GCC ATG GGT GCT GAA TTA CCC GCG CCT CTA-3'), and XhoarrB3-2 (5'-CCG CTC GAG TTA ATA AGC GGT TTT AAC ACC-3'). Two rounds of PCR were required. In the first round, gene fragments upstream and downstream of the mutation were individually amplified, with the primers overlapping at the point of mutation. The PCR conditions included an initial incubation at 95˚C for 5 minutes, followed by 33 cycles at 95˚C for 35 seconds, 58˚C for 40 seconds, and 72˚C for 2 minutes, and finishing with 1 cycle at 72˚C for 10 minutes. In the second round, the two amplified fragments were mixed, and crossover PCR with primers NcoarrA5-2 and

XhoarrB3-2 were used to create the full-length mutant form. The PCR conditions in the second round included an initial incubation at 95˚C for 10 minutes, followed by 30 cycles of 95˚C for 30 seconds and 60˚C for 6 minutes with an increase in 15 seconds for each repetition, and finishing at 72˚C for 10 minutes. Fragments were digested with Nco I and Xho I restriction enzymes (New England Biolabs) and ligated into the appropriate vector.

B.3.3. Activity Assay.

ARR activity was measured using a colorimetric assay. A reaction mix containing 120 μM Methyl viologen, 90 μM Dithionite, 50 mM MOPS buffer at pH 7, and 0.15 M NaCl was placed into a plastic cuvette under anaerobic conditions. Enzyme samples and electron acceptors were added, the cuvetes were plugged with rubber stoppers, and MV oxidation was measured by following loss of blue color at 600 nm using a Beckman spectrophotometer.

B.3.4. Mutational analysis.

Mutational analysis was performed using crude lysates of *E. coli* overexpressing the different forms of ARR in pET32H Bam Hind (Tochio et al. 2001). Cells were lysed with the addition of 100 μL of 0.1 g/mL CelLytic powder (Sigma). Whole cell samples of anaerobic wild-type and a Δ*napA* mutant of *Pseudomonas auruginosa* strain PA14 were used as a positive and negative control for the nitrate reduction assay. *E. coli* grown on DMSO was used as a positive control for DMSO reductase activity.

B.4. Results

B.4.1. Homology Modeling.

ArrA and ArrB were individually modeled to obtain preliminary structural information about each protein. For ArrA, a structure for residues Gly_{54} – Gly_{311} was predicted using the periplasmic DMSO reductase from *Rhodobacter capsulatus* (e60C, 42.8% identity (Bray et al. 2000)), the dissimilatory nitrate reductase from *Desulfovibrio desulfuricans* (2nap, 32.83% identity (Dias et al. 1999)), and formate dehydrogenase H from *E. coli* (1fdo, 26.71% identity (Boyington et al. 1997)) as templates (Figures B.1.A-D.). The conserved region consists of α/ß folds along the periphery and surrounding the entrance of the funnel-shaped cavity leading to the active site of the protein. Additionally, the residue that directly contacts the Mo atom can be narrowed down to Ser_{190} or Ser_{191}, which are predicted to occur on a loop directly above the Mo (Figure B.1.E.).

Figure B.1 Homology model of ArrA. A-D. Comparison of FDH structure (A-top view looking down into funnel cavity, C-side view) with homology model of ArrA (B-top view, D-side view). Conserved region is marked in green. E. Close up of Mo atom showing location of Ser_{140} and Ser_{141} as potential polypeptide ligands.

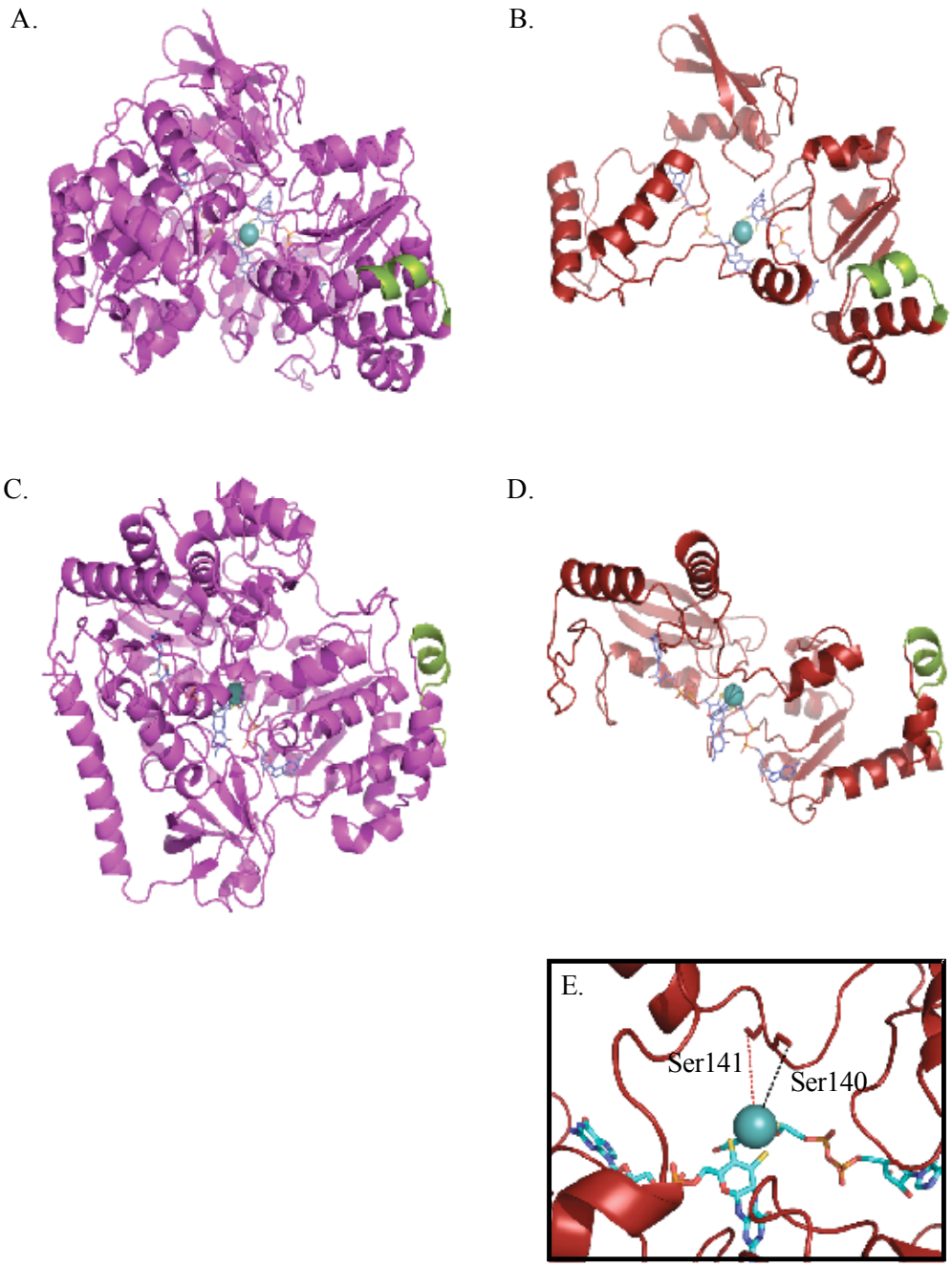

Modeling of ArrB predicted a structure for residues Met_1-Trp_{115} using the pyrogallol-phloroglucinol transhydroxylase from *Pelobacter acidigallici* (1vlf, 37.73% identity (Messerschmidt et al. 2004) and the ethylbenzene dehydrogenase from *Aromatoleum aromaticum* (2ivfB, 38.25% identity (Kloer et al. 2006)) as templates (Figure B.2.). The conserved region allows the assignment of twelve of the sixteen cysteine residues that are thought to coordinate four predicted iron-sulfur clusters. Cys 12, 15, and 18 are assigned to cluster 1. Cys 22 is assigned to cluster 2. Cys 57, 60, 65, and 99 are assigned to cluster 3. And, cys 69, 89, 92, and 95 are assigned to cluster 4. A seven-stranded ß-barrel domain present in the structure of pyrogallol-phloroglucinol transhydroxylase and thought to be involved in membrane anchoring does not seem to be conserved in ArrB.

Figure B.2. Homology model of ArrB. Comparison of FeS containing subunit of pyrogallol-phloroglucinol transhydroxylase and ArrB. Iron sulfur clusters and numbered beginning with the cluster closest to the site of interaction with the large subunit (top right corner).

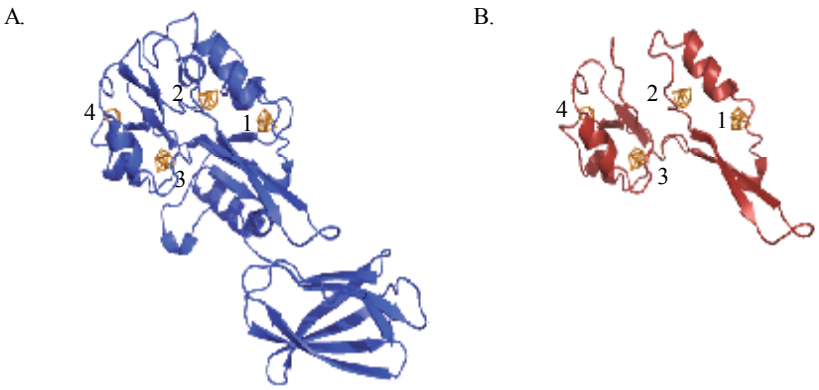

B.4.2. Mutational analysis

Previous studies by our laboratory identified a gene region conserved among all of the known *arrA* sequences while not being conserved among other members of the DMSO reductase family; this allowed the design of degenerate primers that could be used to determine if the gene was expressed in the environment (Malasarn et al. 2004). In the homology model, this conserved region corresponds to residues 237-248 of 1fdo, 239-250 of 2nap, and 257-268 of 1e60C (Figure B.3.A). These residues occur in a region that

is adjacent to and part of an α-helix near the outer edge of the cavity (shown in green in Figures B.1.A-D.).

To determine if the conserved region of ArrA discussed above is essential for enzyme function, site directed mutagenesis of the conserved block was performed. Three chimeric proteins were created in which the regions from the corresponding sequences of 1fdo, 2nap, and e60 were used to replace the native conserved amino acid residues in ArrA. The protein was expressed in the presence of ArrB, and activity was measured. All three of these mutations resulted in complete loss of activity (Figure B.3.B.). To determine if the mutations altered the ability of ARR to reduce alternative substrates, assays of the mutants using nitrate and DMSO were also carried out. No increase in activity was observed with any of the mutants (data not shown).

Two individual residues, W_{293} and K_{295} were also replaced by alanine. Both point mutations resulted in complete loss of activity (data not shown), though the constructs were not sequenced to verify that other mutations were not present.

A.

Shewanella sp. strain ANA-3	EGVWHKPFVGDF
Bacillus selenitireducens	EELWYKPFVDGF
Chrysiogenes arsenatis	KGLWSKEFVDGF
Desulfitobacterium hafniense	DGLWNKDFVDGF
Sulfurospirillum barnesii	EGRWNKSFVDGF
Desulfitobacterium hafniense (NapA)	EELDNPRFWQRY
Rhodobacter capsulatus (DorA)	EDLYDKDFIANY
Escherichia coli (FdhH)	ENLYDKAFVASR

B.

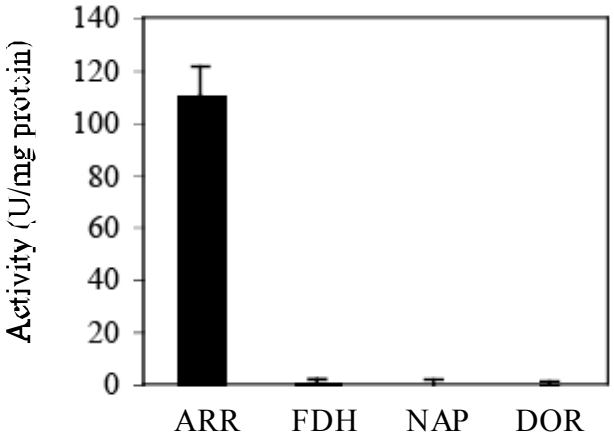

Figure B.3. Arsenate reductase activity of wild-type and chimeric forms of ARR. A. Sequence alignment of conserved region in ArrA from ANA-3, *B. selenitireducens*, *C. arsenatis*, *Desulfitobacterium hafniense*, *Sulfurospirillum barnesii*, *D. desulfuricans*, *R. capsulatus*, *E. coli*. B. Activity of wt form of ArrA (ARR), FDH-ArrA (FDH), NapA-ArrA (NAP), DorA-ArrA (DOR).

B.5. Discussion

Homology modeling predicts that part of ArrA is structurally similar to the MGD-containing subunit of other members of the DMSO reductase family. The conserved region includes partial structure from three of the four domains present in these enzymes. Together, these three domains form the funnel-shaped cavity leading to the active site of the enzyme. Additionally, Ser_{190} or Ser_{191} are presented as being possible direct ligands to the Mo atom. The use of Ser in this role has been found for the DMSO reductase (Schindelin et al. 1996).

Modeling ArrB allowed the assignment of twelve cysteine residues associated with the four predicted Fe-S clusters in this protein. The organization presented here is different from the first prediction based on sequence analysis, which assigned cys 12, 15, 18, and 69 to cluster 1; cys 22, 60, 65, and 57 to cluster 2; cys 89, 92, 95, 183 to cluster 3; and cys 99, 164, 167, and 179 to cluster 4 (Saltikov and Newman 2003).

Mutational analysis of the conserved region identified as being uniquely conserved among ArrA enzymes suggests that it is essential to the function of ARR although, based on the model, this region does not contact the substrate or the MGD cofactor directly. Thus, the role of this region on enzyme activity is unknown. Interestingly, while the known structures all identify this region as being adjacent to and part of an alpha helix, several of the conserved amino acid residues present in the ARR sequence statistically occur less frequently in helices. Possibly, this difference in sequence results in the loss of the helix in ARR and changes the substrate specificity or redox potential of the cofactor. An understanding of the purpose of this conserved region may provide insight into how ARR reduces As(V). To evaluate the accuracy of the models presented here, mutational analysis of residues such as Ser_{190} and Ser_{191} and those thought to be involved in Fe-S cluster coordination are required, as is the further analysis of the conserved region.

B.6. Acknowledgements

We thank Pamela Bjorkman and Shanna Z. Potter for helpful discussions.

B.7. References

Boyington, J. C., V. N. Gladyshev, et al. (1997). "Crystal structure of formate dehydrogenase H: catalysis involving Mo, molybdopterin, selenocysteine, and an Fe4S4 cluster." Science **275**(5304): 1305-8.

Bray, R. C., B. Adams, et al. (2000). "Reversible dissociation of thiolate ligands from molybdenum in an enzyme of the dimethyl sulfoxide reductase family." Biochemistry **39**(37): 11258-69.

Dias, J. M., M. E. Than, et al. (1999). "Crystal structure of the first dissimilatory nitrate reductase at 1.9 angstrom solved by MAD methods." Structure **7**(1): 65-79.

Kisker, C., H. Schindelin, et al. (1997). "Molybdenum-cofactor-containing enzymes: structure and mechanism." Annu Rev Biochem **66**: 233-67.

Kloer, D. P., C. Hagel, et al. (2006). "Crystal structure of ethylbenzene dehydrogenase from *Aromatoleum aromaticum*." Structure **14**(9): 1377-88.

Malasarn, D., C. W. Saltikov, et al. (2004). "*arrA* is a reliable marker for As(V) respiration." Science **306**(5695): 455.

Messerschmidt, A., H. Niessen, et al. (2004). "Crystal structure of pyrogallol-phloroglucinol transhydroxylase, an Mo enzyme capable of intermolecular hydroxyl transfer between phenols." Proc Natl Acad Sci U S A **101**(32): 11571-6.

Saltikov, C. W. and D. K. Newman (2003). "Genetic identification of a respiratory arsenate reductase." Proc Natl Acad Sci U S A **100**(19): 10983-8.

Schindelin, H., C. Kisker, et al. (1996). "Crystal structure of DMSO reductase: redox-linked changes in molybdopterin coordination." Science **272**(5268): 1615-21.

Schwede, T., J. Kopp, et al. (2003). "SWISS-MODEL: An automated protein homology-modeling server." Nucleic Acids Res **31**(13): 3381-5.

Tochio, H., M. M. Tsui, et al. (2001). "An autoinhibitory mechanism for nonsyntaxin SNARE proteins revealed by the structure of Ykt6p." Science **293**(5530): 698-702.

Appendix C

Effects of adsorbed arsenic on HFO aggregation and bacterial adhesion to surfaces

C.1. Introduction

Trace elements can be released to sediment porewaters upon reductive dissolution of iron (Fe) oxides. The rate and extent of Fe(III) oxide reductive dissolution is dependent on crystallinity, mineral solubility, surface area, and the presence of adsorbed ions (Bondietti et al. 1993; Roden and Zachara 1996; Larsen and Postma 2001; Bonneville et al. 2004; Pedersen et al. 2006). Adsorbed anions such as arsenate (As(V)) and arsenite (As(III)) can retard reductive dissolution by chemical reductants, but the effect of adsorbed As on microbial Fe(III) reduction has not been studied in detail. In incubations with *Shewanella* species strain ANA-3, microbial Fe(III) reduction was enhanced by the presence of As(III) adsorbed onto the surface of hydrous ferric oxide (HFO), an amorphous Fe oxyhydroxide (see Chapter 4). *Shewanella* sp. strain ANA-3 wild-type (WT) was incubated with hydrous ferric oxide (HFO) pre-equilibrated with As(III) (HFO/As(III)) or As(V) (HFO/As(V)) or without As (HFO only). ANA-3Δ*arrA*, a mutant unable to respire As(V), was incubated with HFO/As(V) as a control for As(V) reduction. Interestingly, the rates of Fe(III) reduction for the Δ*arrA* mutant on HFO/As(V) and ANA-3 WT on HFO were similar, while the rates of ANA-3 WT grown

on HFO/As(III) and HFO/As(V) were significantly higher. ANA-3 WT reduced the majority of adsorbed As(V) to As(III) within 40 hours of incubation. Once As(III) was the dominant species on the surface, the rates of Fe(III) reduction was comparable to the rates of ANA-3 WT incubated with HFO/As(III). The presence of adsorbed As(III) on HFO increased the rate of Fe(III) reduction. An explanation for this result was not immediately obvious, and could be due to HFO surface properties, aggregation, bacterial adhesion and/or genetic factors. The purpose of this study is to investigate the properties of HFO with adsorbed As(III) compared to HFO with adsorbed As(V) and HFO without adsorbed As in an attempt to explain increased rates of microbial Fe(III) reduction in the presence of adsorbed As(III). Surface properties were investigated by light microscopy and environmental scanning electron microscopy (ESEM). The rates of bacterial and chemical reduction was measured and the extent of bacterial adhesion onto the surface in the presence and absence of As was compared.

C.2. Materials and Methods

All chemicals used were reagent grade and used without further purification. Solutions were prepared with 18 MΩ-cm deionized water (Milli-Q, Millipore) and stored in plastic containers that had been washed in 2-5% nitric acid. For bacterial incubations, all solutions were autoclaved before use with the exception of the bicarbonate buffer, which was filter-sterilized (0.2 μm pore size) and added to the autoclaved medium. The bacterial minimal growth medium was buffered with 50 mM bicarbonate and had a total phosphate concentration of 50 μM and an ionic strength of 0.06 M.

C.2.1. Arsenic-equilibrated HFO preparation

HFO was prepared by the drop-wise addition of 0.5 M NaOH to 0.067 M $Fe(NO_3)_3$ until the solution stabilized at pH 8 (Schwertmann and Cornell 1991). The suspension was equilibrated for >4 h under constant stirring, adjusting any pH drift as necessary with 0.5 M NaOH. The HFO was then washed three times with sterile water and centrifuged. The HFO was not autoclaved after synthesis to avoid changes in mineralogy.

After the final wash, the HFO was resuspended in an As solution, and equilibrated overnight with constant stirring. For the ESEM experiments, 1 g of HFO was equilibrated in 200 mL of 0.01 M of Na_2HAsO_4 (Sigma) or $NaAsO_2$ (Sigma) at pH 8.0. For all other experiments, 0.25 g of HFO was equilibrated in 40 mL of 0.015 M As(III) or As(V) solution. These conditions ensured that all available surface sites for As adsorption were saturated with As at pH 8. The HFO was washed once with sterile water to remove excess As and resuspended in bacterial minimal medium (pH 8) to a final slurry concentration of 3 g_{HFO}/L. In the case of HFO without any adsorbed As, the solid was resuspended directly in bacterial medium after the initial washing and adjusted to pH 8. A subset of HFO, HFO/As(III) and HFO/As(V) solids were resuspended in water rather than bacterial medium as a control for the ESEM experiments.

C.2.2. Incubations with ANA-3

40mL of each type of HFO slurry were transferred into a sterile tube with a screw-cap lid and placed in an anaerobic chamber (80% N_2, 15% CO_2, 5% H_2). *Shewanella* sp. strain ANA-3 and *Shewanella* sp. strain ANA-3Δ*arrA*, a mutant with a

deletion in *arrA*, were used as inocula. See Chapter 5 for more information on the bacterial strains. A summary of the experimental conditions is presented in Table 6.1. Each tube was inoculated with 2 x 10^4 cells of ANA-3 WT or the Δ*arrA* mutant, or left uninoculated. Each condition was measured in duplicate. All tubes were incubated at 30°C in the dark in the anaerobic chamber.

At each time point, dissolved Fe(II) and total Fe(II) concentrations were determined by the ferrozine method (Stookey 1970). A 500 µL aliquot was filtered through a microcentrifuge filter with a 0.2 µm pore size (Costar, nylon Spin-x) in the anaerobic chamber for dissolved Fe(II) analysis. Ten µL of slurry was added directly to 90 µL of 1 M HCl in a 96-well plate for total Fe(II) determination. Time points were collected after 55 hours and 91 hours of incubation.

C.2.3. Environmental Scanning Electron Microscopy (ESEM)

ESEM is a technique particularly suited for imaging surface structures of hydrated solids because the beam can be operated at relatively high pressures. The structure is preserved when the solid is frozen and the water slowly evaporated from the surface. After 91 hours of incubation, all tubes were centrifuged and washed once with sterile deoxygenated water to remove the bacterial minimal medium. The solids were then resuspended in 20 mL of water, and transferred into a sterile Balch tubes. The tubes were capped before removal from the anaerobic chamber.

ESEM images were taken at the Jet Propulsion Laboratory (JPL) on a Phillips XD30 scanning electron microscope, operating in environmental mode. The samples were extracted from the Balch tubes with a syringe and placed on a sample holder.

Excess water was quickly wicked away from the sample before placing the sample holder on a Peltier stage cooled to 3.2-3.3°C. Conditions inside the chamber were maintained at 4.5 torr (~75% relative humidity), and the vacuum was applied such that the water was slowly removed from the sample surface (~15 min). The beam was operated at 20 kV and 332 μA.

C.2.4. Chemical Rates of Reduction

The chemical rates of reduction of HFO, HFO/As(V), and HFO/As(III) were compared by measuring the Fe(II) produced by reaction with l(+)-ascorbic acid (EM Science) at pH 8. All solutions were deoxygenated and the experiment was carried out in an anaerobic chamber. 18 mL of 100 mM of ascorbic acid in HEPES buffer (pH 8) was added to a concentrated stock solution of HFO, HFO/As(V) or HFO/As(III) to a final slurry concentration of 0.3 g/L. Each condition was performed in duplicate. At each time point, 10 μL of sample was added to 90 μL of 1 M HCl in a 96-well plate for ferrozine analysis of total Fe(II).

C.2.5. Bacterial adhesion assay

A *Shewanella* sp. strain ANA-3Δ*arrA* derivative expressing unstable green fluorescent protein (GFP) was created by transferring pTK4 (Teal et al. 2006) into ANA-3Δ*arrA* through conjugation and selection on 15 μg/mL tetracycline. pTK4 expresses a variant of GFP, GFP(AAV), containing a C-terminal oligopeptide extension that makes it susceptible to fast degradation by native intracellular proteases. The *gfp*(AAV) gene is

driven by the *Escherichia coli rrnB* P1 promoter, which is growth regulated such that cells fluoresce when they are actively growing.

Cultures of ANA-3Δ*arrA* carrying pTK4 were grown to midexponential phase on LB supplemented with tetracycline at 15 μg/mL. These cells were washed twice in LB with no antibiotic and resuspended in anaerobic minimal medium to remove tetracycline, which can form complexes with HFO and increase solubility (Gu and Karthikeyan 2005).

Under anaerobic conditions, 100 μL of washed cells at ~5 x 108 cells/mL were mixed with 100μL of HFO, HFO/As(III), or HFO/As(V) slurry and stored at room temperature anaerobically in a glove box for 1 hr. Samples were resuspended by gentle pipetting and 5μL were placed on a slide with no cover slip and brought out of the glove box for microscopy. Images were obtained using a Zeiss Axioplan microscope with a 20x NEOFLUAR plan objective lens using light (exposure time 0.05 seconds) and fluorescent excitation (exposure time 10 seconds).

C.3. Results and Discussion

C.3.1. Biological and chemical rates of reduction

The rate and extent of Fe(II) production for ANA-3 WT (HFO, HFO/As(III), HFO/As(V)) and ANA-3Δ*arrA* mutant (HFO/As(V)) is consistent with the more detailed time course in Chapter 4. The highest concentrations of Fe(II) are found in incubations with ANA-3 WT with HFO/As(V) and HFO/As(III). ANA-3 WT incubated with HFO only produces significantly less Fe(II) than ANA-3 WT incubated with HFO/As(III) and

HFO/As(V). Iron(II) production in ANA-3Δ*arrA* mutant incubations with HFO only and HFO/As(III) are similar. However, increased Fe(II) production is evident in the ANA-3Δ*arrA* mutant HFO/As(III) incubations. Both ANA-3 WT and ANA-3Δ*arrA* mutant incubations confirm the that the presence of adsorbed As(III) increases the rate of Fe(II) production (Table C.1.). Only a background amount of Fe(II) was measured in the control tubes over the course of the experiment, indicating that bacterial contamination was negligible.

Bacterial incubations				
	ANA-3 WT		**ANA-3 *ΔarrA* mutant**	
Incubation time	55 h	91 h	55 h	91 h
HFO	0.23	0.65	0.20	0.38
As(III)/HFO	0.65	1.04	0.67	1.01
As(V)/HFO	3.00	4.24	0.25	0.47
Control tubes (no bacteria)				
	Bacterial medium		**Water**	
Incubation time	55 h	91 h	55 h	91 h
HFO	0.15	0.15	0.14	0.15
As(III)/HFO	0.14	0.14	0.13	0.14
As(V)/HFO	0.12	0.16	0.11	0.16

Table C.1. Total Fe(II) concentrations (mM) from the incubations used in the ESEM experiment after 55 and 91 hours of incubation. Tubes were incubated at 30°C in an anaerobic chamber. The slurry concentration in all tubes is 3 g/L and was buffered at pH 8. The data reported is an average of duplicate tubes.

The amount and rate of Fe(II) production by ascorbic acid is similar for HFO, HFO/As(V), and HFO/As(III) (Figure C.1.). Therefore, the chemical rates of reduction are independent of adsorbed As.

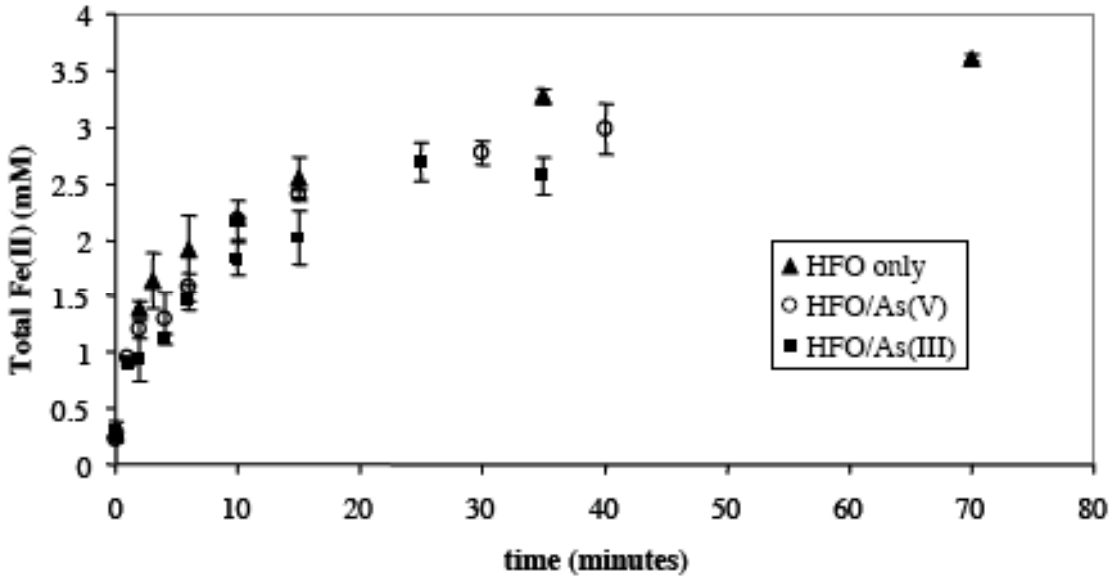

Figure C.1. Total Fe(II) production during the chemical reduction of HFO, As(V)/HFO and As(III)/HFO by 100 mM ascorbic acid at pH 8. The error bars indicate the standard deviation of duplicate samples.

C.3.2. Effect of adsorbed As on HFO aggregation

Adsorbed As(III) made HFO more bioavailable for reduction, presumably by affecting HFO aggregation or surface properties. Slower settling was observed from HFO with adsorbed As(III) (Figure C.2.), suggesting smaller particle size or less efficient aggregation. When imaged by light microscopy after vigorously shaking the tubes, the particle sizes in all three cases appear to be the same size (~50 μm) (Figure C.5.). However, imaging the supernatant after allowing the solid to settle for >24 hours, only

the HFO/As(III) tube had traces of particles that would not settle (Figure C.3.). Although they may comprise only a small fraction of the total mass of HFO/As(III) in the tube, the presence of the small particles may explain the increased rates of Fe(III) reduction.

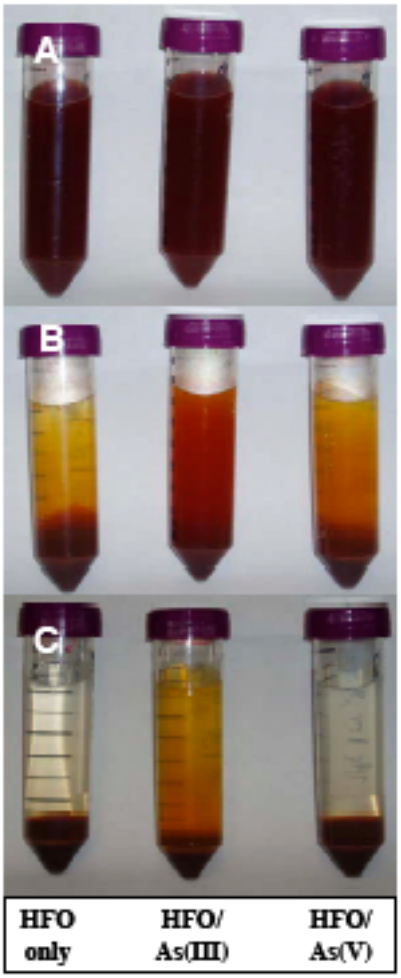

Figure C.2. Tubes of HFO only (left tube), HFO/As(III) (middle tube), and HFO/As(V) (right tube) A. immediately after shaking, B. after 2 hours, and C. after >24 hours of settling. The HFO in all tubes is suspended in bacterial medium (no inoculation, pH 8, ionic strength = 0.01 M).

ESEM was used to observe the surface morphology of HFO in the presence and absence of adsorbed As(III) and As(V). All three solids had similar morphologies, but

there were some subtle differences. HFO and HFO/As(V) had clusters of ball-shaped mounds (Figure C.4.A.,B.). These mounds were actually collections of smaller, nanoparticles of HFO, consistent with previous studies of HFO aggregates (Cornell and Schwertmann 1996). HFO/As(III) had a slightly different surface structure, exhibiting smoother surfaces and fewer ball-shaped mounds (Figure C.4.C.).

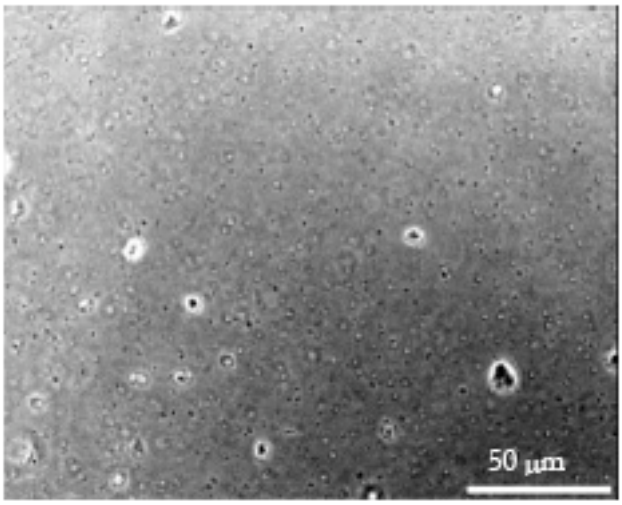

Figure C.3. Light microscope image of the particles in the supernatant of HFO/As(III) that had been left undisturbed for >24 hours.

ESEM images were also taken after 91 hours of incubation with ANA-3 WT and Δ*arrA* mutant. The morphology of all three solids (HFO, HFO/As(III), HFO/As(V)) after incubation with either ANA-3 WT or ANA-3 mutant was similar to the starting material (Figure C.5.A.,B.,C.). In the case of HFO/As(V) incubated with ANA-3 WT, most of the As(V) had been reduced to As(III) after 91 hours of incubation. Even though the majority of the As on the surface was As(III), the morphology was more similar to HFO/As(V). Therefore, the change in oxidation state from As(V) to As(III) did not significantly affect the morphology of the surface.

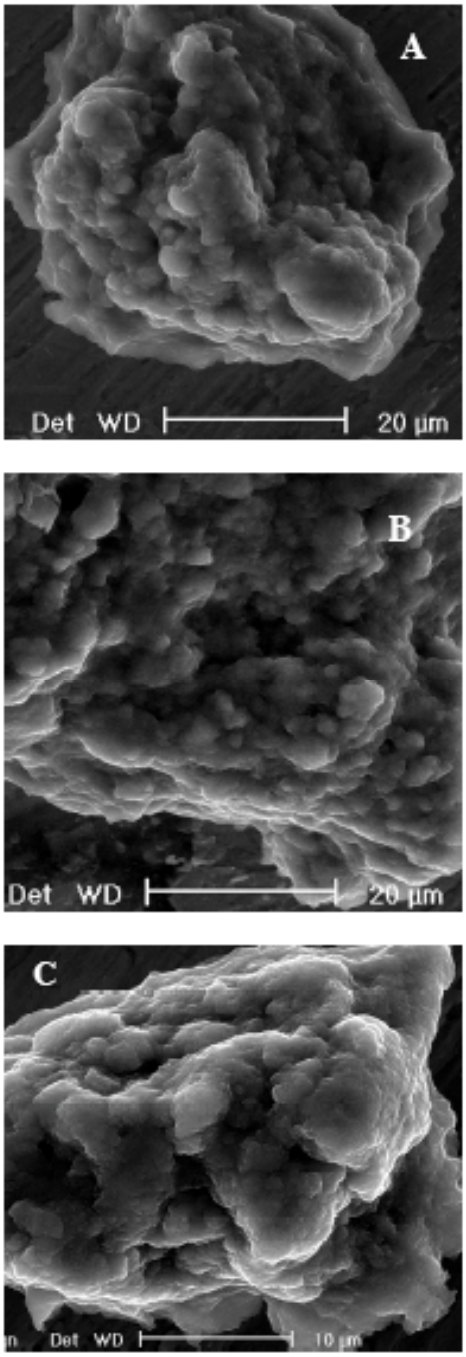

Figure C.4. ESEM images of A. HFO only, B. HFO with As(V), and C. HFO with As(III) without bacteria. The solids were suspended in water. Samples for imaging were taken immediately after shaking the tubes.

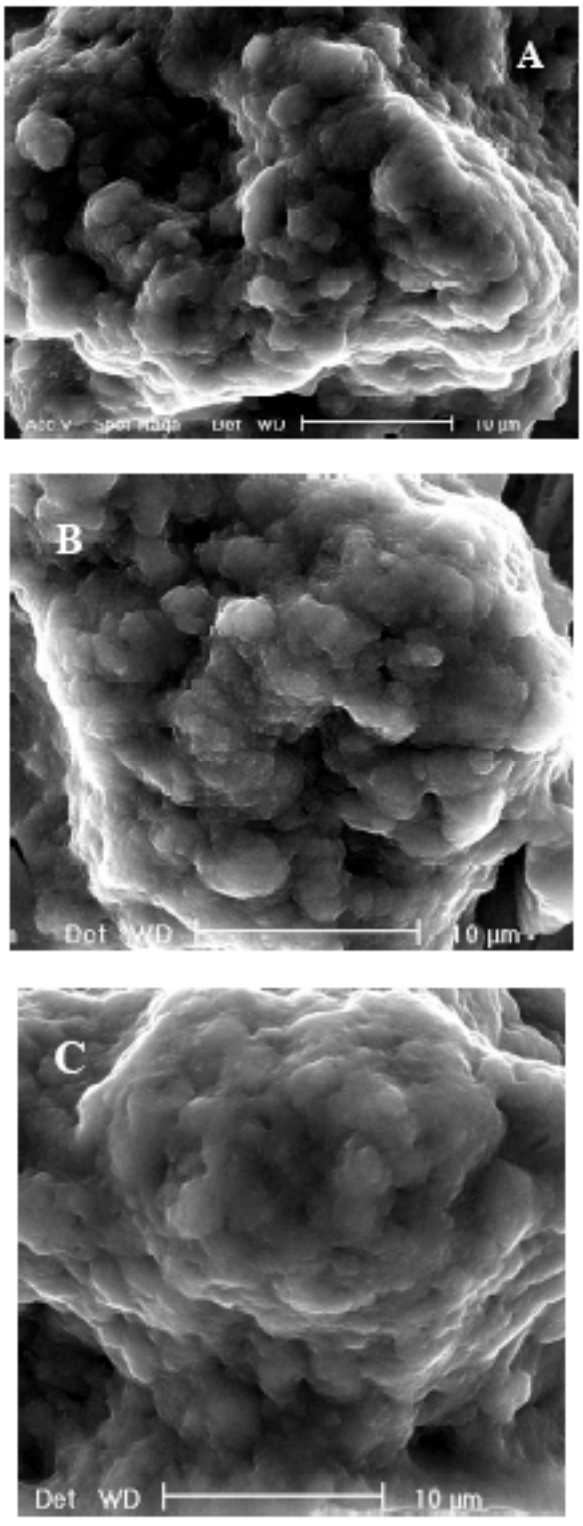

Figure C.5. ESEM images of A. HFO only, B. HFO with As(V), and C. HFO with As(III) after 91 hours of incubation with *Shewanella* sp. strain ANA-3 WT. Samples for imaging were taken immediately after shaking the tubes.

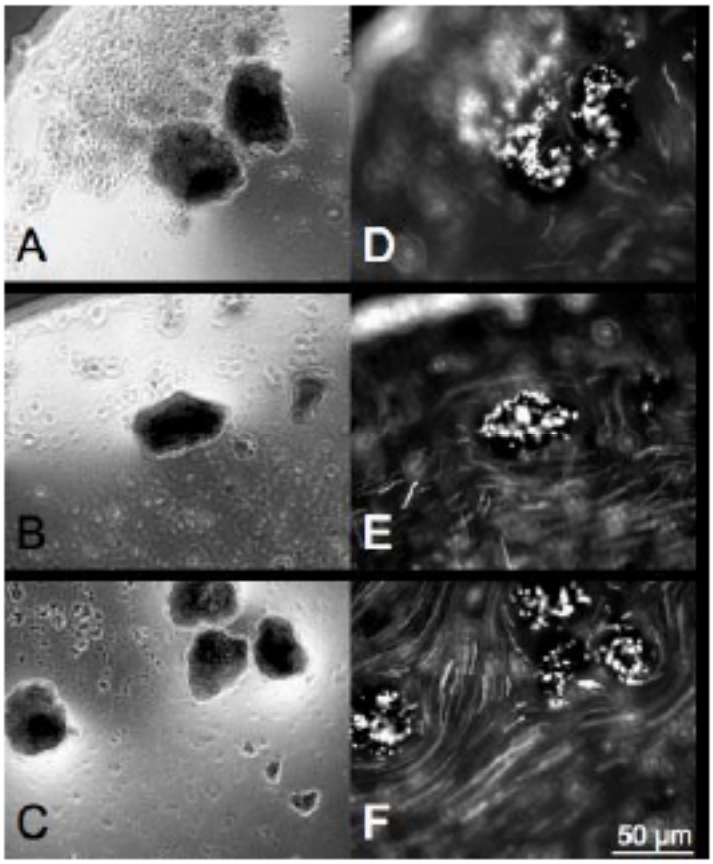

Figure C.6. Adhesion of active *Shewanella* sp. strain ANA-3Δ*arrA* onto HFO. Light microscope images of A. solid HFO, B. As(III)-sorbed HFO, and C. As(V)-sorbed HFO. Fluorescent images of GFP(AAV)-expressing ANA-3Δ*arrA* in the same field of view corresponding to light images in the adjacent panel (D to F).

C.3.3. Bacterial adhesion

To understand the contribution of cell adhesion to the differences in iron reduction rates, adhesion assays were carried out using ANA-3Δ*arrA* expressing a growth-regulated unstable GFP variant. Performance of this assay required a high cell number for a short amount of time to allow visualization to be completed in the absence of growth, which would have resulted in differences in total cell number. Use of the growth-regulated, unstable GFP allowed direct observation of cells that were

metabolically active.

After incubating the cells with the HFO samples for 1 hour, actively growing fluorescent cells were found attached to particles under all three conditions (Figure C.6.). This suggests that the differences in surface properties due to adsorbed As(III) did not significantly affect cell adhesion.

C.3.4 Conclusion

The presence of adsorbed As(III) on the surface of HFO significantly increased the rate of Fe(III) reduction by ANA-3 WT and ANA-3Δ*arrA* mutant, but did not affect the rates of chemical reduction by ascorbic acid. The reduction of As(V) to As(III) by ANA-3 WT did not change the surface morphology, and there was no evidence for preferential bacterial adhesion to HFO/As(III). While most of the particles in all three cases are approximately the same size, the presence of colloidal HFO/As(III) particles may explain the increased rates of Fe(III) reduction. The colloidal particles may be about the same size or smaller than the bacterial cells, which may make the Fe(III) particles more bioavailable for reduction.

Colloidal stabilization of Fe(III) oxides by As(III) adsorption has not been reported in the literature and it would be valuable to investigate this property further (e.g., effects of pH on colloidal stability and the effect of varying As(III) concentration) to determine whether this observation may be relevant to natural sediments. Although the As concentrations used in this study are higher than observed in most natural environments, the presence of As(III)-stabilized Fe oxide colloids may have environmental implications, even at lower concentrations. In Haiwee Reservoir, As(III) is

the dominant species in the Fe reduction zone. Even if only a small fraction of the solid phase is affected by As(III)-stabilized colloids, it may impact the overall rate of Fe reduction. The fraction of Fe and As in the sediments that would have to be mobilized in order to support the observed porewater concentrations is <2.5% (Hering and Kneebone 2001). Thus, even as a small fraction of the total solid phase, the presence of As(III)-stabilized colloids may affect the bioavailability of the Fe phase, and ultimately the mobilization of As.

C.4. Acknowledgements

This work was done in collaboration with Dr. Kate Campbell and Dr. Janet Hering. As lead author, Kate helped in all of the work aside from the bacterial adhesion assays. She performed the chemical reduction experiment and collected ESEM images with Randall Mielke at JPL.

C.5. References

Bondietti, G., J. Sinniger, et al. (1993). "The reactivity of Fe(III) (hydr)oxides: effects of ligands in inhibiting the dissolution." Colloids and Surfaces A: Physiochemical and Engineering Aspects **79**: 157-167.

Bonneville, S., P. V. Cappellen, et al. (2004). "Microbial reduction of iron(III) oxyhydroxides: effects of mineral solubility and availability." Chem Geol **212**: 255-268.

Gu, C. and K. G. Karthikeyan (2005). "Interaction of Tetracycline with Aluminum and Iron Hydrous Oxides." Environ Sci Technol **39**(8): 2660-2667.

Hering, J. and P. Kneebone (2001). Biogeochemical Controls on Arsenic Occuarance and Mobility in Water Supplies. Environmental Chemistry of Arsenic. J. William T. Frankenberger. New York, Marcel Dekker, Inc.**:** 155-181.

Larsen, O. and D. Postma (2001). "Kinetics of reductive bulk dissolution of lepidocrocite, ferrihydrite, and geothite." Geochim Cosmochim Ac **65**: 1367-1379.

Pedersen, H. D., D. Postma, et al. (2006). "Release of arsenic associated with the reduction and transformation of iron oxides." Geochim Cosmochim Ac **70**: 4116-4129.

Roden, E. E. and J. M. Zachara (1996). "Microbial Reduction of Crystalline Iron (III) Oxides: Influence of Oxide Surface Area and Potential for Cell Growth." Environ Sci Technol **30**(5): 1618-1628.

Schwertmann, U. and R. M. Cornell (1991). Iron Oxides in the Laboratory. Weinheim, Wiley-VCH.

Stookey, L. L. (1970). "Ferrozine-A new spectophotometric reagent for iron." Analytical Chemistry **42**(7): 779-781.

Teal, T. K., D. P. Lies, et al. (2006). "Spatiometabolic Stratification of *Shewanella oneidensis* Biofilms." Appl Environ Microbiol **72**(11): 7324-7330.